

CSUN Geological Sciences Fall Field Frolic!

August 20-23, 2008

Northern Mojave/Owens Valley/Long Valley Regions

Welcome to the 2008 Fall Field Fling presented by the Department of Geological Sciences at CSUN. This is an especially significant and poignant trip because it celebrates two important anniversaries:

- 1) The 50th anniversary of California State University Northridge
- 2) The 25th anniversary of the very first fall field frolic, organized and led by George Dunne to the Death Valley region in October of 1983

We are pleased that many alumni have responded to our invitation to participate in this event, reflecting the close ties between alumni and "The Mother Ship" that we have fostered over the years. We hope these ties will maintain and even strengthen over the years ahead.

In addition to celebrating these anniversaries, this trip also celebrates the impact that research by our alumni and faculty has had on our geologic understanding of this fascinating part of California. Many of our stops will be at locations where studies have been carried out by CSUN geologists.

In alphabetical order, your fearless trip organizers and field stop leaders are:

- Dr. Kim Bishop (CSU Los Angeles)
- Dr. George Dunne (CSUN Emeritus Faculty Member)
- Dr. Gene Fritsche (CSUN Emeritus Faculty Member)
- Mike Kaericher (CSUN undergraduate student)
- Dr. Steve Lipshie (Los Angeles County Dept. of Public Works)
- Jean Rains (CSUN graduate student)
- Dr. Cal Stevens (San Jose State University)
- Dr. Paul Stone (U. S. Geological Survey, Menlo Park)
- Brian Swanson (Seward Engineering Geology, Inc.)
- Dr. Jorge Vazquez (CSUN Faculty Member)
- Jeff Woolford (CSUN graduate student)
- Dr. Doug Yule (CSUN Faculty Member)

We thank Mari Flores for helping with the paperwork and information flow regarding trip planning, Dave Liggett and Mike Tacsik for logistical support during the trip, and Natasha Galvez Dunne for planning and preparing our breakfasts.

\N.B. Materials in this informal guidebook are for the educational use of field trip participants and are not to be duplicated or cited as references.

2008 Fall Field Frolic Stop Itinerary

Day 1 (Aug. 20)

STOP #	LOCATION	GEOLOGIC FOCUS	LEADERS
1	El Paso Mtns	Late Pz evolution	J. Rains, K. Marsaglia, G. Dunne
2	Talc City Hills	Pz & Mz deformation; Devonian stratigraphy	C. Stevens, G. Dunne
3	southern Inyo Mtns	Late Pz stratigraphy, structure	P. Stone, B. Swanson
4	Independence	Devonian channel	C. Stevens

Day 2 (Aug. 21)

STOP #	LOCATION	GEOLOGIC FOCUS	LEADERS
1	Poverty Hills/Crater Mtn	Mega landslide	Kim Bishop
2	Ditto	Big Pine Volcanic Field	Jeff Woolford, Jorge Vazquez
3	Ditto	Owens Valley fault zone	Kim Bishop, Doug Yule
4	Northern Inyo Mtns	Late Precambrian stratigraphy	Mike Kaericher, Doug Yule
5	Chalfant	Basal deposits, Bishop tuff	J. Vazquez, S. Lipshie

Day 3 (Aug. 22)

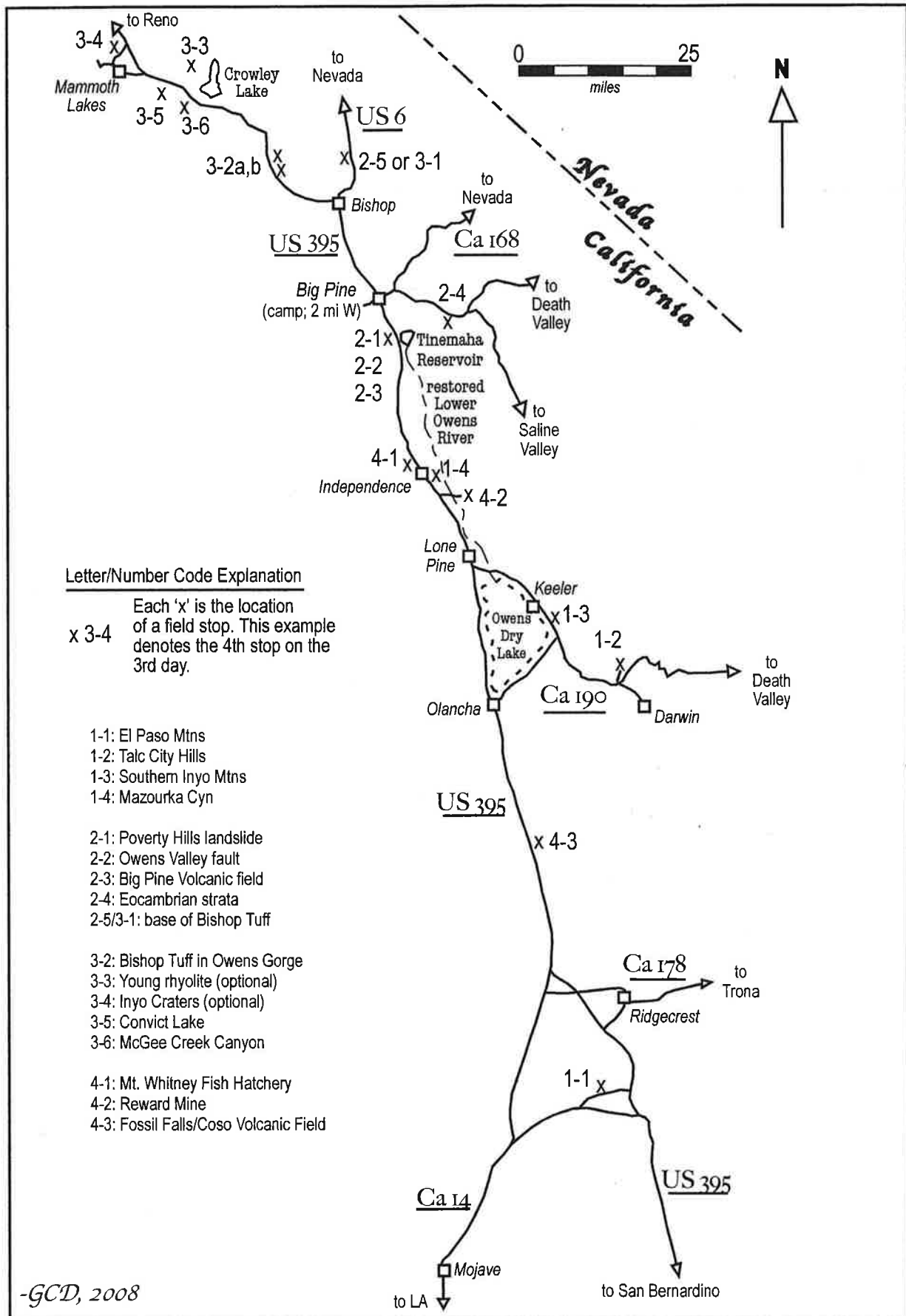
STOP #	LOCATION	GEOLOGIC FOCUS	LEADERS
1	Owens River Gorge	Bishop tuff	J. Vazquez, S. Lipshie
2	Hot Creek Rhyolite	Youngest caldera deposits	J. Vazquez, S. Lipshie
3	Inyo Craters*	Inyo Craters (youngest volcanism)	S. Lipshie
4	Convict Lake	Pz stratig. & structure in Sierran pendants	C. Stevens
5	McGee Creek Cyn	Devonian channel, Pz stratig	C. Stevens

* optional stop, if time permits

Day 4 (Aug. 23)

STOP #	LOCATION	GEOLOGIC FOCUS	LEADERS
1	Independence area	effects of recent debris flows	tba
2	Reward Mine	Permian potholes	C. Stevens
3	Owens Lake	Dust mitigation, river restoration	G. Dunne
4	Fossil Falls	Pluvial drainage, potholes	C. Stevens, G. Dunne
5	Coso Mtns	Coso volcanic field, geothermal energy	J. Vazquez, G. Dunne

2008 CSUN Fall Field Frolic



Character of Middle Permian Subduction Initiation in the El Paso Mountains, California

Jean Rains and Kathie Marsaglia

Paleozoic rocks of the El Paso Mountains (EPM) provide important data about the geological evolution of the western edge of the North American continent. In Late Proterozoic and Early Paleozoic time, the western edge was a passive continental margin, trending north to northeast as revealed by cratonal, miogeoclinal (continental shelf and slope), and eugeoclinal (deep marine and continental rise) sedimentary facies and the isotopic Sr; 0.706 line, among other geologic evidence (Fig. 1) (Kistler and Peterman, 1973; Hamilton and Myers, 1966; Burchfiel and Davis, 1975; Miller et al., 1995; Barth et al., 1997; Dickinson, 2000; Stevens et al., 2005). Younger rocks of the western continental margin, beginning with Pennsylvanian and Permian strata, cut across the older facies belts at a high angle, indicating a rearrangement of the continental margin (Fig. 1). The displacement of the EPM and the Caborca block in Mexico from their respective Lower Permian facies belts, along with other evidence, has been interpreted as supporting continental margin rearrangement and truncation by left-lateral transform faulting (Fig. 1) (Dickinson, 2000; Stevens et al., 2005). Regional sedimentary patterns have been interpreted by some workers as indicating that the EPM were at their present latitude by Pennsylvanian time (Carr et al., 1984, 1997; Martin and Walker, 1995, Stevens et al., 2005). [For alternative hypotheses and further details of displacement of the EPM, see Poole (1974), Snow (1992), Miller et al. (1995) and Stevens et al., (2005)].

The EPM are uniquely informative about the Permian transition from pre-subduction to subduction regimes because they contain a plutonic and volcanic expression of the onset of subduction (Martin and Walker, 1995; Miller et al., 1995) as well as a sedimentary record (Carr et al., 1997). From this initiation of magmatism, the southwestern North America continental margin eventually transitioned to the active Andean-style continental margin that gave rise to the Sierra Nevada Batholith (Fig. 1) in the early Mesozoic.

I have studied the Permian sedimentary record of the Permian transition from pre-subduction to subduction regimes, springboarding my efforts on previous work by others, notably Carr et al. (1997). The focus of my study was the transition from borderland to

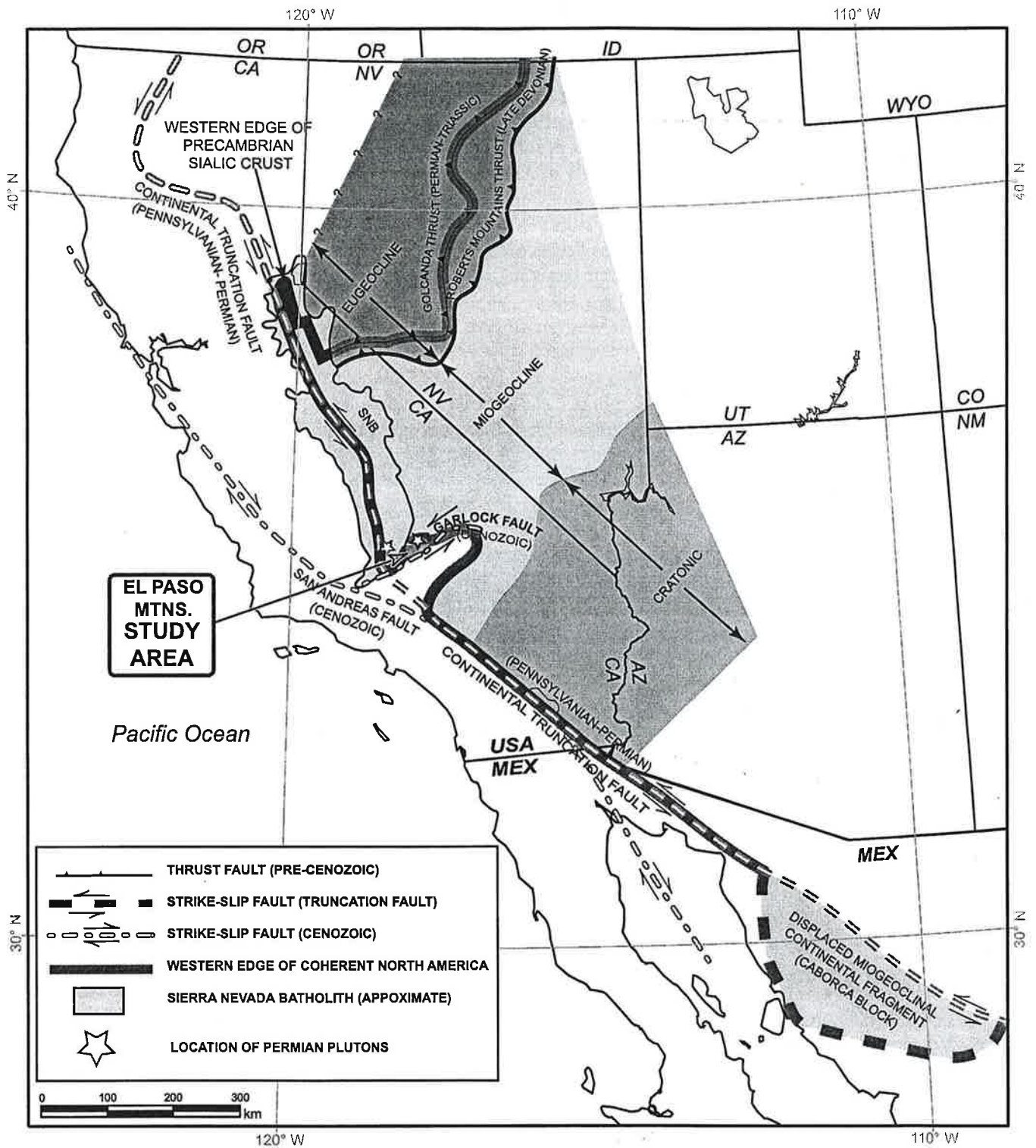
volcaniclastic sedimentation in the Early Permian (~280 - ~260 Ma), up to the overlying latest Early Permian (~262 ± 2 Ma) andesite flows (Carr et al., 1984, 1997; Martin and Walker, 1995). The age of transition from pre-volcanic sedimentation to arc volcanism is constrained by microfossils (Dibblee, 1952, 1967; Carr et al., 1984, 1997) in the metasediments and by U – Pb zircon dating of the overlying volcanics (Martin and Walker, 1995; Miller et al., 1995).







I measured, described, and sampled an apparently continuous, ~950 m-thick stratigraphic section of Early Permian metasediments southwest of Mormon Flat (Fig. 2). Representative samples were thin-sectioned and petrographically analyzed for texture and composition. Although metamorphosed up to greenschist level, sedimentary and mineralogical details are still discernible. My research revealed the following. Above a disconformable contact with underlying Ordovician-Late Cambrian (eugeoclinal) deep-marine passive margin rocks, the Permian section begins with a local basal conglomerate (~33 m), followed by metacarbonate turbidites (~62 m), then mostly covered noncalcareous metashales and metasiltsstones (~393 m). Upsection, the mudstones become more calcareous (~152 m; several beds of meta-arkose interrupt the upper ~64 m. An abrupt change to slightly tuffaceous calcarenite (~10 m) is followed by tuffaceous metasandstones with distinctly zoned plagioclase crystals that dominate the rest of the section (~297 m). Rare interbeds of quartz arenite occur ~15 m above the base of the tuffaceous metasandstones and of bioclastic metalimestone near the top below the andesite flows. These results are consistent with a history of uplift (conglomerate), followed by subsidence and deeper water sedimentation (shale), then gradual shallowing accompanied by onset of nearby volcanism (volcaniclastic and bioclastic sediments) to construction of a volcanic edifice (andesitic lavas) in a shallow marine environment. (Fig. 3).

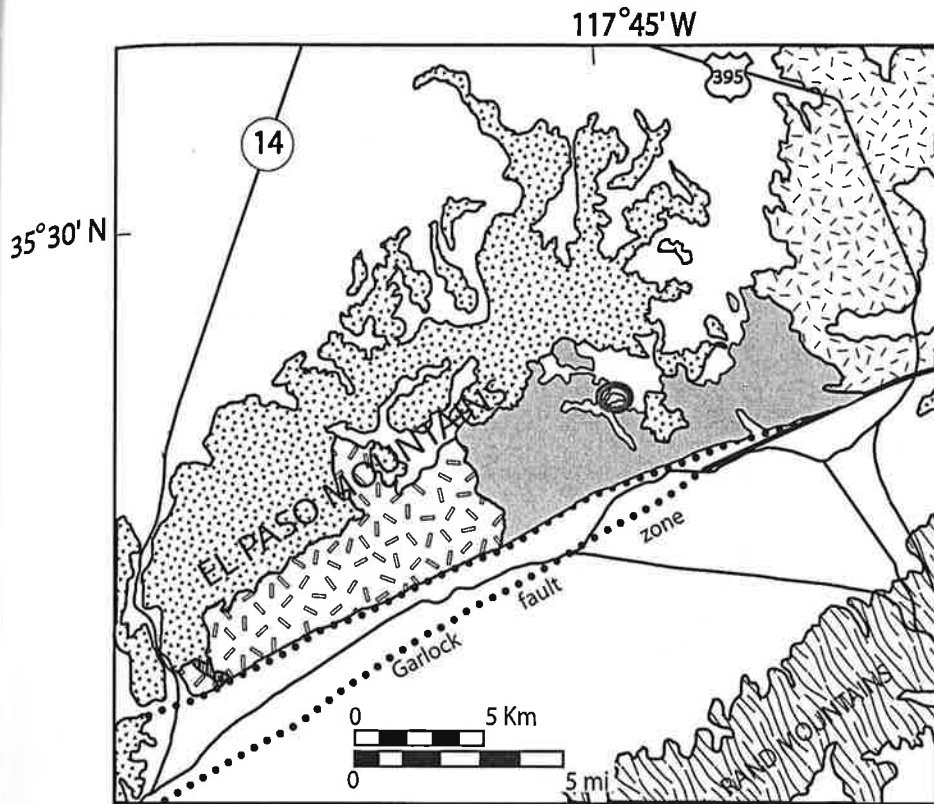
The pattern of uplift followed by subsidence in the upper plate of the nascent subduction zone (EPM) (Fig. 3) is consistent with induced subduction (Hall et al., 2003; Gurnis and Hall, 2004; Stern, 2004) along a transform plate boundary. More speculatively, given transform faulting possibly continuing in the region, the shift in Euler poles for the Pacific and North American plates at 266-267 Ma (Gorden and Van der Voo, 1995, Table 1) may have added a component of convergence along a portion of the boundary, enabling local subduction initiation and the eventual development of the Sierra Nevada Batholith.

REFERENCES:

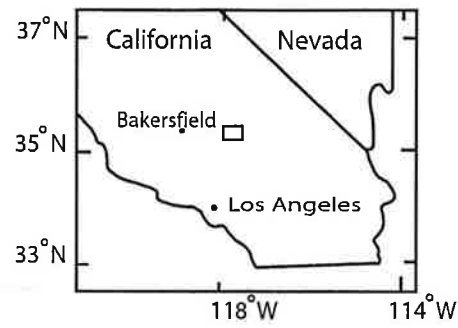
- Barth, A. P., Tosdal, R. M., Wooden, J. L., and Howard, K. A., 1997, Triassic plutonism in southern California: Southward younging of arc initiation along a truncated continental margin: *Tectonics*, v. 16, no. 2, p. 290-304.
- Burchfiel, B.C., and Davis, G. A., 1975, Nature and controls of Cordilleran orogenesis, western United States: Extensions of an earlier synthesis: *American Journal of Science*, v. 275-A, p. 363-396.
- Carr, M. D., Christiansen, R. I., and Poole, F. G., 1984, Pre-Cenozoic geology of the El Paso Mountains, southwestern Great Basin, California – A summary, *in* Lintz, J., Jr., ed., *Western geological excursions: Cordilleran section*, Geological Society of America Fieldtrip Guidebook 7, v. 4, p. 84-93.
- Carr, M. D., Christiansen, R. L., Poole, F. G., and Goodge, J. W., 1997, Bedrock geologic map of the El Paso Mountains in the Garlock and El Paso Peaks 7-1/2' quadrangles, Kern County, California: U. S. Geological Survey Miscellaneous Investigations Series Map I-2389, 9 p., scale 1:24,000.
- Dibblee, T. W., 1952, Geology of the Saltdale quadrangle, California: California Division of Mines and Geology Bulletin 160, 43 p.
- Dibblee, T. W., 1967, Areal geology of the western Mojave Desert: U. S. Geological Survey Professional Paper 522, 153 p.
- Dickinson, W. R., 2000, Geodynamic interpretation of Paleozoic tectonic trends oriented oblique to the Mesozoic Klamath—Sierran continental margin in California, *in* Soreghan, M. J., and Gehrels, G. E., eds., *Paleozoic and Triassic paleogeography and tectonics of western Nevada and northern California*: Boulder, Colorado, Geological Society of America Special Paper 347, p. 209-245.
- Gorden, R. G. and Van der Voo, R., 1995, Mean paleomagnetic poles for the major continents and the Pacific Plate, *Global Earth Physics: A Handbook of Physical Constants*, AGU Reference Shelf I, Table 1, p. 225 – 239.
- Gurnis, M., and Hall, C. E., 2004, Evolving force balance during incipient subduction, *Geochemistry, Geophysics, Geosystems*, AGU, v. 5, no. 7, 31 p., Q07001, doi: 1029/2003GC000681
- Hall, C. E., Gurnis, M., Sdrolias, M., Lavier, L. L., and Muller, D., 2003, Catastrophic initiation of subduction following forced convergence across fracture zones, *Earth and Planetary Science Letters*, Vol. 212, p. 15-30.
- Hamilton, W., and Myers, W. B., 1966, Cenozoic tectonics of the western United States: *Review of Geophysics*, v. 4, p. 509-549.
- Kistler, R. W., and Peterman, Z. E., 1973, Variations in Sr, Rb, K, Na, and initial $^{87}\text{Sr}/^{86}\text{Sr}$ in Mesozoic granitic rocks and intruded wall rocks in central California: *Geological Society of America Bulletin*, v. 84, p. 3489-3512.
- Martin and Walker, 1995, Stratigraphy and paleogeographic significance of metamorphic rocks in the Shadow Mountains, western Mojave Desert, California, *GSA Bulletin*, v. 107, no. 3, p. 354 – 366.
- Miller and others, 1995, Geochronologic and isotopic evidence for Triassic-Jurassic emplacement of the eugeoclinal allochthon in the Mojave Desert region, California: *Geological Society of America Bulletin*, v. 107, no. 12, p. 1441-1457.
- Poole, F. G., 1974, Flysch deposits of the Antler foreland basin, western United States: *Society of Economic Paleontologists and Mineralogists (SEPM) Special Publication*, v. 22, p. 58-82.
- Snow, J. K., 1992, Large-magnitude Permian shortening and continental-margin tectonics in the southern Cordillera: *Geological Society of America Bulletin*, V. 104, p. 80-105.
- Stern, 2004, Subduction initiation: spontaneous and induced,, *Earth Planetary Science Letter* 226, p. 275 – 292, doi: 1016/j.epsl.2004.08.07
- Stevens, C. H., Stone, P., and Miller, J. S., 2005, A new reconstruction of the Paleozoic continental margin of southwestern North America: Implications for the nature and timing of continental truncation and the possible role of the Mojave-Sonora megashear hypothesis, *in* Anderson, T. H., Nourse, J. A., McKee, J. W., and Steiner, M. B., eds., *the Mojave-Sonora megashear hypothesis: Development, assessment, and alternatives*: Geological Society of America Special Paper 393, p.



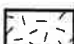
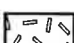

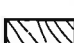




-  THRUST FAULT (PRE-CENOZOIC)
-  STRIKE-SLIP FAULT (TRUNCATION FAULT)
-  STRIKE-SLIP FAULT (CENOZOIC)
-  WESTERN EDGE OF COHERENT NORTH AMERICA
-  SIERRA NEVADA BATHOLITH (APPOXIMATE)
-  LOCATION OF PERMIAN PLUTONS

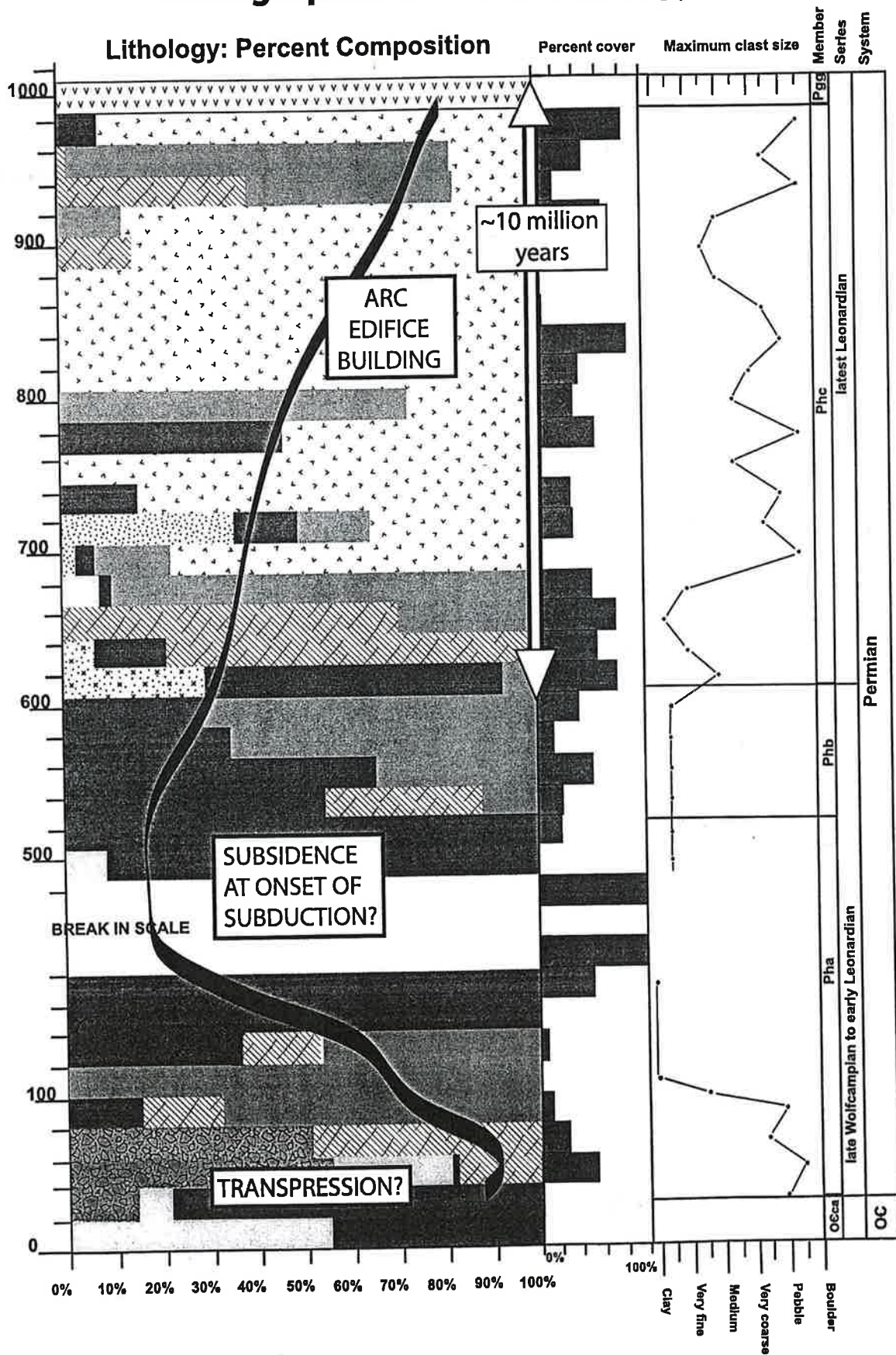


Location map modified from Carr et al. (1984)





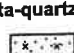






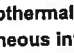



- KEY**
-  Quaternary sediments and cover
 -  Tertiary rocks
 -  Jurassic granitoids
 -  Permian and Triassic plutons
 -  "Bond Buyer" sequence
 -  Rand schist
 -  Paleozoic metasedimentary and metavolcanic rocks
 -  Study area

Stratigraphic Column: Lithology and Cover



KEY

-  Quaternary cover
-  Meta-andesite
-  Meta-argillite, meta-siltstone
-  Meta-quartz arenite
-  Meta-arkose, non-tuffaceous
-  Tuffaceous metasandstone
-  Other metasandstones
-  Metaconglomerate
-  Meta-carbonate
-  Silicified limestone, recrystallized chert
-  Hydrothermal "alterite"
-  Igneous intrusion
- OC**
Ordovician - Cambrian
-  Change in basin depth

The Middle Devonian Mount Morrison submarine fan system

(Abstracted from Cal Stevens and Tina Pelley, 2006)

Overview of Fan

The Mount Morrison submarine fan system developed along the western continental margin of North America in Middle Devonian time, seaward of the immense Paleozoic carbonate shelf that flanked the craton. The quartz sand and lime mud composing the fan were derived from the east and transported across the shelf during a major lowstand of sea level. All elements of the fan system are exposed from the Talc City Hills on the east to the Sierra Nevada on the west.

The Mount Morrison fan system lies above a major sequence boundary of Middle Devonian age. Seven depositional environments are recognized above this sequence boundary of which we will see four on this trip. These latter are: (1) the shelf exposed in the Talc City Hills, (2) an upper slope channel cropping out above Squares Tunnel in the Inyo Mountains, (3) the main distributary channel exposed at McGee Mountain in the eastern Sierra Nevada, and (4) the submarine fan itself exposed at Convict Lake in the Sierra Nevada.

Development of the Mount Morrison fan system was triggered by a rapid drop in sea level that resulted in exposure of the shelf. At that time sand was carried across the shelf, submarine canyons were cut into the shelf margin and upper slope, and fan deposition commenced. Later a rise in sea level resulted in flooding of the shelf cutting off the supply of sand to the shelf as well as to the fan. This event resulted in burial of the submarine fan and the channels cut into the middle and upper slope by the deep-water dark gray argillite and radiolarian chert of the late Middle to Late Devonian Squares Tunnel Formation. On the shelf shallow-water carbonates of the Lost Burro Formation were deposited.

The Mount Morrison fan and distal parts of the main channel are interpreted to have been offset ~65 km in a right-lateral sense on the cryptic Tinemaha fault of possible latest Cretaceous or early Tertiary age (Stevens and Greene, 1999; Kylander-Clark et al., 2005). Reconstruction of this offset aligns lithologically similar channel deposits of the fan system at Tinemaha Reservoir in the western Inyo Mountains and McGee Mountain in the eastern Sierra Nevada.

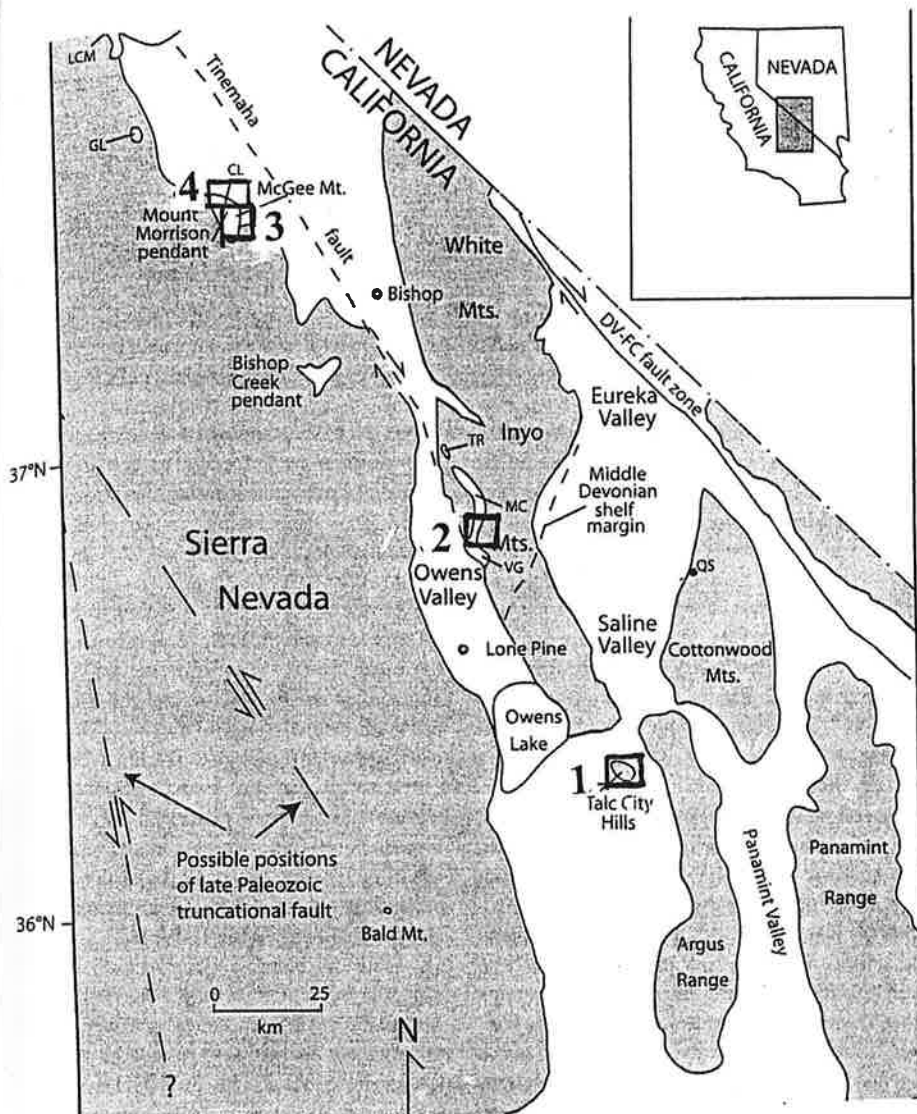
Field Trip Stops for Devonian Mount Morrison fan system

(1) Shelf facies in the Talc City Hills. This facies is represented by the sandy Lippincott Member of the Lost Burro Formation. There is no striking evidence of an unconformity at the base of the lowest sandstone, but as this is the only sandstone unit in this part of the stratigraphic section, it apparently represents a significant geologic event. We suggest that these sandstones are composed of sand reworked during the transgression of the sea that marked the end of deposition of the Mount Morrison fan. The sandstones here are similar to those in the submarine fan facies although they generally lack a calcareous matrix and are thin and unimodal rather than thick and mixed. Conodonts from above and below the Lippincott Member indicate a late Middle Devonian age, essentially coeval with rocks in the submarine fan facies.

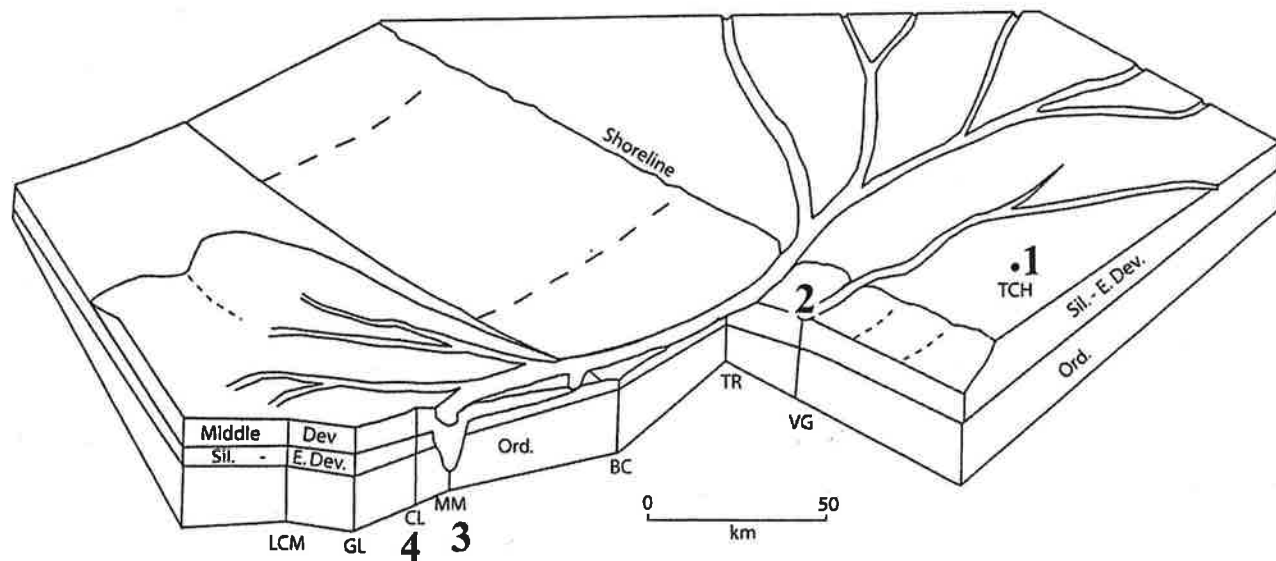
(2) Upper slope channel at Squares Tunnel in Mazourka Canyon. The submarine channel that is well exposed at this locality is cut into the deep-water Vaughn Gulch Limestone of Silurian to early Middle Devonian age and is filled with Late Devonian deep-water dark argillite and radiolarian chert of the Squares Tunnel Formation. Based on regional thickness patterns the depth of the channel is estimated as 125 m.

(3) Main distributary channel at McGee Mountain. Of the ~575-m-thick section exposed here, about two-thirds consists of medium- to coarse-grained, calcareous quartz sandstone containing floating lithoclasts. The remainder of the section is composed of poorly sorted conglomerate with a matrix of coarse-grained, calcareous quartz sand similar to that in the associated sandstone beds. These rocks, assigned to the Mount Morrison Sandstone, fill a channel that has cut out the normally underlying Aspen Meadow Formation and apparently most of the older Convict Lake Formation at its deepest point. Comparison with the thickness of the Mount Morrison Sandstone here with that of the fan facies ~6 km to the northwest at Convict Lake and the amount of missing section below the channel suggests a channel depth on the order of 325 m. The Mount Morrison Sandstone at McGee Mountain is overlain by the Squares Tunnel Formation similar to that in the upper slope channel at Squares Tunnel.

(4) Submarine fan facies at Convict Lake. This facies is represented by rocks assigned to the Mount Morrison Sandstone. Here this formation is composed of massive light- to medium-gray, calcareous quartz sandstone and sandy limestone. Locally clasts of black chert or argillite float in the otherwise mostly massive sandstone. Few sedimentary structures are present. Conodonts show that these rocks are approximately the same age as the Lippincott Member of the Lost



Location map (left) and interpretive diagram (below) of Mount Morrison fan complex, showing field stops 1-4. CL, Convict Lake; GL, Gull Lake pendant; LCM, Log Cabin Mine pendant; MC, Mazourka Canyon; MM, McGee Mountain; QS, Quartz Spring; TCH, Talc City Hills; TR, Tinemaha Reservoir; VG, Vaughn Gulch. Modified from Stevens and Pelley (2006).



Burro Formation in the Talc City Hills. The Mount Morrison Sandstone at Convict Lake is overlain by the Squares Tunnel Formation similar to that elsewhere in the deep-water parts of the fan system.

References

- Kylander-Clark, A.R.C., Coleman, D.S., Glazner, A.F., and Bartley, J.K., 2005, Evidence for 65 km of dextral slip across Owens Valley, California since 83 Ma: *Geological Society of America Bulletin*, v. 117, p. 962-968.
- Stevens, C.H., and Pelley, T., 2006, Development and dismemberment of a Middle Devonian continental-margin submarine fan system in east-central California: *Geological Society of America Bulletin*, v. 118, p. 159-170.
- Stevens, C.H., and Greene, D.C., 1999, Stratigraphy, depositional history, and tectonic evolution of Paleozoic continental-margin rocks in roof pendants of the eastern Sierra Nevada, California: *Geological Society of America Bulletin*, v. 111, p. 919-933.

Structural Setting and Significance of the Talc City Hills

(George Dunne)

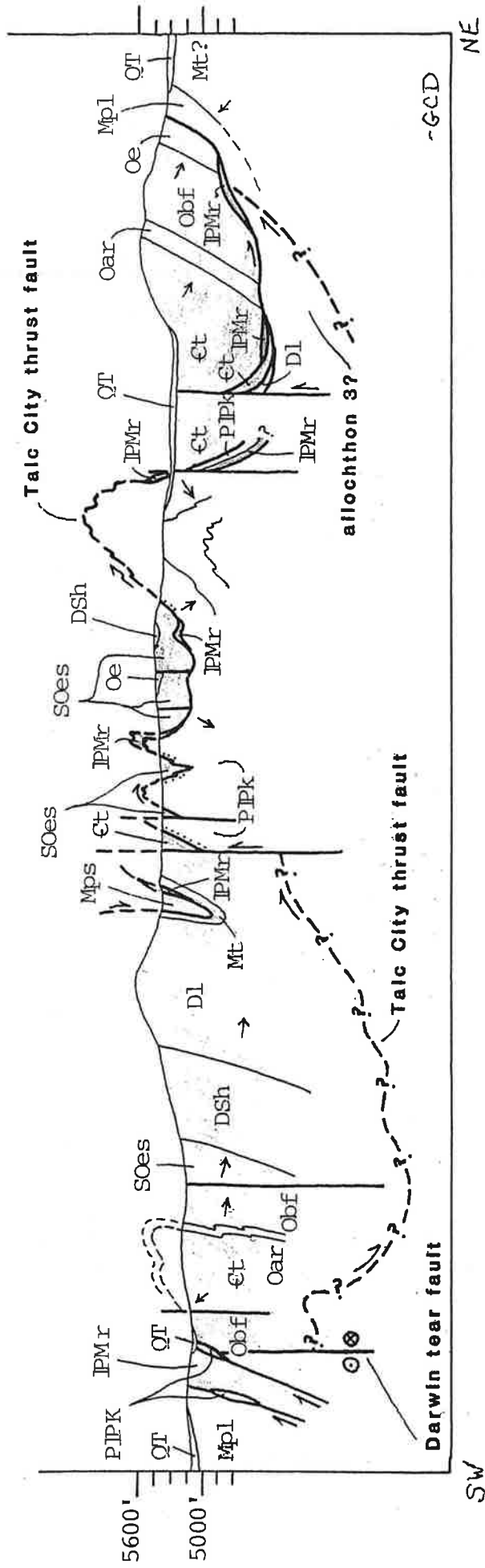
The Talc City Hills and other parts of the Darwin Plateau and adjacent southern Inyo Mountains area were mapped by USGS geologists during and following WWII, at a time when there were still a number of unresolved issues regarding Mississippian and younger Paleozoic stratigraphy. As a result of these issues, some important structural aspects of this region were misinterpreted, and other important structures were simply not recognized. Renewed stratigraphic and structural study of this region beginning in the late 1960's has led to a much improved—yet still evolving—understanding of the geology of this region. The first modern structural study in this region was done in the late 1960's right here in the Talc City Hills by Rachel Gulliver, a Masters Thesis student at UC Santa Barbara. Through detailed mapping here, she was able to document the presence and character of two superposed families of contractional structures. Her work served as a springboard for ongoing studies of these structures over a wide region of eastern California that continue today.

The two suites of structures that Rachel recognized are as follows:

- (1) a relatively older set of imbricate thrust faults and some related folds, at least some and perhaps all of which are of Permian age;
- (2) a relatively younger set of thrust and reverse faults, folds, and locally pervasive cleavage that can be demonstrated to have evolved episodically over a span that may have begun in Triassic time, was most active in Jurassic time, and continued at reduced intensity into the Early Cretaceous.

The older suite of structures was first called the Last Chance thrust system after the most prominent fault within it, and was initially inferred to be of early Mesozoic age. However, its name evolved as additional studies suggested that the suite encompassed many additional structures and cropped out over a broad region in and northwest of Death Valley. Additionally, at least some structures within the system can be demonstrated to be of Permian age. Here in the Talc City Hills, the Talc City thrust fault, thoroughly folded by northwest-trending folds of the younger contractional suite, is a striking representative of this older thrust system.

The relatively younger set of structures came to be called the East Sierran thrust system (ESTS), because it was recognized to trend northwest along the east flank of the Sierran batholith from the Mojave Desert perhaps as far as the Tioga Pass region. Our most detailed knowledge of this system is derived from its exposures between the Garlock fault and the southern Inyo Mountains, where generations of advanced field students and Master's students from CSUN mapped features within the ESTS. A schematic cross section through the Talc City Hills that nicely expresses both suites of structures is presented in the following figure.



Geology of thrust plates in the Talc City Hills and Darwin Hills:

Commentary of Cal Stevens and Paul Stone

A complex group of thrust faults dominates the structure of the Talc City Hills and Darwin Hills. In this area, observed and inferred thrust faults separate four major structural plates, each of which has its own distinctive Paleozoic stratigraphy (see stratigraphic diagram). Especially important for interpretation of the relative displacement are the middle to Upper Mississippian formations which differ significantly from plate to plate.

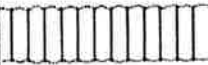






From the structurally lowest to structurally highest, we refer to the plates of this thrust complex as plates 1, 2, 3, and 4. The middle and Upper Mississippian units exposed in these plates represent an increasingly westward (offshore) paleogeographic position with respect to the carbonate shelf edge as indicated by regional stratigraphic studies (Stone et al., 1989; Stevens et al., 1995, 1996).


The parautochthonous structural plate 1 is distinguished by the presence of the Stone Canyon Limestone and Santa Rosa Hills Limestone. The Stone Canyon Limestone, mainly composed of dark-gray cherty limestone, is interpreted as a relatively deep-water carbonate platform deposit, whereas the overlying light-gray, pelmatozoan-rich Santa Rosa Hills Limestone accumulated in a well-agitated, shallow-water platform environment. This sequence therefore represents a prograding carbonate platform of middle to Late Mississippian age. A thin Upper Mississippian unit of quartzite and shale (Indian Springs Formation) overlies the Santa Rosa Hills Limestone.

By contrast, the middle to Upper Mississippian sequence of structural plate 2 consists of the Stone Canyon Limestone and the overlying Rest Spring Shale, a deep-water unit approximately coeval with the Indian Springs Formation. This sequence represents a relatively offshore position beyond the progradational limit of the Santa Rosa Hills Limestone.

Structural plates 3 and 4 are distinguished by the presence of the Upper Mississippian Mexican Spring Formation, composed of quartzose siltstone and minor calcareous turbidites, and the overlying Rest Spring Shale. This sequence represents a basinal environment of deposition. Plate 3 differs structurally from plate 4 in having a completely overturned stratigraphic section.

The four plates of the thrust complex were juxtaposed after the Early Permian and probably before emplacement of a 174-Ma (early Middle Jurassic) pluton that intruded the Ophir

AGE	STRUCTURAL PLATE			
	4	3	2	1
TRIASSIC				Union Wash Formation
PERMIAN				
				Owens Valley Group
PENNSYLVANIAN		Keeler Canyon Formation	Keeler Canyon Formation	
				Keeler Canyon Fm?
				Tihvipah Limestone
MISSISSIPPIAN	Rest Spring Shale	Rest Spring Shale	Rest Spring Shale	Indian Springs Formation
			Stone Canyon Limestone	Santa Rosa Hills Limestone
	Mexican Spring Fm	Mexican Spring Fm		Stone Canyon Limestone
		Stone Canyon Ls(?) and Tin Mountain Ls, undivided	Tin Mountain Limestone	Stone Canyon Limestone
DEVONIAN	Tin Mountain Limestone		Lost Burro Formation	
	Lost Burro Formation	Lost Burro Formation		
SILURIAN	Hidden Valley Dolomite		Hidden Valley Dolomite	
	Ely Springs Dolomite			
ORDOVICIAN	Eureka Quartzite			
	Badger Flat Limestone			
	Al Rose Formation			
CAMBRIAN	Tamarack Canyon Dolomite			

 Stratigraphic hiatus


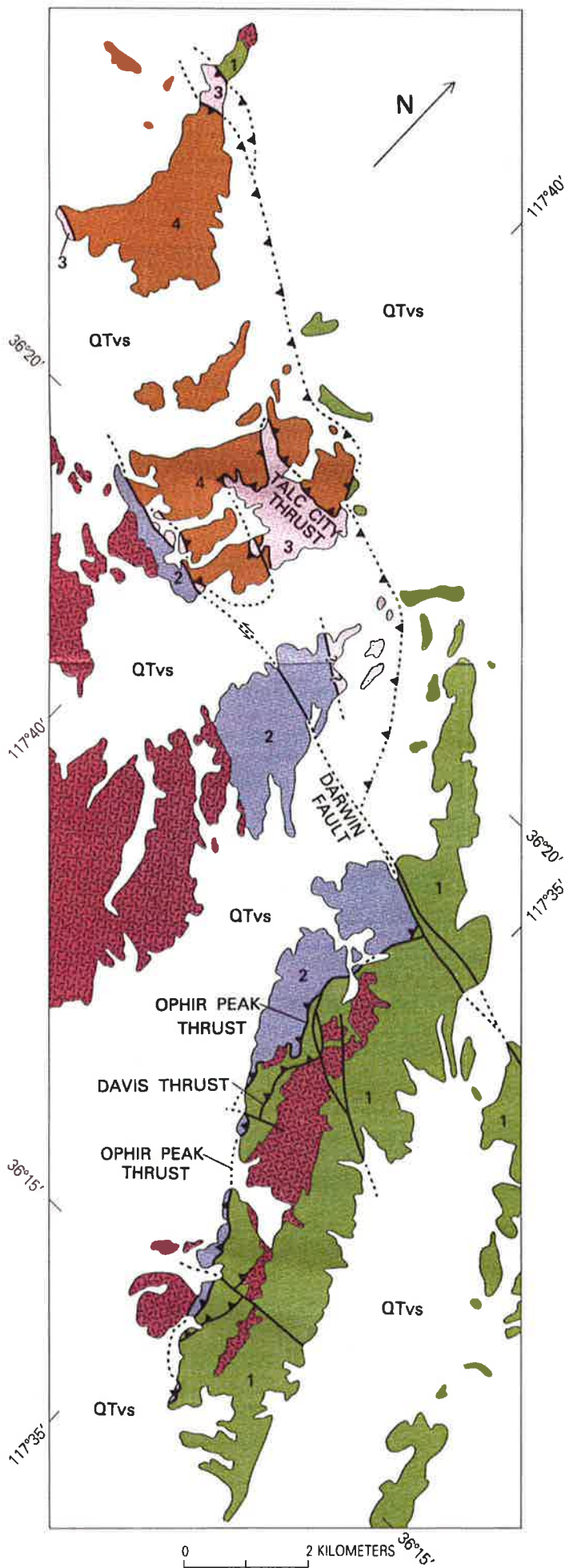
 Rocks absent due to faulting

Chart showing stratigraphic units present in each of four major structural plates in Darwin Hills and Talc City Hills (modified from Stone et al., 1989). Mississippian units from plates 1 to 4 indicate an increasingly westward paleogeographic position with respect to the paleoshelf at the time of deposition.

Peak thrust in the Darwin Hills (Stone et al., 1989). Stevens and Stone (2005) recently suggested that this thrust complex is part of the regionally extensive, Late Permian Sierra Nevada-Death Valley thrust system that includes the Inyo Crest thrust of Swanson (1996) exposed ~15 km northwest of the Talc City Hills.

References:

- Stevens, C.H., and Stone, P., 2005, Structure and regional significance of the Late Permian(?) Sierra Nevada-Death Valley thrust system, east-central California, *in* Calzia, J.P., ed.: Earth Science Reviews, v. 73, issues 1-4, Fifty Years of Death Valley Research, A volume in honor of Lauren A. Wright and Bennie Troxel, p 103-113.
- Stevens, C.H., Klingman, D., and Belasky, P., 1995, Development of the Mississippian carbonate platform in southern Nevada and eastern California on the eastern margin of the Antler Foreland Basin, *in* Dorobek, S.L., and Ross, G.M., eds.: Stratigraphic evolution of foreland basins: SEPM (Society for Sedimentary Geology) Special Publication 52, p. 175-186.
- Stevens, C.H., Klingman, D., Sandberg, C.H., Stone, P., Belasky, P., Poole, F.G., and Snow, J.K., 1996, Mississippian stratigraphic framework of east-central California and southern Nevada with revision of Upper Devonian and Mississippian stratigraphic units in Inyo County, California: U S Geological Survey Bulletin 1988-J, p. J1-J39.
- Stone, P., Dunne, G.C., Stevens, C.H., and Gulliver, R.M., 1989, Geologic map of Paleozoic and Mesozoic rocks in parts of the Darwin and adjacent quadrangles, Inyo County, California: U S Geological Miscellaneous Investigation Series, scale 1:31,250.
- Swanson, B.J., 1996, Structural geology and deformational history of the southern Inyo Mountains east of Keeler, Inyo County, California [MS thesis]: California State University, Northridge, 125 p.



EXPLANATION

- QTvs Volcanic and sedimentary rocks (Quaternary and Tertiary)
- Granitoid rocks (Jurassic)
- 4 Sedimentary rocks of structural plate 4 (Mississippian to Cambrian)
- 3 Sedimentary rocks of structural plate 3 (Permian to Devonian)
- 2 Sedimentary rocks of structural plate 2 (Permian to Silurian)
- 1 Sedimentary rocks of structural plate 1 (Triassic to Mississippian)
- Contact
- ⇌ Fault—Showing relative horizontal movement; dotted where concealed, queried where inferred
- ▲ Thrust fault—Sawteeth on upper plate; dotted where concealed

Simplified tectonic map of Darwin Hills and Talc City Hills showing faults bounding four major structural units (reproduced from Stone et al., 1989).

Geologic history of the southern Inyo Mountains

Brian Swanson and Paul Stone

Paleozoic and younger rocks exposed in the southern Inyo Mountains record a complex history of deposition, intrusion, uplift, and deformation. The following summary is based on a number of published reports and the M.S. thesis of Swanson (1996), who mapped the southernmost part of the Inyo Mountains in detail and reconstructed the Permian and later deformational history.

In early Paleozoic time the southern Inyo Mountains area was part of the western continental shelf of North America. Cambrian to Lower Mississippian carbonate and subordinate quartzose rocks exposed in the area are composed of shallow-water marine sediments that accumulated on the southwest-trending shelf (Stevens, 1986). By contrast, the overlying Upper Mississippian Mexican Spring Formation and Rest Spring Shale represent deposition in a deep-water marine basin originally formed by downwarping related to the latest Devonian to Mississippian Antler orogeny. The margin of this basin lay just southeast of the southern Inyo Mountains, where Upper Mississippian carbonate shelf strata are exposed.

In Pennsylvanian to earliest Permian time, limestone turbidites of the Keeler Canyon Formation were deposited above the Rest Spring Shale, indicating a continuation of basinal conditions in the southern Inyo Mountains (Stevens et al., 2001). These turbidites are interpreted to have been derived from a broad carbonate shelf to the east, where the coeval Bird Spring Formation accumulated (Stevens and Stone, 2007). Pennsylvanian to earliest Permian turbidite sedimentation along the western margin of the Bird Spring Shelf, above Upper Mississippian shelf strata, reflects subsidence interpreted to have been related to left-lateral truncation of the continental margin farther west (Stevens et al., 2005).

In middle Early Permian time, thrust faulting and folding occurred at the current location of the southern Inyo Mountains. This deformation, which Stevens and Stone (2005a) interpreted as related to emplacement of the Last Chance allochthon, formed a northeast-trending uplift that separated two lithologically distinct deep-water marine basins. The very fine grained Lone Pine Formation was deposited northwest of the ridge, and the coarser-grained, informally named sedimentary rocks of Santa Rosa Flat were deposited to the southeast (Stone et al., 1989). This depositional regime persisted into latest Early or Middle Permian time.

A second episode of thrust faulting and folding took place in the Late Permian. This event is represented primarily by the east-vergent Inyo Crest thrust and Upland Valley footwall syncline, which deform the Keeler Canyon Formation and the sedimentary rocks of Santa Rosa Flat. Uplift and erosion of at least 610 m of the Keeler Canyon Formation resulted from this event, as indicated by an unconformity with up to 90 degrees of angular discordance between the folded Pennsylvanian to Early Permian rocks and the overlapping Late Permian to Early Triassic Conglomerate Mesa Formation (Swanson, 1996). Stevens and Stone (2005b) have proposed that the Inyo Crest thrust was part of a regional Late Permian thrust belt that extended from the eastern Sierra Nevada to the Death Valley area.

During Early to Middle Triassic time, the Union Wash Formation was deposited above the Conglomerate Mesa Formation in a deep- to shallow-water marine environment (Stone et al., 1991). This fine-grained formation, which accumulated during a period of relative tectonic quiescence, represents the youngest marine deposition in the region.

Development of the Sierran magmatic arc began west of the Inyo Mountains in Late Triassic to Early Jurassic time. Continued uplift, erosion and volcanic activity associated with the Sierran arc led to deposition of volcanic flows, ash deposits and associated volcanoclastic sediments of the Inyo Mountains Volcanic Complex (Dunne et al., 1998) primarily during the Middle to Late Jurassic.

Compression on the east margin of the Sierran arc and heating associated with emplacement of granitic plutons led to the development of northwest-trending folds and thrust faults in the weakened rocks of the southern Inyo Mountains and adjacent areas. These Mesozoic structural features are part of the East Sierran Thrust System (Dunne and Walker, 2004). The dominant fault of this system, east of the town of Keeler is the Flagstaff thrust, which placed the Lower Permian Lone Pine Formation over the Triassic Union Wash Formation and the Jurassic volcanic complex. The minimum amount of slip on this fault east of Keeler is estimated to be approximately 3900 m (Swanson, 1996). The folds and thrust faults are overprinted by a set of conjugate strike-slip faults that indicate later, minor, northeast-directed compression.

In late Miocene to Pleistocene time, basalt flows and alluvial fans were deposited as uplift of the present Inyo Mountains commenced. Northwest-trending normal faults and right-lateral oblique faults developed in response to Basin and Range extension, producing the Inyo Mountains horst and Owens Valley graben observed today.

References Cited

- Dunne, G.C., and Walker, J.D., 2004, Structure and evolution of the East Sierran thrust system, east central California: *Tectonics*, v. 23, TC4012, doi:10.1029/2002TC001478, 23 p.
- Dunne, G.C., Garvey, T.P., Osborne, M., Scheiderei, D., Fritsche, A.E., and Walker, J.D., 1998, Geology of the Inyo Mountains Volcanic Complex: implications for Jurassic paleogeography of the Sierran magmatic arc in eastern California: *Geological Society of America Bulletin*, v. 110, p. 1376-1397.
- Stevens, C.H., 1986, Evolution of the Ordovician through Middle Pennsylvanian carbonate shelf in east-central California: *Geological Society of America Bulletin*, v. 97, p. 11-25.
- Stevens, C.H., and Stone, P., 2005a, Interpretation of the Last Chance thrust, Death Valley region, California, as an Early Permian décollement in a previously undeformed shale basin: *Earth-Science Reviews*, v. 73, p. 79-101.
- Stevens, C.H., and Stone, P., 2005b, Structure and regional significance of the Late Permian(?) Sierra Nevada-Death Valley thrust system, east-central California: *Earth-Science Reviews*, v. 73, p. 103-113.
- Stevens, C.H., and Stone, P., 2007, The Pennsylvanian-Early Permian Bird Spring carbonate shelf, southeastern California: fusulinid biostratigraphy, paleogeographic evolution, and tectonic implications: *Geological Society of America Special Paper* 429, 82 p.
- Stevens, C.H., Stone, P., and Miller, J.S., 2005, A new reconstruction of the Paleozoic continental margin of southwestern North America: implications for the nature and timing of continental truncation and the possible role of the Mojave-Sonora megashear, *in* Anderson, T.H., Nourse, J.A., McKee, J.W., and Steiner, M.B., eds., *The Mojave-Sonora megashear*

hypothesis: development, assessment, and alternatives: Geological Society of America
Special Paper 393, p. 597-618.

Stevens, C.H., Stone, P., and Ritter, S.M., 2001, Conodont and fusulinid biostratigraphy and
history of the Pennsylvanian to Lower Permian Keeler Basin, east-central California:
Brigham Young University Geology Studies, v. 46, p. 99-142.

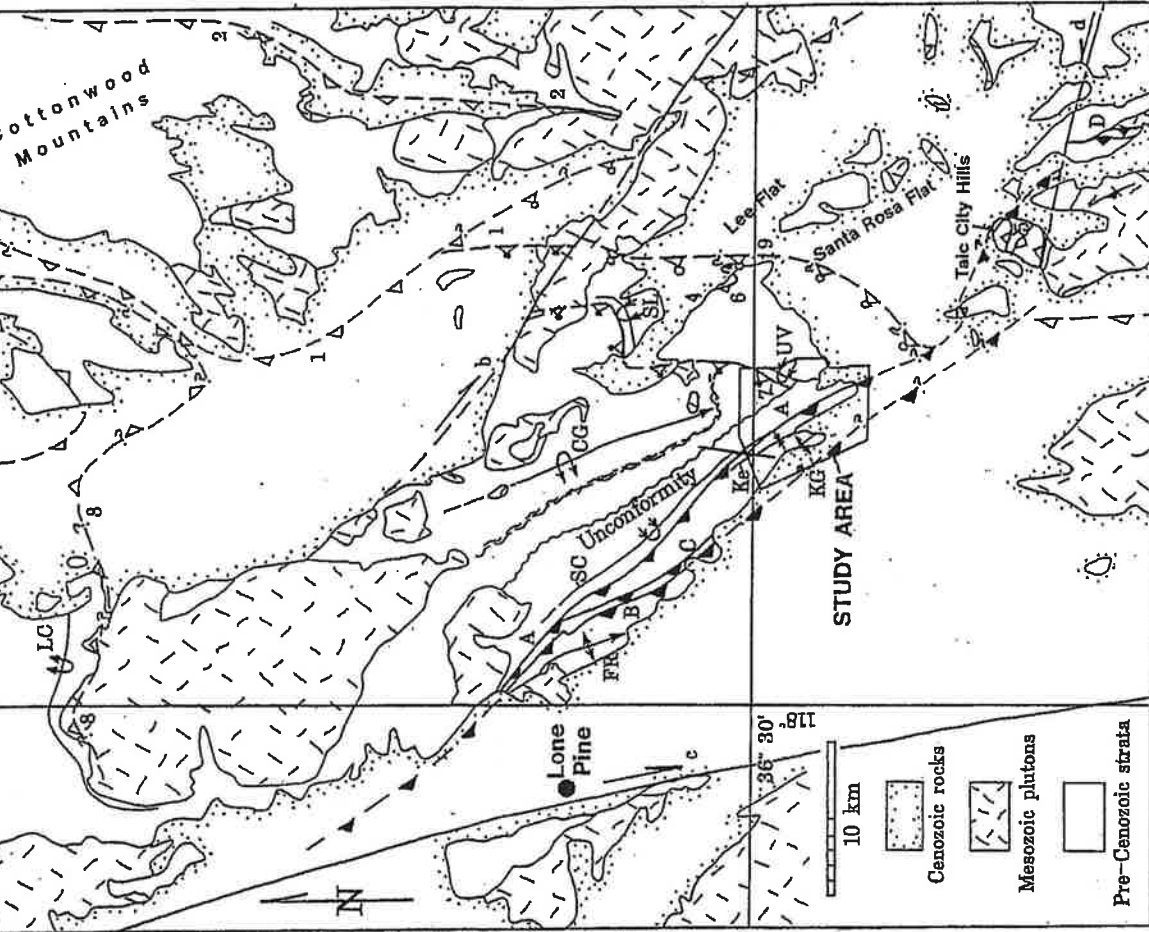
Stone, P., Dunne, G.C., Stevens, C.H., and Gulliver, R.M., 1989, Geologic map of Paleozoic and
Mesozoic rocks in parts of the Darwin and adjacent quadrangles, Inyo County, California:
U.S. Geological Survey Miscellaneous Investigations Series Map I-1932, scale 1:31,250.

Stone, P., Stevens, C.H., and Orchard, M.J., 1991, Stratigraphy of the Lower and Middle (?)
Triassic Union Wash Formation, east-central California: U.S. Geological Survey Bulletin
1928, 26.

Swanson, B.J., 1996, Structural geology and deformational history of the southern Inyo
Mountains east of Keeler, Inyo County, California: Northridge, California State University,
M.S. thesis, 125 p.

EXPLANATION

FAULTS - Dashed where concealed of inferred



Faults of the Death Valley thrust belt; based on Snow (1992)

- 1, Least Chance thrust; 2, Raceback thrust; 3, Marble Canyon thrust; 4, Lemoigne thrust; 5, Tale City thrust; 6, Fishhook thrust; 7, Inyo Crest thrust; 8, Eureka thrust; 9, Lee Flat thrust

Trace of Inferred Lee Flat thrust and southern trace of Least Chance thrust proposed by Snow (1992)

Trace of Inyo Crest thrust and revised southern trace of Least Chance thrust; based on this study and mapping by Stone (1996, written commun.)

Sheared belt of Rest Spring Shale

Faults of the East Sierran thrust system; based on Dunne et al. (1978) and Dunne (1986)

- A, Flagstaff thrust; B, Dolomite Canyon thrust; C, Swansea thrust; D, Davis thrust; E, Argus-Staring thrust; F, Ophir thrust; G, Sand Canyon thrust; H, Layton Well thrust

Major strike-slip faults

- a, Death Valley-Furnace Creek fault zone; b, Hunter Mountain fault; c, Owens Valley fault; d, Darwin tear fault; e, Garlock fault

FOLDS

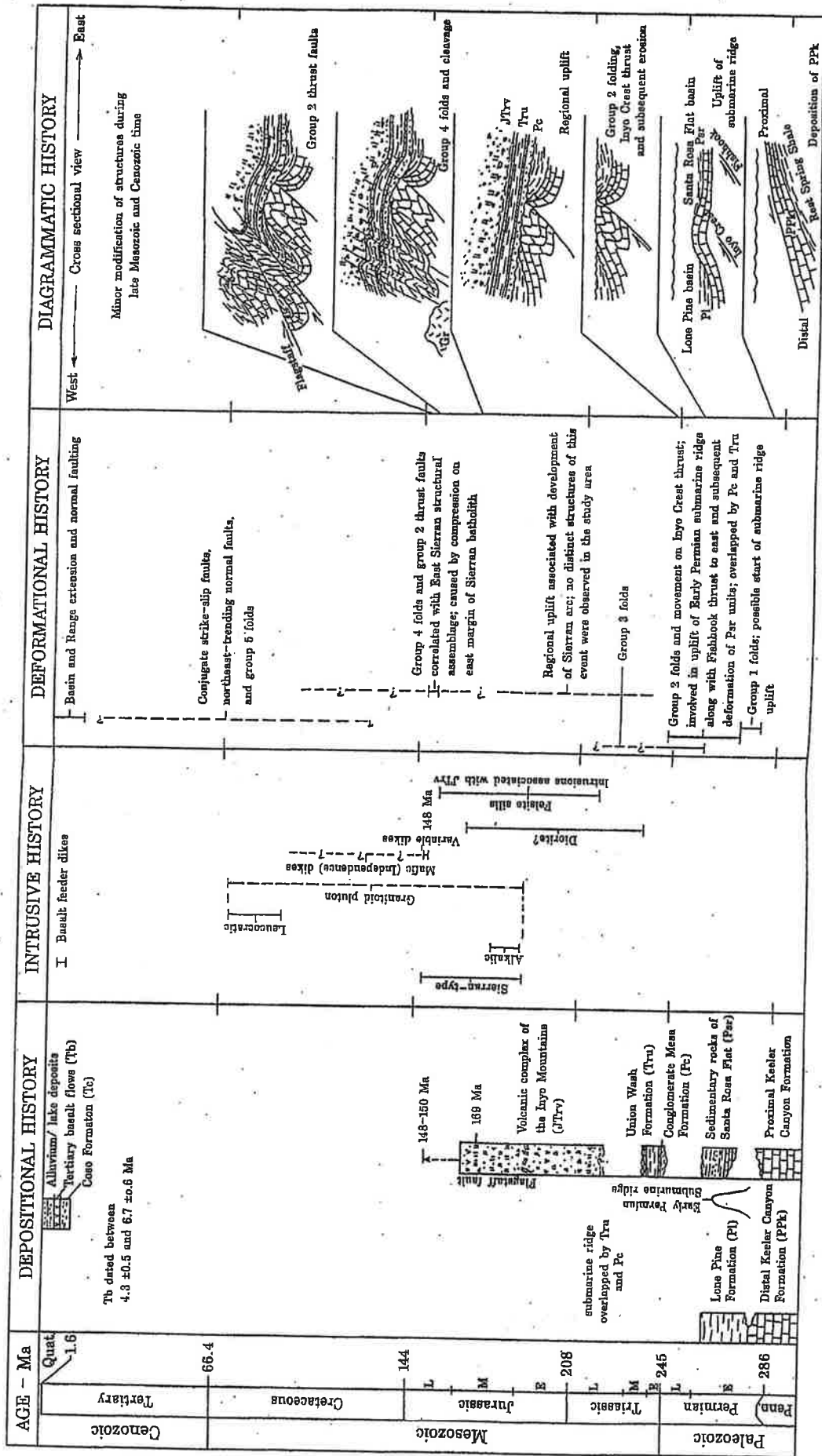
Anticline - Upright and overturned

- LC, Lead Canyon anticline; CG, Cerro Gordo anticline; FR, Front Ridge anticline; KG, Keeler Gold anticline; WT, White Top backfold

Syncline - Upright and overturned

- SL, San Lucas Canyon syncline; UV, Upland Valley syncline; SC, Slate Canyon syncline; Ke, Keeler syncline

Regional structural index map of east-central California and western Nevada. Modified from Dunne, et al. (1978), Stone (1984), Dunne (1986), Snow, et al. (1991), Stone, et al. (1989), Snow (1992) and from mapping during this study.

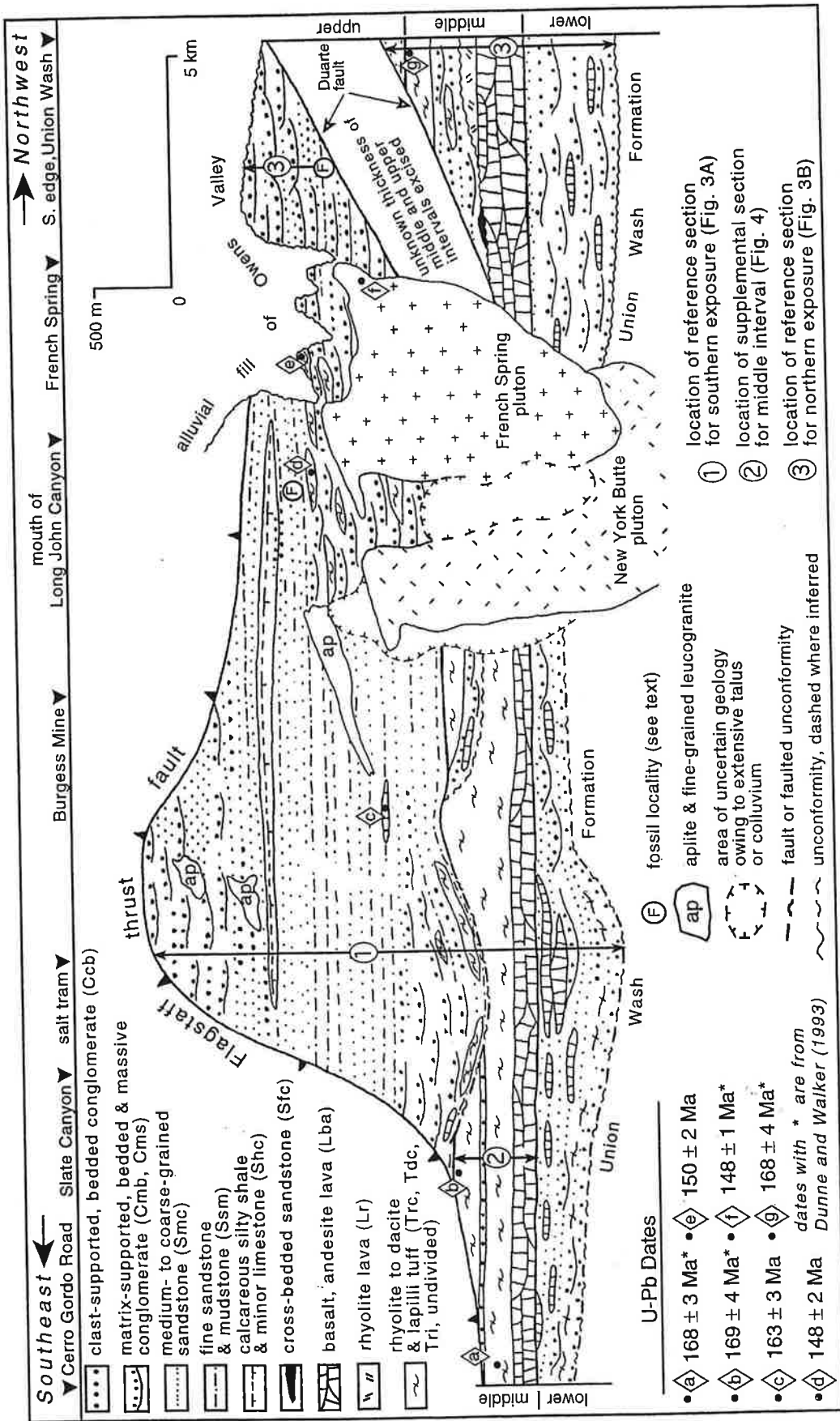


Summary diagram illustrating the inferred geologic history of the study area since the Pennsylvanian Period.

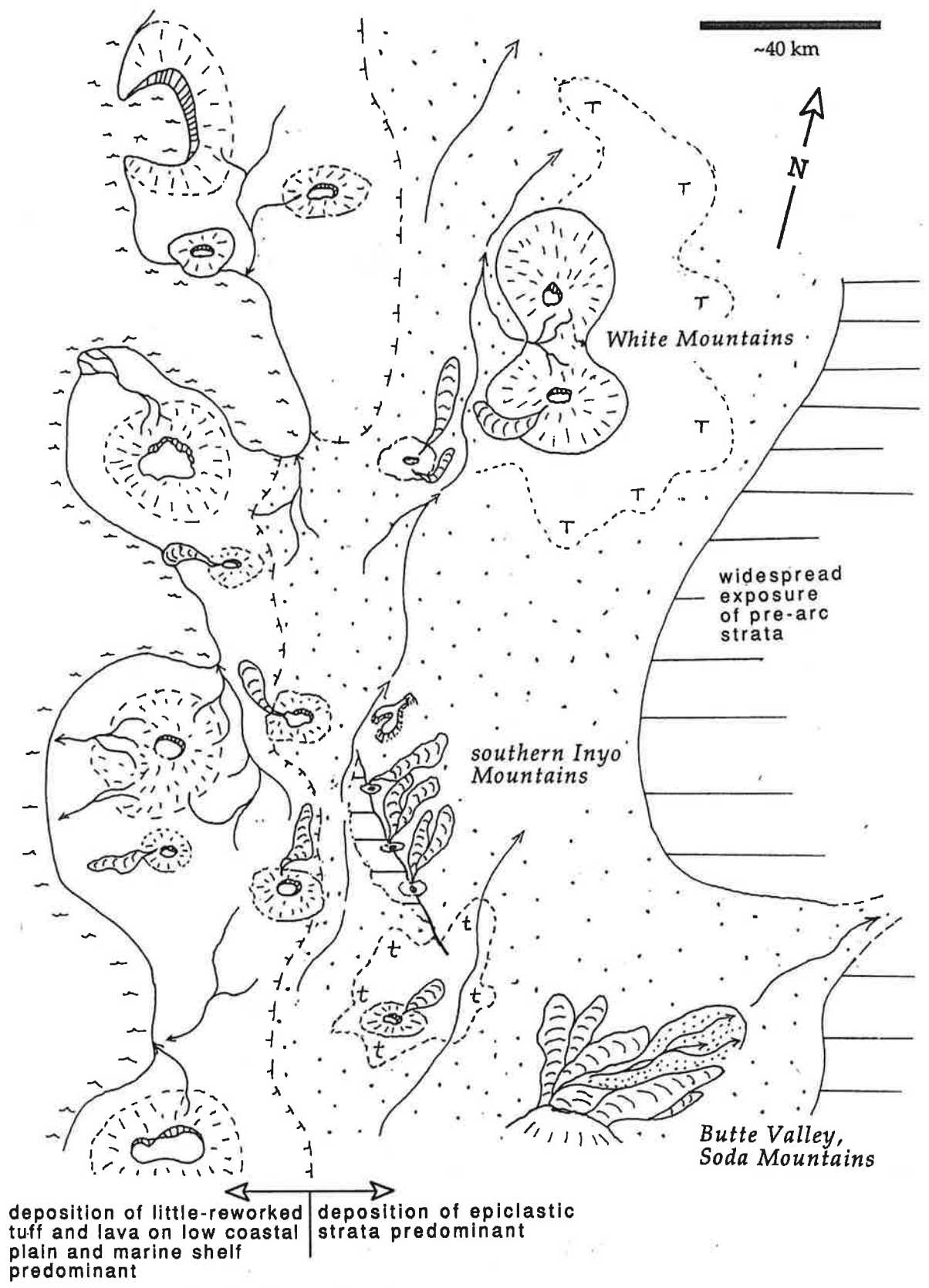
Inyo Mountains Volcanic Complex, Southern Inyo Mountains

George Dunne

In order to successfully map out the East Sierran thrust system (ESTS) in the southern Inyo Mountains, I necessarily had to gain an understanding of the stratigraphy of the prominent but little-studied Mesozoic volcanic and volcanoclastic sequence that crops out along the west flank of the range here. I was fortunate to capture the interest of a number of Masters and Senior Thesis students from CSUN in this sequence of rocks. Over time, aided by hoards of CSUN advanced field mapping students and by U-Pb dating work by Doug Walker at Kansas, we were able to develop a nice story regarding these rocks, which represent the eastern, subaerial fringe of the volcanic cover of the Sierran igneous arc. We named these rocks the Inyo Mountains Volcanic Complex. Our study of these rocks provides a knowledge bridge between well known Mesozoic arc sections lying farther to the west, in the core of the arc, and coeval sedimentary sections—locally containing arc-derived intercalations of airfall tuff and fine volcanoclastic debris—that lie east of the arc in the western interior of the U.S. The first of the following two figures presents a schematic, vertically exaggerated cross section of the Complex. The second figure presents a paleogeographic map representing aspects of how the region might of looked in Jurassic time.



Schematic stratigraphic cross section of the Inyo Mountains Volcanic Complex. fossil localities (F), which contain identical fossil assemblages, into approximate alignment. That part of the complex extending ~3 km south of Cerro Gordo Road (see Fig. 2) is not shown owing to complex faulting and abundant hypabyssal intrusions in that area. The datum for the section is the base of the middle interval. See Figure 2 for locations noted thickness of strata excised by the Duarte fault was arbitrarily selected so as to bring the two across the top of the section.



Schematic mid-Jurassic paleogeography of the east flank of the Sierran volcanic arc in eastern California.

Owens Lake dust mitigation, and restoration of the lower Owens River.

Dust mitigation on Owens Dry Lake.

Pluvial Owens Lake expanded and shrank through glacial and interglacial periods of the last Ice Age. It reached its last maximum extent and depth between 2000 and 3000 years ago when it covered about 240 square miles and had a maximum depth greater than 250 feet. It was maintained primarily by inflow from the Owens River to the north.

By the late 1800's it had diminished to about 100 square miles and had typical depths between 30 and 50 feet. Los Angeles completed its Owens Valley aqueduct in 1913, and began diverting almost all of the flow of the Owens River into it. As a result, the river quickly shrank to a seasonal stream. As a further result, within 15 years Owens Lake was dry except for a seasonal shallow brine pond covering its west-central portion.

As the lake bed was exposed and dried out, huge dust storms arose during windy periods. During storms, the dust plumes could be seen from space, and the worst ones represented the lift-off of an estimated 70 tons of dust per second. Of the 25 highest airborne dust readings ever recorded in the United States, 23 were from Owens Dry Lake.

Passage of amendments to the Federal Clean Air Act in 1990 provided legal tools to force the Los Angeles Department of Water and Power to agree to mitigate the dust storms, with major reductions required by 2006 and involving the largest dust sources that cover about 30 square miles. LADWP implemented a dust-reduction plan utilizing (1) shallow water flooding of some areas, with water diverted from the aqueduct (the most widely used method); (2) planting of salt-tolerant grasses and bushes in others; and (3) spreading of a gravel veneer in still other areas.

To date LADWP has spent about \$500 million dollars on the project, with ongoing costs of about \$40 million per year. As a result of these efforts, major dust storms have been reduced by about 50%. Because they failed to attain their 2006 dust reduction targets, LADWP is required to expand its dust mitigation measures to an additional ~13 square miles by 2010.

One positive side effect of the rewetting of Owens Lake is that tens of thousands of birds, including 26 species of waterfowl, 16 species of birds of prey, 33 species of shorebirds, and five species of owls, have returned to feast on the freshwater shrimp and brine flies.

Lower Owens River Revitalization, 2007 and forward

During the interval 1970-1990, Los Angeles DWP engaged in an aggressive program of ground water removal via well pumping in the central and southern Owens Valley. As a result, springs dried up, as did marshy areas with shallow water table, leading to progressive desertification of significant parts of the Valley floor. After 20 years of court battles over excessive groundwater pumping, LADWP in 1997 agreed to reduce ground water withdrawal rates and to restore water flow in a 62-mile-long stretch of the Lower Owens River, using water diverted from the aqueduct. After an additional 10 years of foot dragging, water finally

began flowing in the lower river in 2007, bringing it slowly back to life. Near the river's delta at the north end of Owens Dry Lake, the river water is recaptured; most is now used for additional dust control on Owens Lake, with the remainder piped back to the aqueduct and on to Los Angeles.

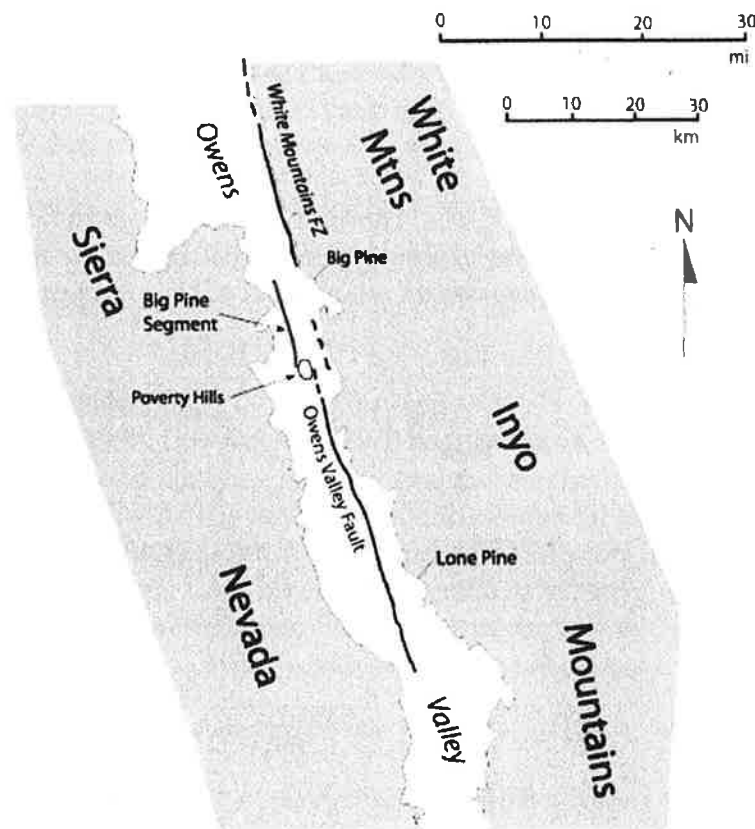
After one year, mud hens dive for food and blue herons patrol the banks. Bass, carp and catfish occupy deeper pools. Some local residents swear they have even seen river otters. So much reedy tule has sprouted along the banks that officials have called in a huge floating weed whacker to cut through it and help keep the water flowing. In most areas the river now is 2 to 3 feet deep and 15 to 20 feet across. The river is beginning its rebirth.

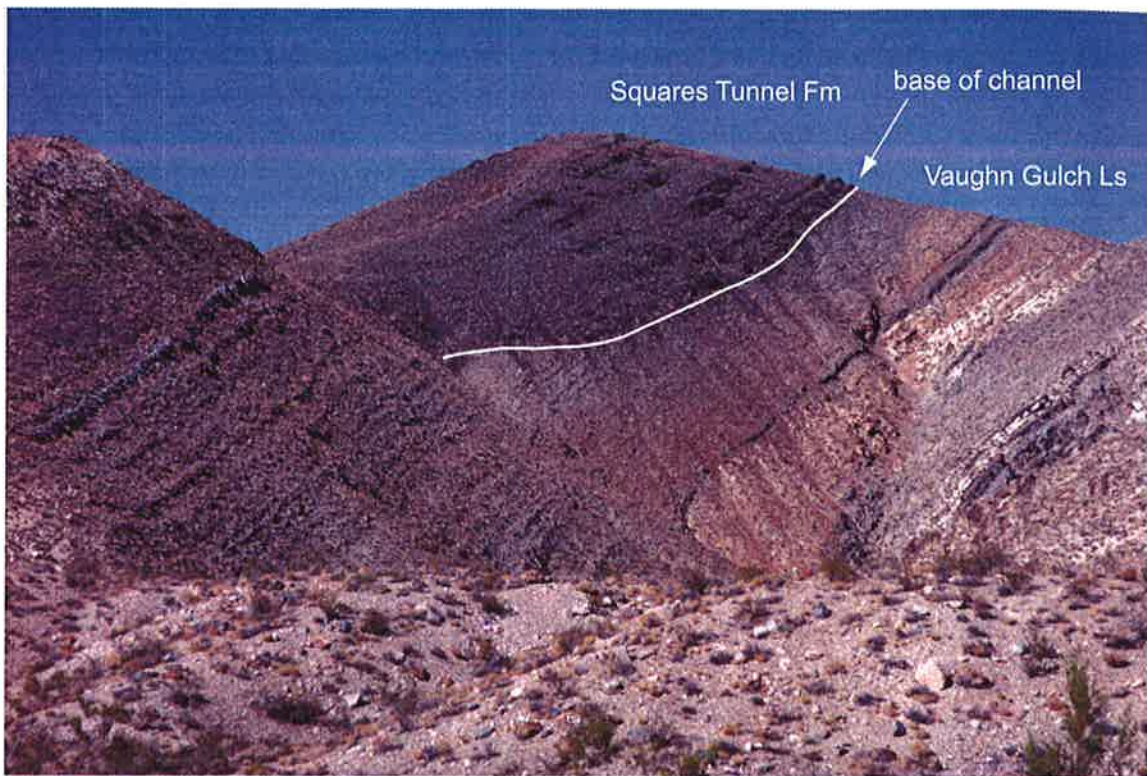
Poverty Hills and Owens Valley Fault Stops

Kim M. Bishop

The Poverty Hills are a 5 square km outcrop of Paleozoic metasedimentary and Mesozoic intrusive rock exposed along the Owens Valley fault in the axial part of Owens Valley (Fig. 1). Two models have been proposed to explain the origin of the hills. The prevailing model for the past couple decades suggests the hills are a tectonic uplift created by horizontal shortening at a left step in the right-lateral Owens Valley fault zone (Taylor and Dilek, 2001; Taylor, 2002). A recently advocated second model suggests the hills are a landslide mass derived from the adjacent mountains (Bishop, 1999; Bishop and Clements, 2006), although this model was actually first suggested in the 1960's by Pakiser et al. (1964) based on a gravity survey of the valley. If the hills are indeed a landslide, the long-runout distance classifies it as a rock avalanche. Correct interpretation of the origin of the hills is important because it has implications for understanding the kinematics of the Owens Valley fault.

Stop 1: Poverty Hills: It is mainly the presence of widespread brecciation across the hills that led Bishop and Clements (2006) to suggest the hills are a landslide deposit. The first stop will be to view roadcuts along Tinemaha Road at the northwest side of the Poverty Hills, where the best breccia exposures are present. Rock in the roadcuts to be viewed consists of Paleozoic metasedimentary Keeler Canyon Formation. We will walk a few hundred meters along Tinemaha Road. WATCH FOR CARS! Of particular interest in the roadcuts is the exposure of a brecciated light-colored stratigraphic unit within dark colored units near where we will park. The color contrast of the light unit with the darker unit allows one to clearly delineate the results of cataclastic flow deformation of the breccia. The light colored unit thickens and thins across the outcrop and has a contorted shape (Fig 2). It is proposed that the heterogeneous stress field required to create this





Channel cut into deep-water Silurian-lower Middle Devonian Vaughn Gulch Limestone and filled by deep-water radiolarian chert of the Upper Devonian Squares Tunnel Formation.

pattern is the result of fluctuating internal stresses created by vibration and/or variable traction as the landslide mass moved rapidly across an irregular surface. The deformed geometry of the light-colored unit is quite reminiscent to the geometry of deformed stratigraphic units present in the Blackhawk landslide, a well-known rock avalanche deposit in the southern Mojave Desert (Fig. 2).

Advocates of the transpressional uplift model for the Poverty Hills suggest the roadcuts expose fault breccia (Taylor, 2002). In this hypothesis, a thrust fault accommodating uplift is present just below the road level. A counterargument to this idea is that the stress field from tectonic faulting could be expected to be relatively homogenous across the width of the outcrop. Thusly faulting would not be expected to cause the contorted shape the light colored unit.

If the hills are a landslide mass, then the landsliding likely occurred several hundred thousand years ago based on the degree of erosional dissection in the Poverty Hills. The source of the landslide is probably the Inyo Mountains where bedrock units of the same age and lithologies are exposed in the Santa Rita Flat pluton area.

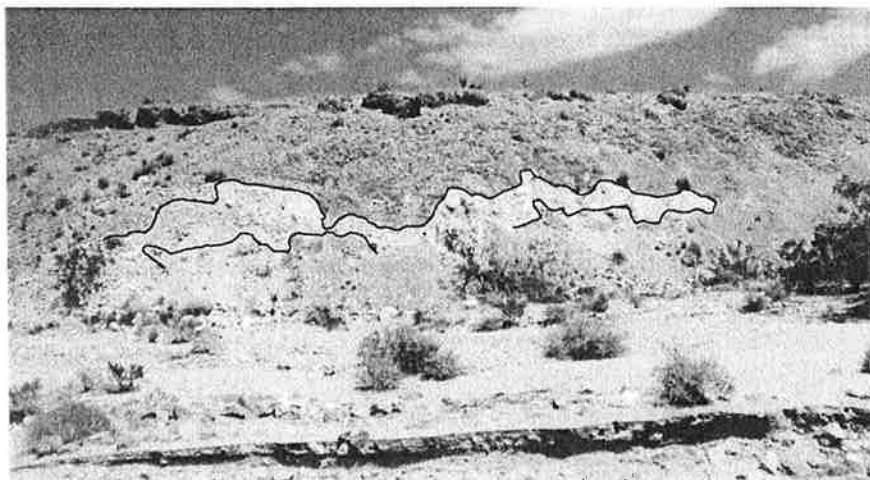
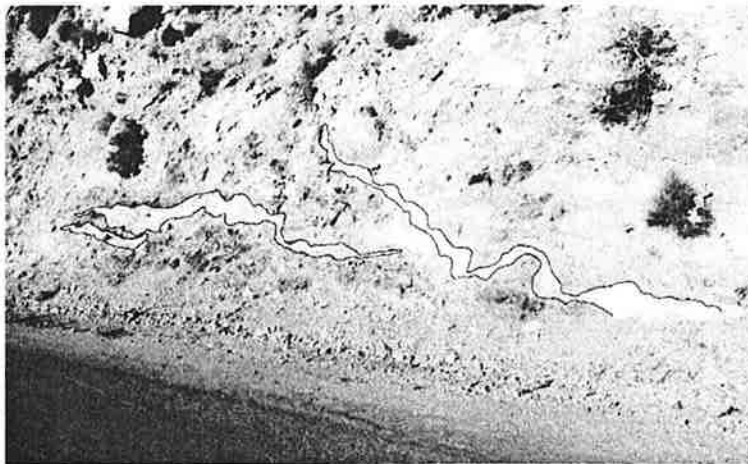


Figure 2. Layers contorted by cataclastic flow of breccia. Top photo from Poverty Hills along Tinemaha Road and bottom photo from Blackhawk rock avalanche in the Mojave Desert. Distorted layers have been outlined.

Stop 2: Owens Valley Fault: As it has been previously mapped, the Owens Valley fault zone contains a 3 km left step between segments southwest and northeast of the Poverty Hills (Fig. 1). According to the transpressional model for development of the hills, right-lateral displacement on both the Central segment fault south of the hills and the Big Pine segment fault north of the hills has created a zone of horizontal compression and uplift between the two segments. Clearly, for the transpressional model to be correct, right-lateral displacement on both fault segments is required. Although evidence has been proposed by Beanland and Clark (1994) for dextral slip on the Big Pine segment, the evidence is weak and there is, in fact, contrary evidence indicating dip-slip only. From this, I question the premise that the Big Pine fault should even be considered a part of the Owens Valley fault.

Probably the most important reason that the Big Pine segment historically has been considered as part of the Owens Valley fault zone is the often stated notion that the segment ruptured in 1872 during the great Owens Valley earthquake (eg. Jennings, 1994; Beanland and Clark, 1994; Slemmons et al., 2008). In opposition, there appears to be solid evidence that the segment did not rupture in 1872. At the Big Pine transfer station stop, we will observe and discuss evidence that argues against both the notion of a right lateral component of slip along the Big Pine segment fault and that the fault ruptured in 1872.

At the stop we will view the following: 1) a stream channel incised in both the hanging wall and the footwall of a strand of the Owen Valley fault and not horizontally offset, 2) the lateral edge of a debris flow that crosses the fault without horizontal offset, 3) the presence of desert varnish on basalt exposed in the fault scarp that argues against 1872 offset, and 4) fault scarp morphology in alluvial fan material that suggests the most recent displacement occurred more than a thousand years ago.

Regarding the last item, some background information is useful. We will observe that the fault scarp has, at its maximum, an angle-of-repose gradient where it cuts alluvial fan deposits. The gradients on the Big Pine segment indicate the scarp is significantly more degraded than the scarp at Lone Pine (Fig. 3), where the fault is well-documented to have ruptured in 1872. This contrast in degradation where the fault scarps are developed in similar coarse alluvial fan materials casts strong doubt that the Big Pine segment ruptured in 1872.

Additional evidence comes from Wallace (1977), who studied fault scarp degradation in the Great Basin and describes three stages. In the first stage of degradation, the fault scarp maintains a scarp free face in which in-situ material is exposed in the fault scarp. The free face will have a gradient of 45 degrees or more and will slowly retreat from its initial location as it also decreases in height. Wallace (1977) concluded that fault scarp free faces persist on the order of 2000 years in the Great Basin. Assuming his model applies to this area, which is not unreasonable, the lack of a free face along the entire Big Pine fault segment where the fault scarp is developed in alluvial fan materials suggests that the last rupture was conservatively more than a thousand years ago.

Discussion

An interesting question is why have so many geologists accepted that the Big Pine segment ruptured in 1872 given that the geomorphic and desert varnish evidence suggests otherwise? The answer is probably that they have uncritically relied on reports made shortly after the earthquake. The most prominent report was made by J.D. Whitney (Whitney, 1872) after he traveled the length of the valley four months following the earthquake.

Stop 2: Owens Valley Fault: As it has been previously mapped, the Owens Valley fault zone contains a 3 km left step between segments southwest and northeast of the Poverty Hills (Fig. 1). According to the transpressional model for development of the hills, right-lateral displacement on both the Central segment fault south of the hills and the Big Pine segment fault north of the hills has created a zone of horizontal compression and uplift between the two segments. Clearly, for the transpressional model to be correct, right-lateral displacement on both fault segments is required. Although evidence has been proposed by Beanland and Clark (1994) for dextral slip on the Big Pine segment, the evidence is weak and there is, in fact, contrary evidence indicating dip-slip only. From this, I question the premise that the Big Pine fault should even be considered a part of the Owens Valley fault.

Probably the most important reason that the Big Pine segment historically has been considered as part of the Owens Valley fault zone is the often stated notion that the segment ruptured in 1872 during the great Owens Valley earthquake (eg. Jennings, 1994; Beanland and Clark, 1994; Slemmons et al., 2008). In opposition, there appears to be solid evidence that the segment did not rupture in 1872. At the Big Pine transfer station stop, we will observe and discuss evidence that argues against both the notion of a right lateral component of slip along the Big Pine segment fault and that the fault ruptured in 1872.

At the stop we will view the following: 1) a stream channel incised in both the hanging wall and the footwall of a strand of the Owen Valley fault and not horizontally offset, 2) the lateral edge of a debris flow that crosses the fault without horizontal offset, 3) the presence of desert varnish on basalt exposed in the fault scarp that argues against 1872 offset, and 4) fault scarp morphology in alluvial fan material that suggests the most recent displacement occurred more than a thousand years ago.

Regarding the last item, some background information is useful. We will observe that the fault scarp has, at its maximum, an angle-of-repose gradient where it cuts alluvial fan deposits. The gradients on the Big Pine segment indicate the scarp is significantly more degraded than the scarp at Lone Pine (Fig. 3), where the fault is well-documented to have ruptured in 1872. This contrast in degradation where the fault scarps are developed in similar coarse alluvial fan materials casts strong doubt that the Big Pine segment ruptured in 1872.

Additional evidence comes from Wallace (1977), who studied fault scarp degradation in the Great Basin and describes three stages. In the first stage of degradation, the fault scarp maintains a scarp free face in which in-situ material is exposed in the fault scarp. The free face will have a gradient of 45 degrees or more and will slowly retreat from its initial location as it also decreases in height. Wallace (1977) concluded that fault scarp free faces persist on the order of 2000 years in the Great Basin. Assuming his model applies to this area, which is not unreasonable, the lack of a free face along the entire Big Pine fault segment where the fault scarp is developed in alluvial fan materials suggests that the last rupture was conservatively more than a thousand years ago.

Discussion

An interesting question is why have so many geologists accepted that the Big Pine segment ruptured in 1872 given that the geomorphic and desert varnish evidence suggests otherwise? The answer is probably that they have uncritically relied on reports made shortly after the earthquake. The most prominent report was made by J.D. Whitney (Whitney, 1872) after he traveled the length of the valley four months following the earthquake.

According to Whitney (1872), "...nowhere are the effects of the earthquake in fissuring and depressing the surface so manifest as in the vicinity of Big Pine. A large body of water issues from the gorges of the Sierra west of this place, and this water spreads out after leaving the sagebrush slope, and runs in numerous channels through a low and swampy meadow, several hundred acres in extent.

Here there is a series of extensive fissures, which may be traced uninterruptedly for several miles." Although this description can be interpreted to indicate that the Big Pine fault segment ruptured in 1872, a critical analysis suggests otherwise. First, Whitney did not have the knowledge to perceive between tectonic rupture and liquefaction features. The "series of

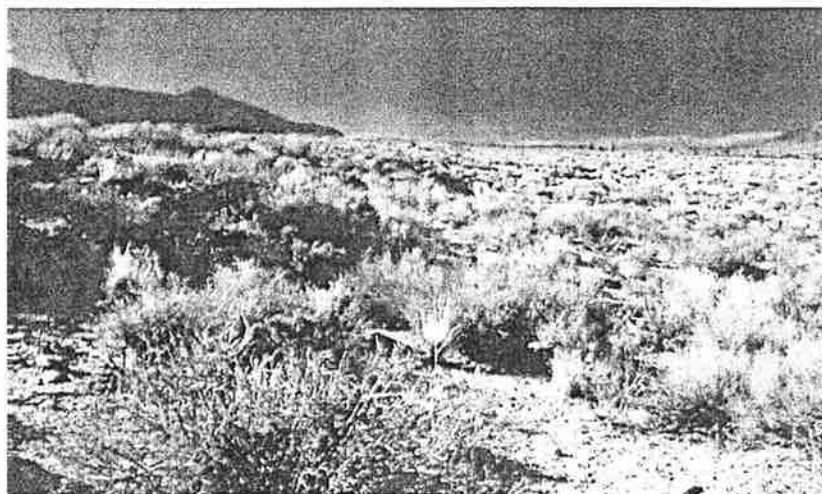


Figure 3. Fault scarp photos from Big Pine fault segment (top) and Lone Pine segment of the Owens Valley fault west of Lone Pine (bottom). The Lone Pine fault is well-documented to have ruptured in 1872. Note the free face present in the bottom photo and absence in upper photo.

extensive fissures" in the Big Pine area observed by Whitney could have just as readily been caused by liquefaction as by fault rupture. Second, the location described by Whitney is not clear. I suggest the most likely area that Whitney describes is a 550 acre meadow area 2.5 km west of Big Pine and 1.5 km west of the Big Pine segment fault (Fig 4). This area is a structural graben that has a shallow groundwater table evidenced by the abundant green vegetation growing in the area. Two major streams, Baker and Big Pine, flow through the meadow after disgorging

from the "sagebrush slope" of the Sierra Nevada. (The Bernasconi Center where we are staying for this event is located in this meadow area.)

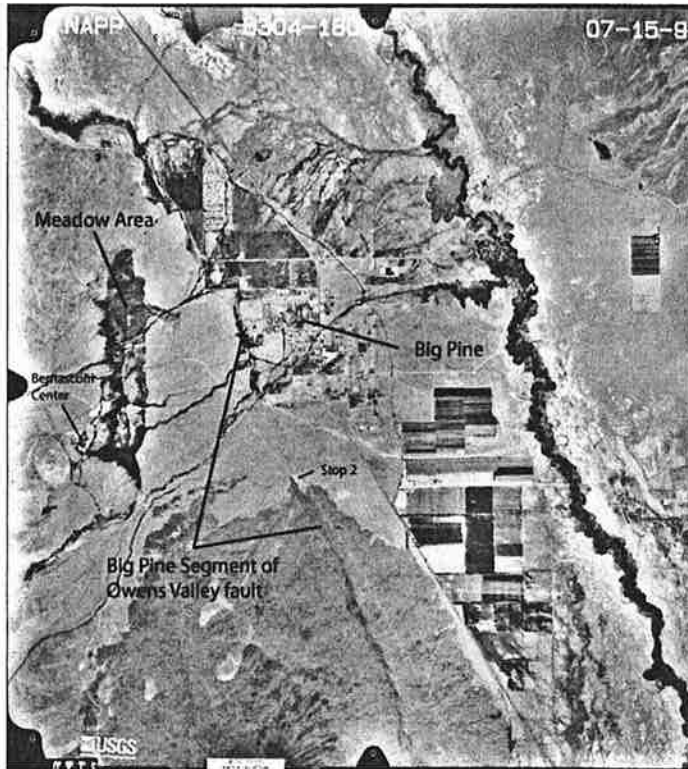


Figure 4. Aerial photo of Big Pine area. Approximate scale is 1 inch = 3 km.

From the ideas discussed above, it is suggested that the Big Pine segment is not strongly linked kinematically to the Owens Valley fault and thus could be considered a separate fault. I propose that the Owens Valley fault dies out east or northeast of the Poverty Hills and its displacement partitioned to other faults. The right-lateral component is suggested to be transferred eastward to the White Mountain fault zone and the dip-slip component transferred westward to the Big Pine fault. This proposal is permissible within the framework of present knowledge including regional kinematics deduced from space geodesy (Dixon et al., 2000) and the results of field studies of the White Mountain fault zone indicating the presence of a releasing bend southeast of the Poverty Hills (Slemmons et al., 2008). If this proposal for the Big Pine fault segment is correct, then the transpressional uplift model for the origin of the Poverty Hills appears untenable. This, in turn, supports the landslide model for the origin of the Poverty Hills.

References

Beanland, S., and Clark, M.M., 1994, The Owens Valley fault zone, eastern California, and surface rupture associated with the 1872 earthquake: U.S. Geological Survey Professional Paper 1982, 29 p.

- Bishop, K.M., 1999, Megarock avalanche and rock slide deposits of the Owens Valley, eastern California, in Baldwin, J., Hughes, K., Sharp, G. M., Steiner, E., and West, M. D., eds., *The Long Valley Caldera, Mammoth Lakes and Owens Valley Region, Mono County, California*, South Coast Geological Society Annual Field Trip Guidebook No. 27, South Coast Geological Society, Santa Ana, CA, pp. 66-92.
- Bishop, K.M. and Clements, 2006, The Poverty Hills, Owens Valley, California – transpressional uplift or ancient landslide deposit?: *Environmental and Engineering Geoscience*, v. 12, no. 4, p. 301-314.
- Dixon, T.H., Robaudo, S., Lee, J., and Reheis, M.C., 1995, Constraints on present-day Basin and Range deformation from space geodesy: *Tectonics*, v. 14, pp. 755-772.
- Frankle, K.L., and 17 others, 2008, Active tectonics of the eastern California shear zone, in Duebendorfer, E. M., and Smith, E.I., eds., *Field Guide to Plutons, Volcanoes, Faults, Reefs, Dinosaurs, and Possible Glaciation in Selected Areas of Arizona, California, and Nevada*, Geological Society of America Field Guide 11, p. 43-81.
- Jennings, C.W., 1994, Fault activity map of California and adjacent areas with locations and ages of recent volcanic eruptions: California Division of Mines and Geology Data Map Series 6, 92 p. 2 plates, scale 1:750,000.
- Pakiser, L.C., Kane, M.F., and Jackson, W.H., 1964, Structural Geology and Vocanism of Owens Valley Region, California – A Geophysical Study, U.S. Geological Survey Professional Paper 438, 65 p.
- Slemmons, D.B., Vittori, E., Jayko, A.S., Carver, G.A., and Bacon, S.N., 2008, Quaternary fault and lineament map of Owens Valley, Inyo County, eastern California: Geological Society of America Map and Chart 96, scale 1:100,000, 2 plates, 25 p. text. Wallace, R.E., 1977, Profiles and ages of young fault scarps, north-central Nevada: *Geological Society of America Bulletin*, v. 88, p. 1267-1281.
- Taylor, T.R., 2002, Origin and structure of the Poverty Hills, Owens Valley Fault Zone, Owens Valley, California: unpublished M.S. Thesis, Department of Geology, Miami University, 93 p.
- Taylor, T.R. and Dilek, Y., 2001, Origin of the Poverty Hills, Owens Valley, California and implications for the tectonic evolution of the Owens Valley Basin: *Geological Society of America Abstracts with Programs*, v. 33, no. 6, p. A-395.
- Wallace, R.E., 1977, Profiles and ages of young fault scarps, north-central Nevada: *Geological Society of America Bulletin*, v. 88, p. 1267-1281.
- Whitney, J.D., 1872, The Owens Valley earthquake: *Overland Monthly*, v. 9, p. 130-140, 266-278. Reprinted by Goodyear, WA., 1888, in Eighth Annual Report of the State Mineralogist: California State Mining Bureau, p. 288-309.

Big Pine volcanic field

(Jorge Vazquez and Jeff Woolford)

Overview:

The Big Pine volcanic field (BPVF) is located along the western boundary of the Basin and Range province in east-central California, approximately 25 kilometers south of the town of Bishop within the N-S trending Owens Valley (Figure 1). Like many other Quaternary volcanic fields in the western United States, BPVF is located along the margins of the Basin and Range province where present-day extension is greatest and concomitant mantle melting and basaltic volcanism are most active. (Best and Brimhall, 1974, Wang et al., 2002). The Owens Valley is bounded by active oblique-slip range-front faults of the Sierra Nevada and Inyo Mountains. Extension is active in the area and locally controls the distribution of volcanic vents (Gillespie, 1992). Scoria cones of the BPVF are aligned along the scarps of approximately N-S trending faults that offset Quaternary alluvial fans (Moore, 1963; Conner and Conway, 2000; Zehfuss et al., 2001). Vertical slip rates over the last 300,000 years in the BPVF area are ~ 0.2 mm/1000 yr (Zehfuss et al., 2001), with the most recent large earthquake (M 7.4) occurring in 1872 AD. At Coso volcanic field, located ~ 100 km south of BPVF and also at the Basin and Range margin, crustal extension rate is a first-order control on the recurrence of basalt and rhyolite volcanism, and the same is likely the case at BPVF (Bacon, 1982).

Approximately 0.5 km^3 of mafic lavas flows comprise the BPVF (Ormerod, 1991, Beard and Glazner, 1995). Most of the volcanic products are basaltic in composition, with a single high-silica rhyolite dome located in the west-central portion of the volcanic field. On average, individual lavas cover approximately 190 km^2 , with average individual lava volumes of 0.065 km^3 (Woolford and Vazquez, 2007). Pyroclastic fallout from the field is rare, but occurs locally beneath lavas and alluvium. Lavas have bulk compositions that range from basalt to basaltic andesite with alkaline and subalkaline affinities, including some tholeiitic examples (Varnell, 2006). Several lavas contain mantle-derived ultramafic xenoliths (spinel lherzolite, wehrlite, and pyroxenites) and reflect relatively fast magma ascent and negligible storage in the crust (Beard and Glazner, 1995; Mordick and Glazner, 2006). Calculated melting depths for the BPVF basalts range from 45-60 km depth in the upper mantle (Wang et al., 2002). Field mapping (Woolford and Vazquez, 2007) in the Aberdeen area of the BPVF reveals two general groups of mafic lavas: 1) xenocryst-rich and 2) xenolith-poor. Xenolith-rich basalts contain variable

amounts of ultramafic, mafic (gabbro), granitic, and metamorphic lithologies, whereas xenolith-poor lavas are dominated by olivine phenocrysts. In both north and south portions of the Aberdeen area, flows composing the base of the volcanic stratigraphy are the xenolith-rich variety, and are typically overlain by xenolith-poor flows. In general, these younger xenolith-poor lavas are ~25% larger in volume than the older xenolith-rich lavas.

Geochronology of BPVF lavas yields Quaternary ages, with most ages less than ca. 0.5 Ma (Gillespie, 1992). K-Ar, $^{40}\text{Ar}/^{39}\text{Ar}$, and (U-Th)/He analyses of lavas and lava-hosted xenoliths yield ages between 1.2 Ma and 0.03 Ma (Wasserburg, 1983; Gillespie et al., 1984; Turrin and Gillespie, 1986; Bierman et al., 1991; Conner and Conway, 2000; Blondes et al., 2007, 2008). Several lavas are dated using cosmogenic ^3He exposure methods, and yield ages of ca. 110 ka to 25 ka (Stone et al., 1993). However, ages for the same lavas using different techniques are discordant: a lava at Goodale Creek yields a K-Ar age of ca. 130 ka (Bierman et al., 1991) and an exposure age of ca. 25 ka (Stone et al., 1993), and a lava at Crater Mountain yields a K-Ar age of ca. 290 ka (Bierman et al., 1991) and an exposure age of ca. 110 ka (Stone et al., 1993). Obsidian from the lone rhyolite dome yields a K-Ar age of 0.99 ± 0.04 Ma (Cox et al., 1963); recent U-Pb dating of zircons from this dome by ion microprobe mass spectrometry yields ages of ca. 0.9 Ma (Janet Harvey, personal communication).

Fish Springs high-silica rhyolite.

The Fish Springs rhyolite comprises a single thick coulee with a volume of at least 0.05 km^3 (dense rock equivalent) of highly evolved (76 wt.% SiO_2) magma (Lidzbarski and Vazquez, 2007). The Fish Springs rhyolite is unique because it is the only silicic magma identified in the BPVF. At nearby Coso volcanic field, an abundance of rhyolite relative to basalt suggests crustal melting by mafic magmas stored in mid to upper crustal reservoirs, whereas the paucity of rhyolite relative to basalt at BPVF suggests only brief crustal residence of ascending mafic magmas (Mordick and Glazner, 2006). The outer portions of the rhyolite are autobrecciated and felsitic rhyolite. Where exposed by quarrying, the internal portions of the rhyolite are pumiceous perlite with local obsidian. Fish Springs rhyolite is crystal poor (~1%), with very small (<0.5 mm) crystals of generally euhedral to subhedral plagioclase, quartz, orthopyroxene, clinopyroxene, biotite, hornblende, Fe-Ti oxides, apatite, pyrrhotite, and very rare zircon, as well as apparent xenoliths and xenocrysts of metamorphic and igneous wallrocks (Lidzbarski and

Vazquez, 2007). Biotite, hornblende, and some clinopyroxene are likely to be xenocrysts based on their oxidation and disequilibrium textures. Trace element concentrations in Fish Springs rhyolite are very low for elements such as Ba (~15 ppm), Sr (~8 ppm), La (~10 ppm) and Zr (~80 pm). These concentrations, together with a pronounced europium anomaly, are comparable to other highly fractionated high-silica rhyolites at Coso and Long Valley, and suggest extensive degrees of feldspar and accessory mineral fractionation.

References:

- Bacon, C.R., 1982, Time-predictable bimodal volcanism in the Coso Range, California: *Geology*, v. 10, p. 65-69.
- Beard, B.L., and Glazner, A.F., 1995, Trace element and Sr and Nd isotopic composition of mantle xenoliths from the Big Pine volcanic field, California: *Journal of Geophysical Research*, v. 100, p. 4169-4179.
- Best, M.G., and Brimhall, W.H., 1974, Late Cenozoic alkalic basaltic magmas in the western Colorado Plateaus and the Basin and Range transition zone, U.S.A., and their bearing on mantle dynamics: *Geological Society of America Bulletin*, v. 85, p. 1677-1690.
- Bierman, P., Gillespie, A., Whipple, K., and Clark, D., 1991, Quaternary geomorphology and geochronology of Owens Valley, California: *Geological Society of America Field Trip in Walawender, M.J., and Hanan, B.B., (eds.), Geological Excursions in Southern California and Mexico: Guidebook for the Geological Society of America Annual Meeting*, p. 199-223.
- Blondes, M.S., Reiners, P.W., Edwards, B.R., and Biscontini, A., 2007, Dating young basalt eruptions by (U-Th)/He on xenolithic zircons: *Geology*, v. 35, p. 17-20.
- Blondes, M.S., Reiners, P.W., Ducea, M.N., Singer, B., and Chesley, J., 2008, Temporal-compositional trends over short and long time-scales in basalts of the Big Pine volcanic field, California: *Earth and Planetary Science Letters*, in press.
- Cox, A., Doell, R.R., and Dalrymple, G.B., 1963, Geomagnetic polarity epochs and Pleistocene geochronometry: *Nature*, v. 198, p. 1049-1051.
- Gillespie, A.R., 1992, Big Pine in Wood, C.A., and Kienle, J., eds., *Volcanoes of North America*: Cambridge University Press, p. 236-237.
- Gillespie, A. R.; Huneke, J. C.; Wasserburg, G. J., 1984, Eruption age of an approximately 100,000-year-old basalt from $^{40}\text{Ar}/^{39}\text{Ar}$ analysis of partially degassed xenoliths: *Journal of Geophysical Research*, v. 89, p. 1033-1048.
- Lidzbarski, M.I., and Vazquez, J.A., 2007, High-silica rhyolite magmatism in the Big Pine volcanic field, eastern California: American Geophysical Union annual meeting, San Francisco, CA
- Moore, J.G., 1963, *Geology of the Mount Pinchot Quadrangle, southern Sierra Nevada California*: US Geological Survey Bulletin 1130, 152 p.
- Mordick, B.E., and Glazner, A.F., 2006, Clinopyroxene thermobarometry of basalts from the Coso and Big Pine volcanic fields, California: *Contributions to Mineralogy and Petrology*, v. 152, p.111-124.
- Ormerod, D.S., Rogers, N.W., and Hawkesworth, C.J., 1991, Melting in the lithospheric mantle: inverse modeling of alkali-olivine basalts from the Big Pine volcanic field, California: *Contributions to Mineralogy and Petrology*, v. 108, p. 305-317.
- Stone, J.O., Hammerschmidt, K., Friedrichsen, H., and Hilton, D., 1993, Cosmogenic He-3 ages of basalts at Big Pine, California: Constraints on uplift across the Owens Valley: EOS, Transactions of the American Geophysical Union.

- Turrin, B., and Gillespie, A. R. (1986), K/Ar ages of basaltic volcanism of the Big Pine volcanic field, California: Implications for glacial stratigraphy and neotectonics of the Sierra Nevada (abs.), Geol. Soc. Am. 18:777.
- Varnell, A., 2006, Petrology and geochemistry of the Big Pine volcanic field Inyo County, California: Unpublished thesis, California State University-Pomona.
- Wang, K., Plank, T., Walker, J.D., and Smith, E.I., 2002, A mantle melting profile across the Basin and Range, SW USA: Journal of Geophysical Research, v. 107
- Wasserburg, G. J., Eruption age of a pleistocene basalt from ^{40}Ar - ^{39}Ar analysis of partially degassed xenoliths: Journal of Geophysical Research, v. 88, p. 4997-5008.
- Woolford, J., and Vazquez, J.A., 2007, Distribution and stratigraphy of basaltic lavas in the southwest portion of the Quaternary Big Pine volcanic field, California: American Geophysical Union annual meeting, San Francisco, CA.
- Zehfuss, P.H., Bierman, P.R., Gillespie, A.R., Burke, R.M., and Caffee, M.W., 2001, Slip rates on the Fish Springs fault, Owens Valley, California, deduced from cosmogenic ^{10}Be and ^{26}Al and soil development on fan surfaces: Geological Society of America Bulletin, v.113, p. 241-245.

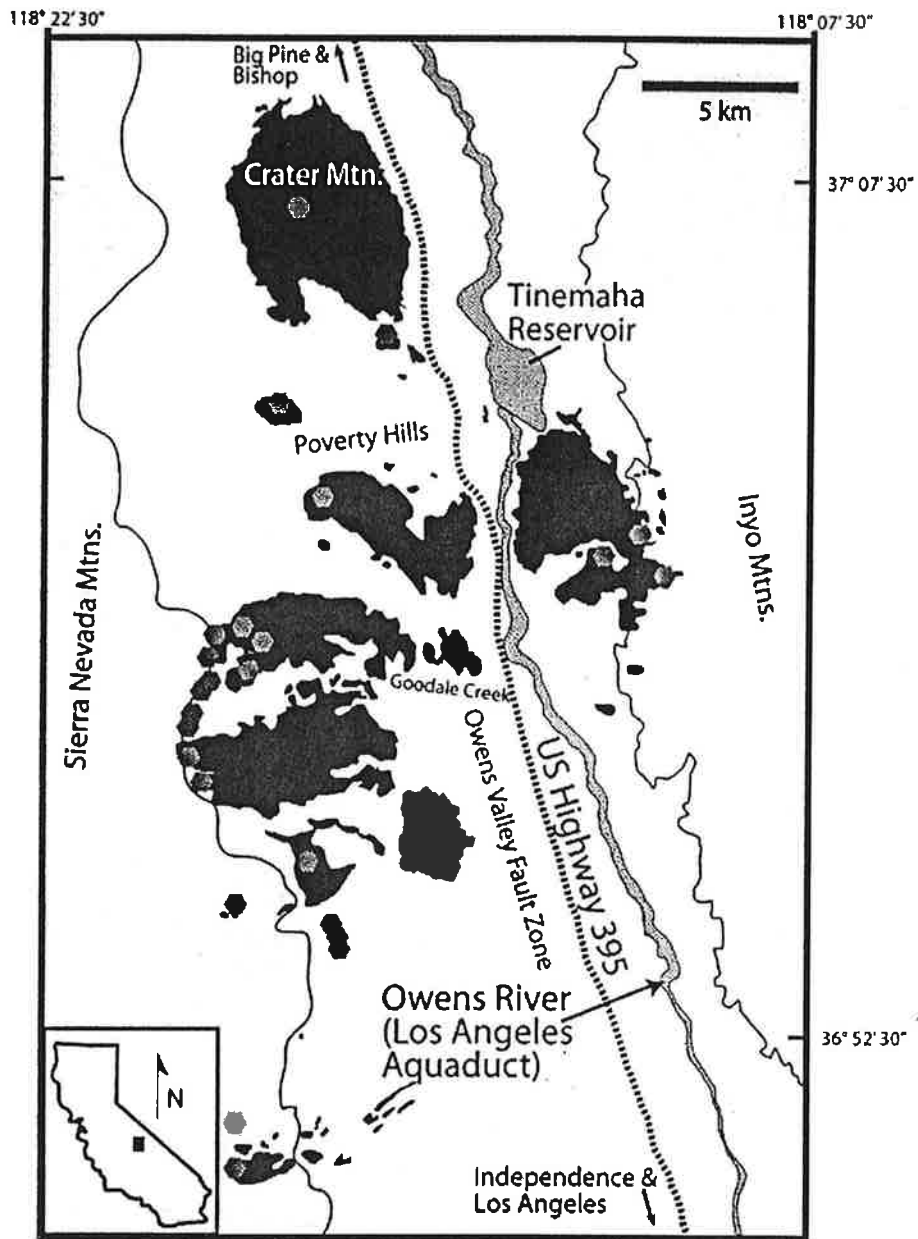


Figure 1. Map showing exposed lavas (black) of the Big Pine volcanic field in Owens Valley, CA, and their proximity to US Hwy. 395 (dashed line) and the Los Angeles Aqueduct (blue). Red hexagons denote apparent locations of scoria cone vents. Individual volcanic units are not distinguished on existing maps of the area. Adapted from Moore (1963) and Blerman et al. (1991).

Right-Lateral Faulting in Owens Valley (Summarized from published literature by George Dunne)

Young geomorphic features and active tectonism reveal that Owens Valley and its flanking ranges are the sites of both normal and right-lateral faulting. While the great vertical relief between valley floor and steep-faced, adjacent mountain peaks was recognized by 19th century geologists as attesting to the normal faulting, the important role of right-lateral faulting was not widely recognized until later. It was not widely appreciated at the time, for example, that the great Owens Valley earthquake of March, 1872, produced more right slip than normal dip slip. The following summary focuses on the evolution of right-lateral strike slip in the Owens Valley.

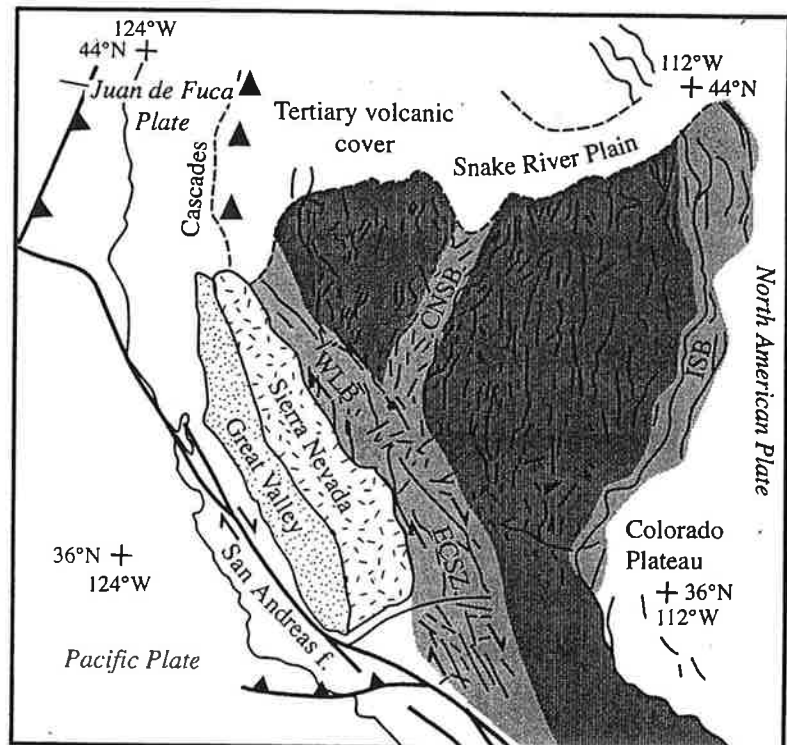
Attempts in the 1960's to match up geologic units across the Owens Valley as a way of assessing possible right slip within the valley yielded right-slip values of no more than 10 kilometers. Contrary views began to emerge in the 1990's. Based on studies of active northwest-trending right-strike-slip faults in the Mojave Desert, combined with analysis of the relative motion between North American and Pacific plates, Roy Dokka, an alumnus of CSUN, suggested that a 50- to 100-km-wide zone of right-lateral faulting trending northwest across the Mojave was accommodating a significant portion of the overall relative plate motion, with the remainder of motion being accommodated by the better-known San Andreas fault system. He named this zone the Eastern California Shear Zone, and speculated that it continued northward and connected in some way with the Walker Lane Belt of western Nevada (see Fig. 1). Various kinds of indirect evidence suggest that the Eastern California Shear Zone became active about 3 m.y. ago (at least in the Owens Valley area) and that it is accommodating between 2 and 4 mm/year of right slip across Owens Valley. Extrapolating Holocene slip rates across the zone yields a total right slip of between 6 and 9 km, the latter value being broadly consistent with earlier geologic estimates for right slip across the valley.

Different kinds of data published beginning in the 1990's have yielded much larger estimates of accumulated right slip across Owens Valley. Summarizing two decades of measuring initial Strontium isotopes in granitic plutons, plots of an initial Strontium = .706 isopleth from these data by Ron Kistler of the USGS revealed an apparent right step of approximately 65 km as the isopleth crossed the northern Owens Valley (Kistler, 1993). Subsequently, Cal Stevens of San

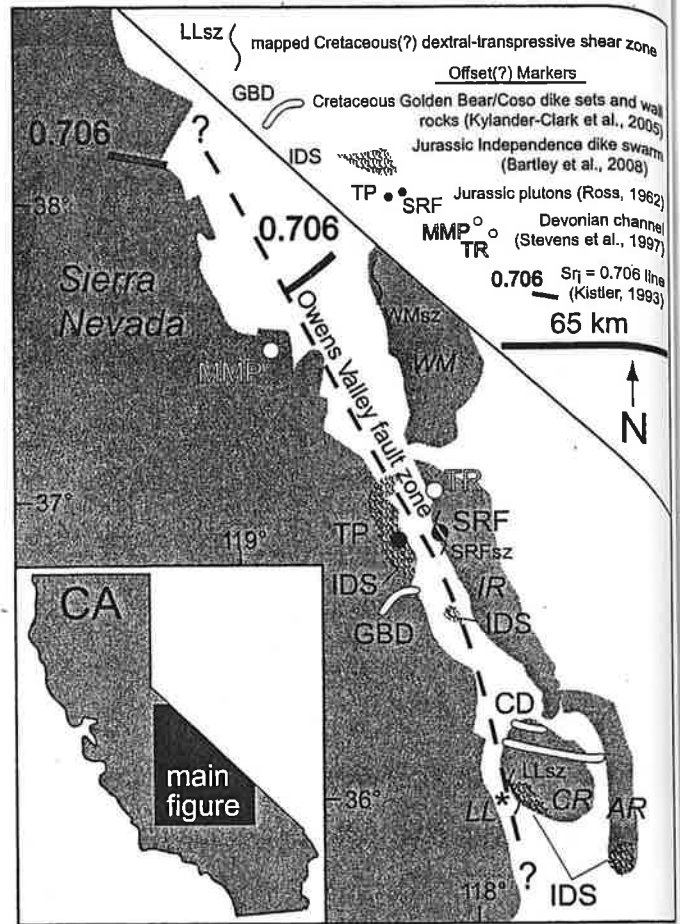
Jose State (1997) was able to locate right-separated parts of a Devonian submarine channel that was offset about 65 km as it crossed Owens Valley. More recently, Kylander-Clark et al. (2005) demonstrated that the Cretaceous-age Golden Bear dike in the Sierra and the Coso dike set in the Coso Range were almost certainly continuations of one another, and that they now are right-separated from one another by about 65 km as they cross southern Owens Valley. Finally, reanalysis of the boundaries of the Independence dike swarm led Bartley et al. (2008) to conclude that the swarm was offset right laterally by a similar amount as it crossed Owens Valley.

The upshot of these more recent studies is that about 55 km of right slip accumulated on a largely cryptic fault running the length of Owens Valley, in addition to another ~10 km of slip accommodated by the presently active basin-and-range faults operating over the past 3 m.y. or so. One possible exposure of the 'mystery' fault zone is present at the narrowest gap between the Sierra and the Coso Range, near Little Lake along Highway 395. Timing of this large amount of right slip is speculative, but it may have been linked to the Late Cretaceous/early Tertiary episode of distinctly right-oblique convergence in the subduction zone along the plate boundary. Slip occurred sometime following the emplacement of the Golden Bear and Coso dikes at ~83 Ma.

Figure 1. Simplified tectonic map of the western part of the U.S. Cordillera showing the major geotectonic provinces and modern plate boundaries. Basin and Range extensional province in dark gray; CNSZ (central Nevada seismic zone), ECSZ (eastern California shear zone), ISB (intermountain seismic belt), and WLB (Walker Lane belt) in light gray.



Locations of markers that support 65+ km of dextral offset across Owens Valley. Although correlation of the Tinemaha (TP) and Santa Rita Flat (SRF) plutons suggested little lateral offset (Ross, 1962), plutons of similar age and lithology are widespread on both sides of Owens Valley. Offset markers include (1) the densest part of the Independence dike swarm (Bartley et al., 2008); (2) the Sr 0.706 isopleth (Kistler, 1993); (3) a Devonian submarine channel at Tinemaha Reservoir and in the Mount Morrison pendant (Stevens et al., 1997); (4) the 83 Ma Golden Bear (GBD; Stop 8, Fig. 1) and Coso dike sets (CD; Stop 6, Fig. 1; Kylander-Clark et al., 2005); and (5) the 102–103 Ma plutons that the Golden Bear and Coso dikes intrude (Kylander-Clark et al., 2005). AR—Argus Range; CR—Coso Range; IDS—Independence dike swarm; IR—Inyo Range; LL—Little Lake; LLsz—Little Lake shear zone of Bartley et al. (2008; Stop 5, Fig. 1); MMP—Mount Morrison pendant; SRFsz—Santa Rita Flat shear zone of Vines (1999); TR—Tinemaha Reservoir; WM—White Mountains; WMsz—White Mountain shear zone of Sullivan and Law (2007).



Background Information, Neoproterozoic of the White-Inyo Mtn Region
(Mike Kaericher and Doug Yule)

The predominantly carbonate Neoproterozoic succession in the White-Inyo Mountains is thought to have been deposited on a passive margin following the rifting of Rodinia. However, a siliciclastic unit, the Hines Tongue, progrades over the passive margin carbonates and represents a significant sea level fall. Two competing hypothesis exist for the origin of this sea level fall. One hypothesis proposes that there could have been a snowball earth situation during which the earth was completely glaciated owing to high albedo from an equatorial supercontinent. This in turn would cause a low hydrologic cycle to occur, cause sea ice to cover the oceans, lower the overall sea level, cease photosynthesis in the oceans, and ultimately crash the ecosystem (Lorentz, 2007). A second hypothesis is that the White-Inyo Mountains area could have experienced uplift and retreat of marine waters as a result of possible tectonic rifting of Rodinia, The Laurentian margin could have experienced two stages of rifting causing the Rodinia breakup to take place. The first rifting happened circa 750 Ma and the second phase circa 570 Ma causing the uplift. Rifting is supported by faulting and breccias, thickness changes in the Lower Reed, thermal subsidence curve, and lateral units showing extension (Pers. Comm., N.J. Lorentz, 2007).

C-isotope record from the Neoproterozoic Wyman Formation, White-Inyo Mountains, California and possible correlation to the Johnnie Formation, Death Valley

Michael Kaericher

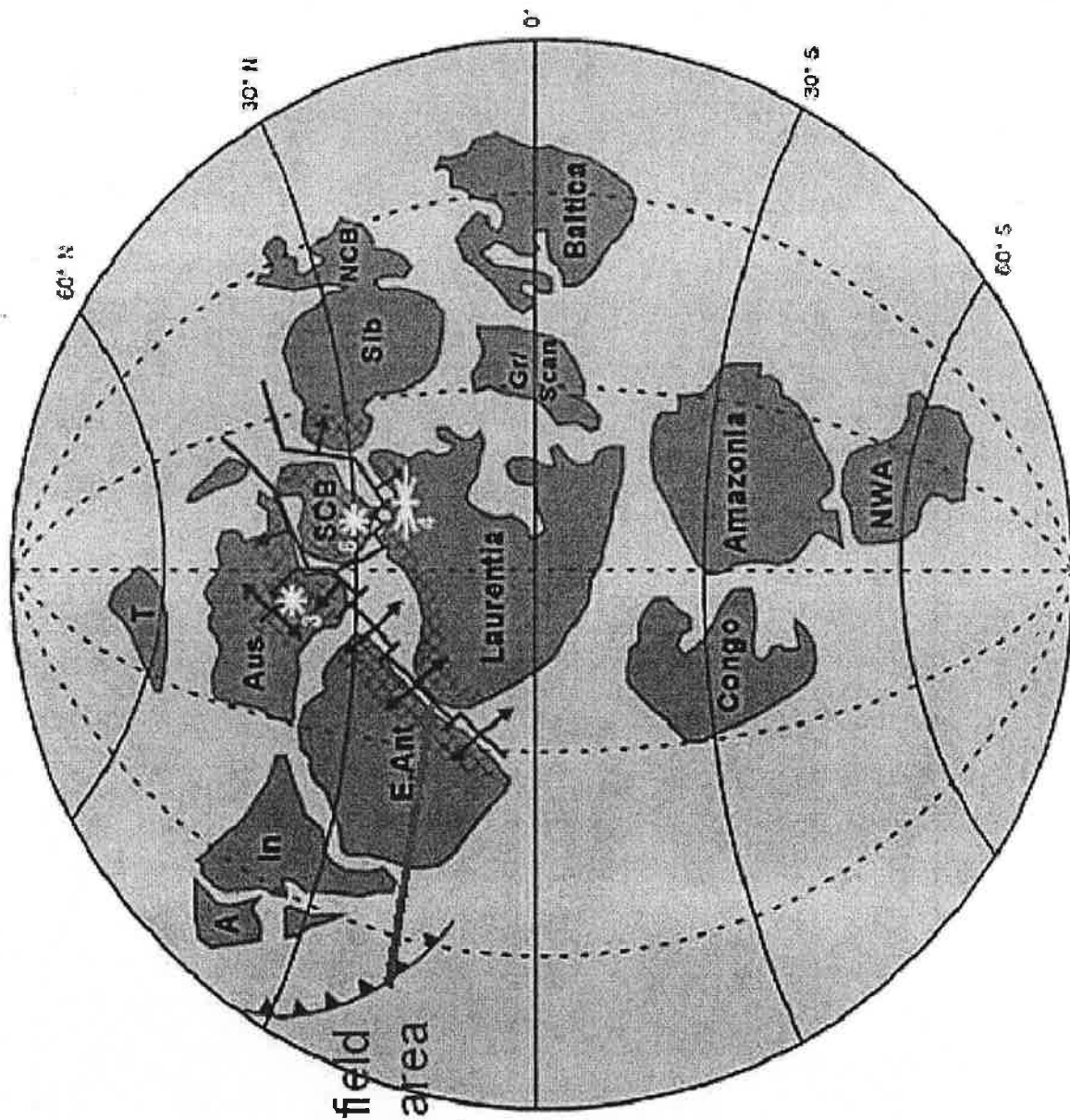
Department of Geological Sciences, California State University, Northridge, Northridge, California 91330

Faculty Advisors: Dr. Douglas Yule and Dr. Nathaniel Lorentz

The carbon-isotope record of Neoproterozoic (1000 to 542 million years old) carbonate-rock sequences provides a way to correlate rock sequences across the Basin and Range province, western North America. This type of study is used here to refine the understanding of the super-continental rifting processes that are currently used to explain the Death Valley succession. This study focuses on carbonates within the upper part of the Wyman Formation, located in the

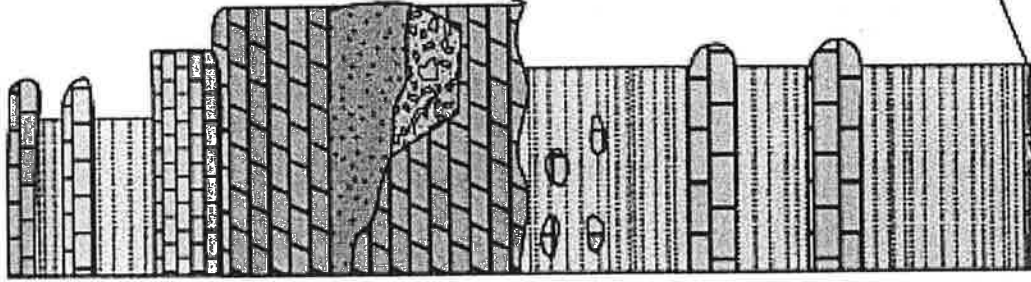
White-Inyo Mountains of eastern California. Here, the Wyman Formation consists of interbedded carbonate and shale. Hand samples collected at 1.5-m intervals were cut, polished, and drilled to produce milligrams of rock powder. The drilled samples had their C-isotopic values measured by means of mass spectrometry (at USC, Dr. Lowell Stott). Carbonates from near the upper contact of the Wyman Formation show a $\delta^{13}\text{C}$ ratio ranging from negative 2.5 per mil to positive 1.0 per mil (VPDB). However, it is interesting to note that these values in the Wyman Formation do not reach -11 per mil (VPDB) as they do in the Johnnie Formation. One possible explanation is that sediment with C-isotope values approaching -11 per mil was eroded away to form the unconformity at the top of the Wyman Formation. Though the Wyman Formation is a more distal-marine unit than the Johnnie Formation, the carbon-isotope data reported here from lenticular oolitic carbonates (from near the top of the Wyman Formation) strengthen a correlation between it and the Johnnie Formation.

Super-continent breakup, 750-580 ma.

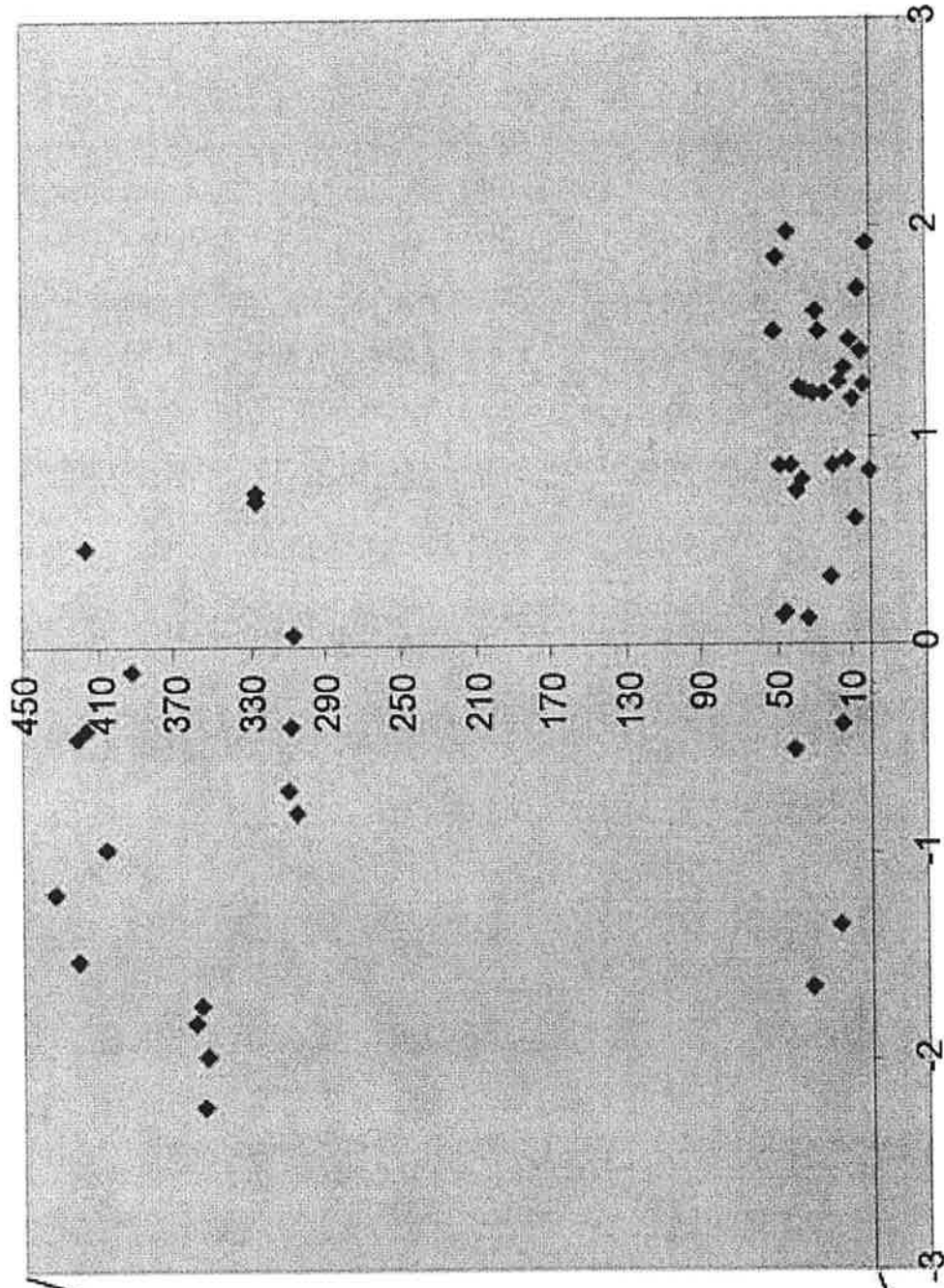


Eyles and Januszczyk (2004)

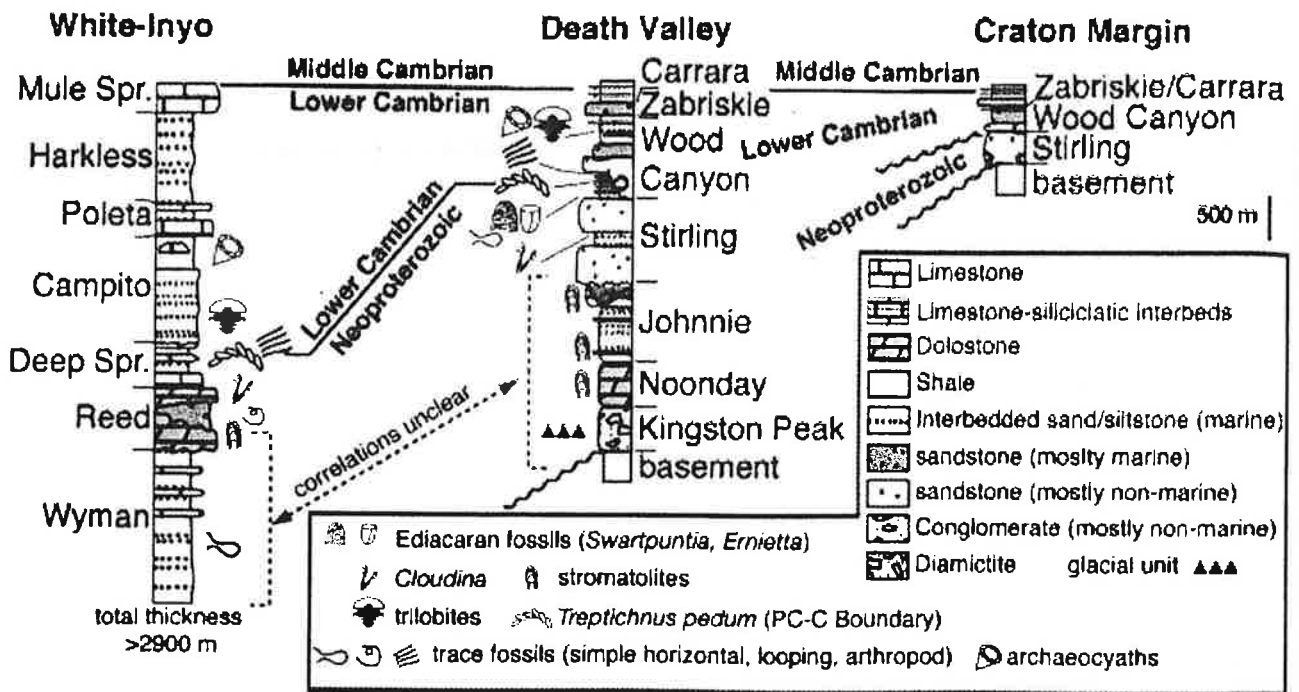
WHITE-INYO



Not to scale







Generalized lithostratigraphic columns for the PC-C transition interval in the southern Great Basin (after Nelson, 1962, 1976; Stewart, 1970; Fedo and Cooper, 2001). Whereas the Lower Cambrian portion is well constrained and correlated between the intervals, correlations between Neoproterozoic strata are less well constrained. Base of the Sauk I Sequence removes some of the Neoproterozoic-Lower Cambrian interval in more proximal (Craton Margin) settings. The Death Valley succession contains a Neoproterozoic glacial-cap-carbonate succession, but no known correlatives exist in the White-Inyo succession. Fossil symbols represent first occurrences of key taxa.

GEOLOGICAL OVERVIEW OF THE LONG VALLEY CALDERA AND THE INYO-MONO CRATERS REGION

The margin of the Long Valley caldera is poorly defined by physiographic features in the vicinity of Crowley Lake. We crossed the caldera boundary somewhere around Tobacco Flat before we turned off of U.S. Highway 395 to go to Convict Lake. Now that we are in the caldera, it is appropriate to summarize the geologic history of the volcano-tectonic depression of Long Valley (Figs. 18 and 19). This summary is intended to provide a reference frame for understanding the relationships of the various geologic features described in Legs 2 through 4 of the guidebook. The overview of the caldera is based on detailed mapping by Roy Bailey (1989) and K-Ar chronology by Brent Dalrymple and Marvin Lanphere (in Bailey and others, 1976, and revised in Mankinen and others, 1986).

The oldest volcanic rocks that are associated with the Long Valley magma chamber are the rhyolite flows of Glass Mountain, which were extruded in the northeast sector of the not-yet-formed caldera between 2.1 and 0.8 m.y. ago (Metz and Mahood, 1985, p. 11,122). The next major event in the formation of the caldera was the cataclysmic extrusion of the Bishop Tuff about 0.76 m.y. ago. The eruption began from a vent along the south-central margin of the proto-caldera immediately west of the Hilton Creek fault (Hildreth and Mahood, 1986, p. 400). As the eruption proceeded and the caldera began to subside, multiple vents developed along a ring-fracture system.

As the ring fracture propagated around the subsiding caldera, the earlier ash flows erupted toward the east, southeast, and southwest, and the later, hotter flows erupted toward the north (Hildreth, 1979, p. 47). About 125 cu mi (500 cu km) of Bishop Tuff were emplaced over a very short time span, perhaps less than a week (see Stop 4). The eruption also produced about 75 cu mi (300 cu km) of air-fall ash, which was carried as far east as Kansas and Nebraska. As the eruption of the Bishop Tuff partially emptied the magma chamber, its roof collapsed and formed the caldera, an elliptical topographic depression that measures about 10 miles (16 km) from north to south and 18 miles (29 km) from east to west (Fig. 18). Caldera subsidence totals 2 miles (3 km), of which one third is reflected in present topographic relief and the other two thirds are represented by post-caldera basin fill.

Shortly after collapse of the caldera, the central part underwent resurgent doming during which rhyolite flows ("older rhyolite" of Table 6) and rhyolitic tuff breccia were extruded. The rhyolite was emplaced from at least 12 vents during an interval of perhaps 100,000 years, between about 0.73 and 0.62 m.y. ago (Mankinen and others, 1986, p. 633). The doming and rhyolite extrusion in the central area were probably completed by 0.5 m.y. ago, thus producing what Smith and Bailey (1968, p. 616) called a "resurgent cauldron" with an uplifted central dome surrounded by a low-lying "moat."

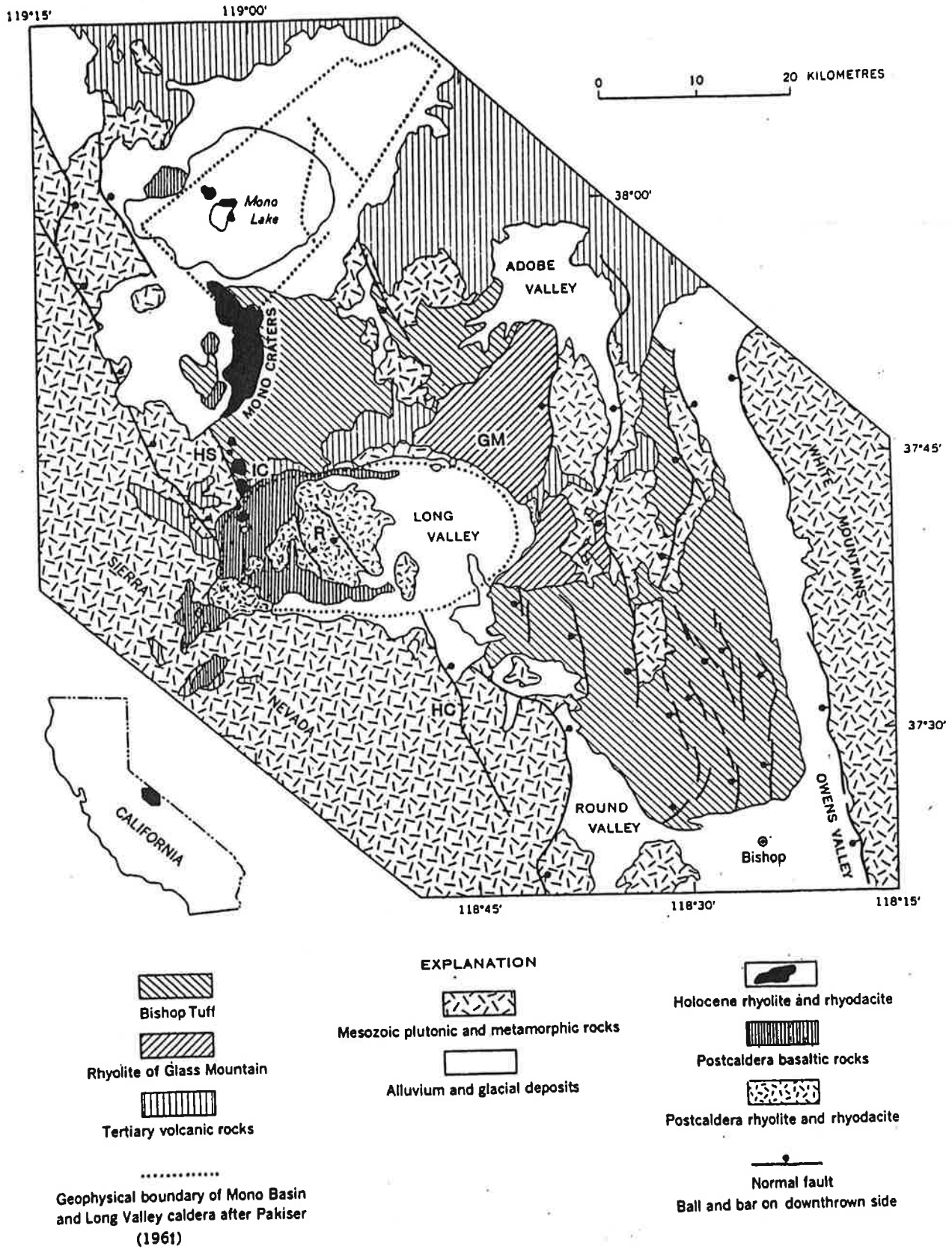


Figure 18. Generalized geologic map of Long Valley-Mono Basin region. The Volcanic Tableland is the area of Bishop Tuff between the Long Valley caldera and the town of Bishop. GM = Glass Mountain Ridge; HC = Hilton Creek fault; HS = Hartley Springs fault; IC = Inyo Craters; R = resurgent dome of Long Valley caldera and its medial graben. (Modified from Bailey and others, 1976, *Jour. Geophys. Research*, © American Geophysical Union)

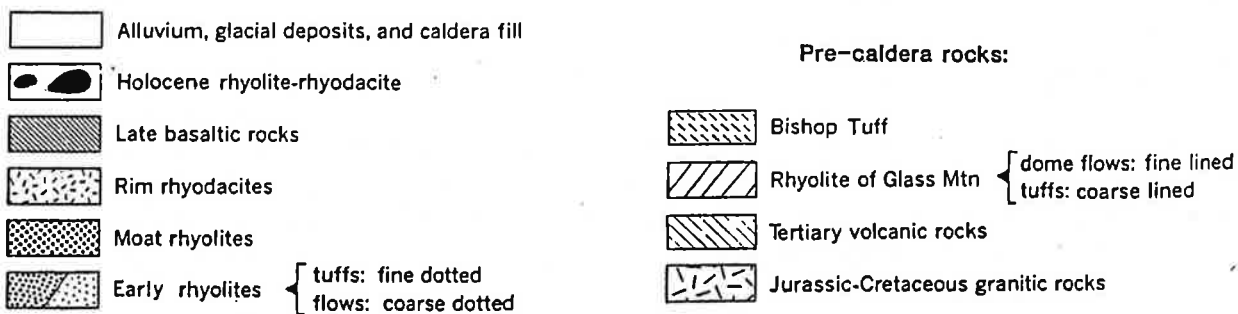
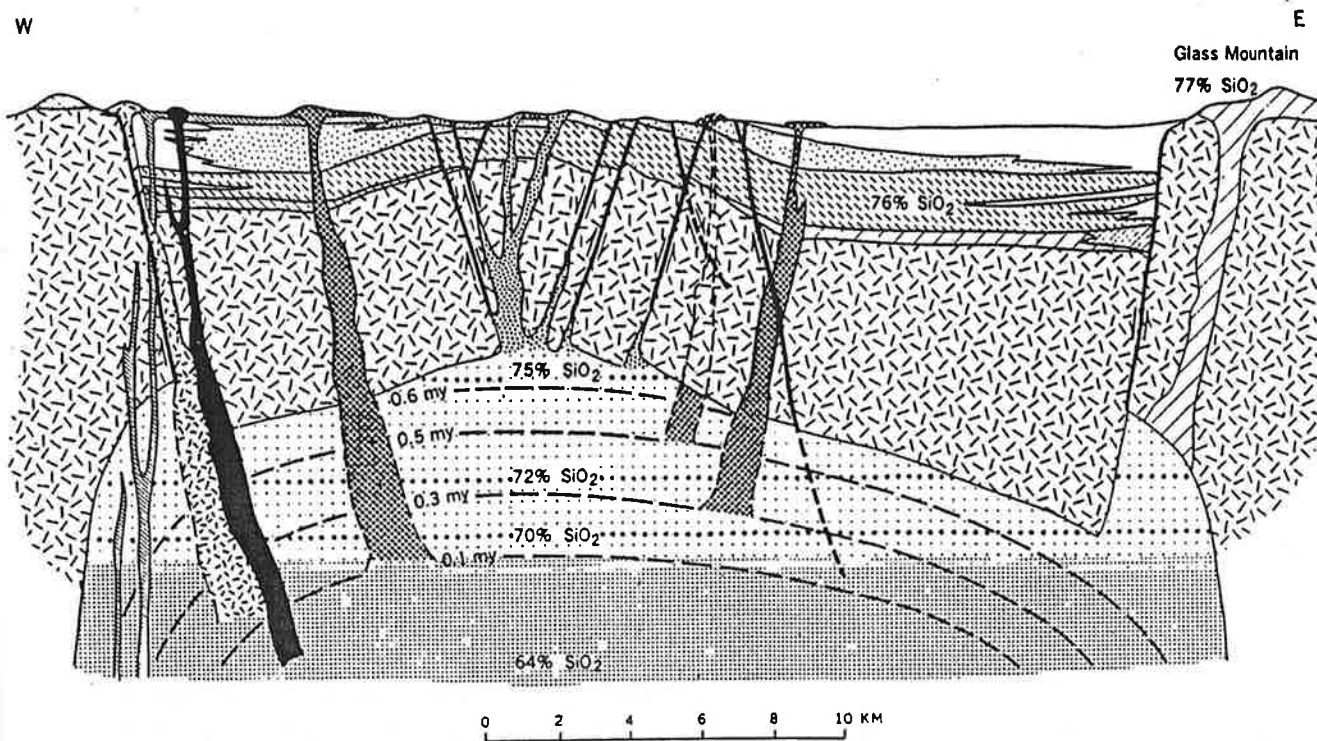


Figure 19. Schematic east-west cross section through Long Valley caldera and its subjacent magma chamber. Heavily dotted part of chamber is rhyodacite magma; lightly dotted part is rhyolite magma. Horizontal dotted lines show silica gradient in vertically zoned chamber. Curved dashed lines show depth to residual magma at specified times. Because the diagram is intended to be a simplified rather than precise representation and because of gaps and uncertainties in subsurface data, the vertical scale is unspecified. Pre-Cenozoic metamorphic rocks are included with granitic rocks in the cross section. (From Bailey and others, 1976, *Jour. Geophysical Research*, © American Geophysical Union)

The next phase of volcanism involved the emplacement of marginal (moat) rhyolites in three discrete episodes spaced at 0.2-m.y. intervals: 0.5, 0.3, and 0.1 m.y. ago. The moat rhyolites (the "younger rhyolite"

of Table 6), which were emplaced on the periphery of the central dome, are probably related to ring fractures around the resurgent dome. A later stage of volcanism produced rim rhyodacites (Fig. 19)

from at least ten vents in the western part of the caldera. The main mass of these hornblende-biotite rhyodacite flows is Mammoth Mountain (Table 6), which consists of flows and plugs that range in age from about 220,000 to 50,000 years.

At the same time that Mammoth Mountain was being formed, basalt and andesite flows (Table 7) were extruded in the west moat of the Long Valley caldera. The flows have K-Ar ages that range from 239,000 to 64,000 years (Mankinen and others, 1986, p. 637-638). Near the town of Mammoth Lakes, basalt flows are interbedded with pre-Wisconsin glacial deposits.

Bailey and others (1976, p. 740) reported a decrease in silica content with decreasing age of the extrusive rocks derived from the Long Valley magma chamber (Table 5). They interpreted this decrease in silica content of successive eruptives as indicating progressive downward crystallization of a zoned magma chamber that is more silicic in its upper part. Most of the basalt and andesite flows have silica content between 48 and 56 percent (Lipshie, 1974, fig. 5), which is signifi-

cantly different from that of the contemporaneous rhyolitic rocks. Bailey and others (1976, p. 740) suggested that the basalt and andesite were derived from a much deeper source than the Long Valley magma chamber and that the mafic and silicic magmas did not interact to any great extent.

More recent volcanic activity has occurred north of Long Valley, in the Mono Craters region near Mono Lake (Fig. 18). Rhyolitic magma began erupting in the Mono Craters about 40,000 years ago, and eruptive episodes continued until about 600 years ago (Wood, 1977a, p. 18; Wood and Brooks, 1979). The Mono Craters volcanism ultimately produced more than thirty domes, craters, and flows (coulees) that lie along a concave-westward arc. The Mono Craters rocks are rhyolitic in composition, and the exposed materials consist primarily of pumice, obsidian, and ash deposits. The trace-element chemistry of the rhyolite indicates that the Mono Craters lavas were not derived from the Long Valley magma chamber. Kelleher and Cameron (1990, p. 17,657-17,658) suggested that, based on variations in trace elements and

Table 5. Silica Content of Volcanic Rocks of the Long Valley Caldera

VOLCANIC ROCK UNIT	AGE (M.Y.)	SILICA CONTENT (%)
Glass Mountain rhyolite	2.1 - 0.8	77
Bishop Tuff	0.76	76
Older (resurgent dome) rhyolite	0.73 - 0.62	75
Younger (moat) rhyolite	0.5 - 0.1	72
Hornblende-biotite rhyodacite	0.22 - 0.05	64 - 70

accessory minerals, the Mono Craters rhyolites were derived from multiple magma sources and may include a large component of mantle material.

The most recent volcanism in the Mono Craters has been at the north end of the arcuate chain, where the Panum Crater dome was emplaced between A.D. 1270 and 1350, based on radiocarbon dating (Wood and Brooks, 1979). Farther north, Paoha Island in Mono Lake is thought to have been uplifted by subsurface emplacement of a volcanic plug sometime between A.D. 1720 and 1850 (Stine, 1984, p. 47). This is based on the observation by Stine (p. 46-47) that the highest strand line that can be recognized on Paoha Island is well below the highest recent level of Mono Lake (6456 ft or 1968 m), which occurred around A.D. 1660 (see p. 224).

Almost contemporaneously with the formation of Panum Crater, volcanic activity also occurred along the Inyo Craters chain to the south (Fig. 18). The chain lies along a north-trending fracture that straddles the northwest margin of the Long Valley caldera (Bailey and others, 1976, p. 735). The fracture is subparallel to and east of the Hartley Springs fault (Fig. 18) and extends northward from the caldera to the south end of the Mono Craters chain. The Inyo Craters chain consists of a series of craters and domes that range in age from about 6000 to 550 years (Miller, 1985, p. 14; Wood, 1977b, p. 92).

Bailey and others (1976, p. 735) originally suggested that the Inyo Craters rhyolite formed by mixing of magmas from the

Long Valley and Mono Craters magma chambers. This suggestion was ultimately confirmed by subsequent geochemical studies (Sampson and Cameron, 1987, p. 10,419). Drilling of four slanted borings along the Inyo Craters chain in the 1980's showed that the north-trending fracture postulated by Bailey and others (1976, p. 741) provided the conduit for a rhyolite feeder dike. Eichelberger and others (1988, p. 13,218) inferred that the feeder dike system tapped more than one magma chamber along its length, resulting in chemical differences among the rhyolites of the Inyo domes.

Although no volcanic eruption is reported to have occurred in the Long Valley-Mono Craters region for hundreds of years, the region is still volcanically active. (An alleged volcanic event at Mono Lake in 1890 can safely be discounted—see Stop 40.) Hot springs and fumaroles abound within the Long Valley caldera, particularly along the south and east margins of the "resurgent dome" and, to a lesser extent, at Mammoth Mountain. Seismic activity that began in 1978 and continues today is associated with 2 ft (0.6 m) of dome-shaped uplift that occurred between 1979 and 1995 in the western part of the resurgent dome (Goldstein and Stein, 1988, p. 13,187; Hill and others, 1995, p. 12,986). Whether the seismic activity is a volcanic or a purely tectonic manifestation is still a topic of controversy that remains to be resolved. In any event, the widespread geothermal activity that continues today in the caldera indicates that the Long Valley magma chamber should still be considered capable of generating further volcanic activity, despite its present quiescence.

PUMICE QUARRY IN BISHOP ASH DEPOSITS.

Although this quarry has been a well-known point of geologic interest for many years, it was not until Wes Hildreth and Colin Wilson undertook their epochal studies of the Bishop Tuff that some of the complexities of the eruptive history of the ash exposed here were revealed. The work of Wilson and Hildreth (1997; 1998) expanded upon the earlier work of Hildreth (1979) and Hildreth and Mahood (1986), which in turn built upon the pioneering studies of Gilbert (1938). But before looking at the features exposed in this quarry, it would be useful to set the scene with a simplified overview of the distribution and eruptive history of the Bishop Tuff.

The Bishop Tuff covers an area of about 580 sq mi (1500 sq km) between Bishop and Mono Lake, with the Volcanic Tableland north of Bishop comprising the largest part of the outcrop area (Fig. 1). Most of the tuff is a rhyolitic ignimbrite, formed by widespread deposition and consolidation of ash-flow deposits. The ignimbrite consists of ash deposits that grade downward from sillar (tuff in which induration is due to recrystallization rather than welding) into true welded tuff. The welded zone grades downward into nonwelded basal pumice ash that overlies 10 to 15 ft (3 to 4½ m) of basal air-fall ash (Bateman, 1965, p. 151-158; Sheridan, 1970, p. 865).

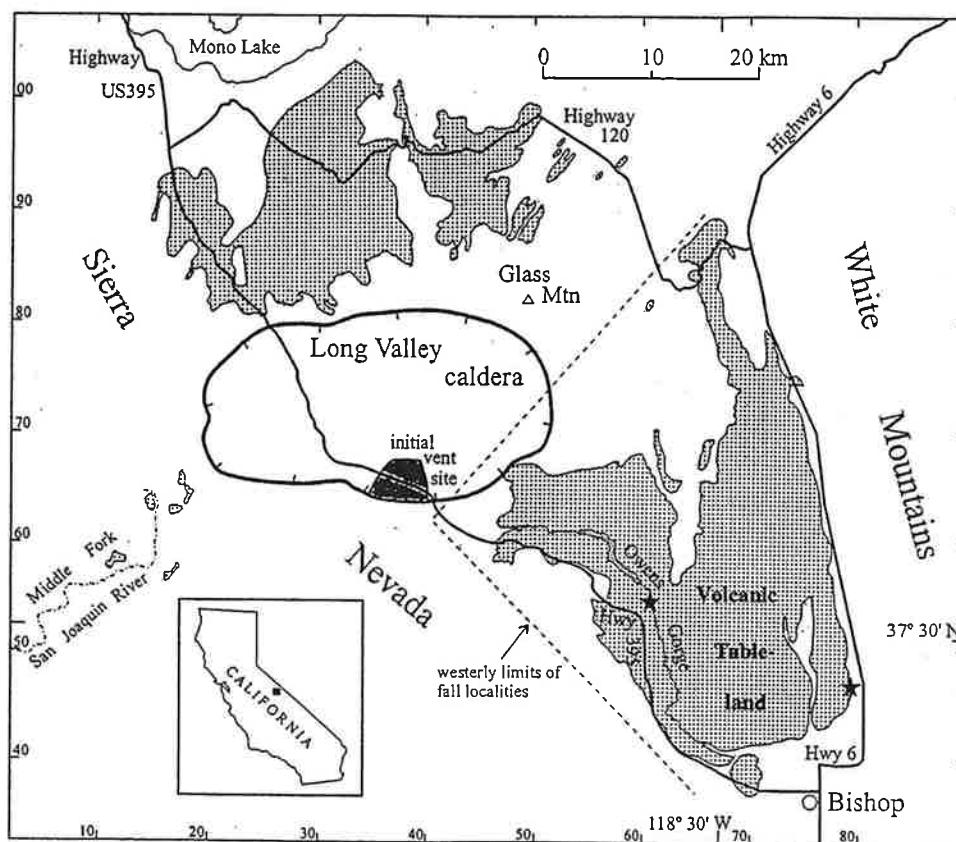


Figure 1. Areal distribution of the Bishop Tuff. The stippled pattern marks areas in which the tuff is presently exposed. The largest exposure area comprises the Volcanic Tableland north and northwest of Bishop. The ring-fracture boundary of the Long Valley caldera, the source area of the tuff, is also shown. The initial eruptions of Bishop ash came from the south-central margin of the caldera. Because it was blown eastward by west winds, air-fall ash deposits are found only east of the vent area, as indicated by dashed lines in the figure. Locations of the two field trip stops to look at the Bishop Tuff are indicated by black stars. (Figure is modified from Wilson and Hildreth, 1997, p. 408.)

The unit generally is 400 to 500 ft (120 to 150 m) thick but locally is up to 800 ft (240 m) thick (Gilbert, 1938, p. 1833; Rinehart and Ross, 1957). In the vicinity of the pumice quarries, which are on the edge of the Volcanic Tableland, the basal Bishop pumice ash is typically about 15 ft (4½ m) thick and is overlain by as much as 75 ft (23 m) of poorly consolidated Bishop Tuff (Chesterman, 1956, p. 60). The unit has been radiometrically dated at 760,000 years (Bogaard and Schirnick, 1995).

Gilbert (1938, p. 1852-1860) in his classic study of the Bishop Tuff inferred that the unit originated as a series of *nuées ardentes* that erupted from a group of vents in the vicinity of Long Valley. Bailey and others (1976, p. 730-731) concluded that the volcano-tectonic depression of the Long Valley caldera formed when the Bishop Tuff erupted, producing 125 cu mi (500 cu km) of ash-flow deposits and 75 sq mi (300 sq km) of air-fall ash deposits. Bishop air-fall ash from the eruption event has been reported as far east as Kansas and Nebraska (Izett and others, 1970, p. 122). Hildreth (1979, p. 44-48; written communication, 1976) used Fe-Ti oxide geothermometry to determine that the basal air-fall ash equilibrated at a temperature of about 720°C (1330°F) and a pressure of 1 kb or less (2 to 3 km depth) and that the last eruptions of ash flows equilibrated at about 790°C (1450°F) and about 4.5 kb (13 km depth). He (oral communication, 1976) cautioned, however, that the latter pressure determination has a very large uncertainty. Hildreth (1979, p. 47) attributed the final stages of eruptive activity to expulsion of hotter, deeper-level magma through the northern segment of the ring fracture, which finally opened as the Long Valley caldera block continued to collapse.

Hildreth (1979, p. 61) originally considered the eruptive process to have involved progressive tapping a single zoned magma chamber, with temperature and depth increasing throughout the eruptive sequence. Later work by Wilson and Hildreth (1997, p. 437), however, indicated that the eruptive process was more complex, in that some pyroclastic units with different temperatures and chemical compositions erupted simultaneously rather than sequentially. They also suggested that chemical compositions may have varied laterally as well as vertically in the magma chamber. Their main evidence for lateral variations in composition was their determination that, as the eruptive vents migrated around the developing caldera, pyroxene-bearing and pyroxene-free magma erupted simultaneously along different segments of the proto-caldera rim.

As a result of their detailed stratigraphic studies of the Bishop Tuff, Wilson and Hildreth (1997, p. 436) concluded that the air-fall ash and pyroclastic flow (ignimbrite) eruptions were largely contemporaneous. They (p. 430-432) used field data combined with modeling of explosive eruption deposits to infer a time history for the eruption of the Bishop Tuff:

- (1) the air-fall ash eruptions lasted slightly more than 4 days;
- (2) the southeast-directed ash flows were emplaced during essentially the same time, starting about 10 to 15 hours after the beginning of the air-fall ash eruptions;
- (3) the latest and thickest north-directed ash flows were emplaced in not more than 1½ days, possibly starting 3½ to 4 days after the ash-flow eruptions began.

The chronology derived by Wilson and Hildreth suggests that the cataclysmic eruption of the Bishop Tuff spanned a week or less.

Xenoliths in the basal tuff indicate that the eruption began at a vent along the south-central margin of the proto-caldera (Hildreth and Mahood, 1986, p. 400). As the eruption proceeded and the caldera began to subside, multiple vents developed along the ring-fracture system. Wilson and Hildreth (1997, p. 437) concluded that vents along the southern margin of the caldera propagated eastward (counter-clockwise) from the initial vent area. As the southern vent activity propagated eastward, additional vents opened up along the northern margin of the caldera. The northern vents propagated from west to east (clockwise), gradually incorporating more and more lithic debris from the Glass Mountain rhyolitic rocks (Wilson and Hildreth, p. 425), for which Metz and Mahood (1985, p. 11,122) reported radiometric ages between 2.1 and 0.8 million years. Hildreth and Mahood (1986, p. 403) concluded that the magma probably erupted along ring-fracture fissures as elongate "curtains" of ash. Their vivid description of the process is worth quoting: "Foundering of the cauldron block into the magma reservoir could open fissures hundreds of meters wide, promoting enormous discharge rates and sustaining such curtains in segments, perhaps discontinuous, each many kilometers long."

This Bishop Tuff material exposed in the quarry walls at this stop (Fig. 2) is poorly consolidated pumice ash and lapilli. The quarry was operated in the 1920's by the California Quarries Company and later, at least into the 1950's, by Insulating Aggregates, Inc., of Bishop (Chesterman, 1956, p. 60). The latter company's mill is still standing, about 2000 ft (600 m) north of this stop. Pumice from the quarry was used mostly in plaster but was also used in stucco, cement, cleanser, and soap.

Figure 2 shows a simplified version of the stratigraphy worked out by Wilson and Hildreth (1997, p. 418) for this locality. The basal ash exposed in the quarry wall is part of the package of air-fall ash that erupted along the southeastern rim of the Long Valley caldera. It is characterized by the absence of pyroxene phenocrysts and extreme sparsity of lithic fragments derived from Glass Mountain rhyolitic rocks. Pumice lapilli up to 1 in. (2½ cm) across are common, and lapilli up to 3 in. (8 cm) across can be found in this unit. Wilson and Hildreth identified the basal air-fall ash exposed here (labeled "afa1" in Fig. 2) as their air-fall

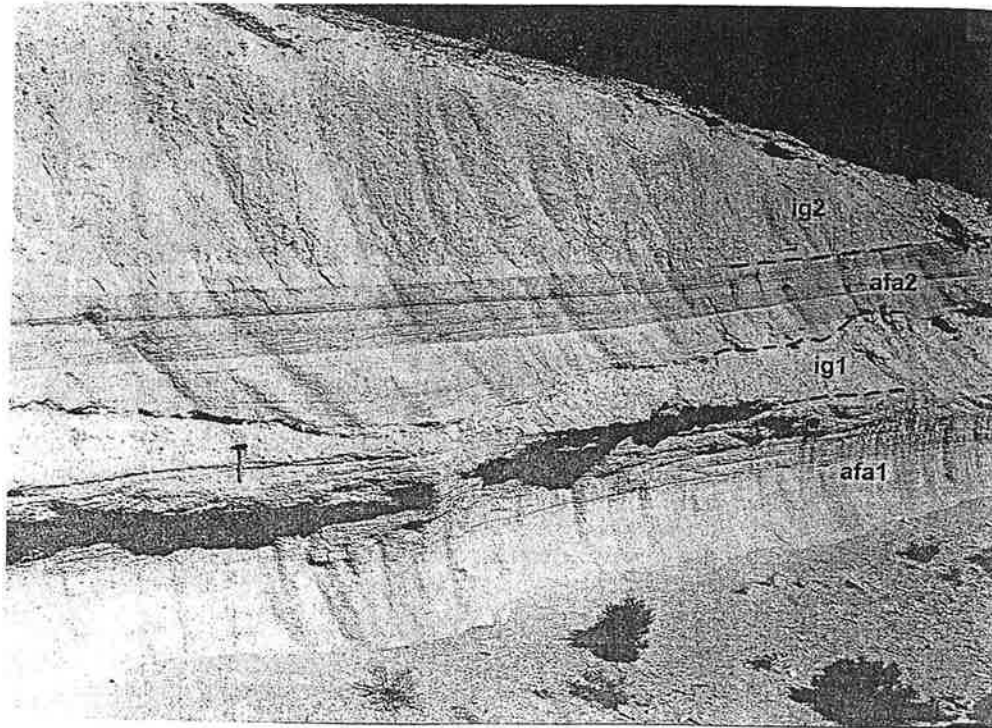


Figure 2. The wall of abandoned quarry at the stop near Rudolph Road north of Laws, looking northwest. Quarry wall exposes several zones of air-fall ash and ignimbrite deposits within the Bishop Tuff: "afa1" is early air-fall ash, "ig1" is early ash-flow deposit, "afa2" is later air-fall ash, and "ig2" is later ash-flow deposit. Wilson and Hildreth (1997, p. 409, 415) report that the two early units lack pyroxene phenocrysts and have very few xenoliths of Glass Mountain rhyolitic rocks, whereas the two later units have some pyroxene phenocrysts and Glass Mountain-derived xenoliths. Note the local cross-bedding in the air-fall ash deposits. A hammer (15 in. or 38 cm long) toward the left in the photo provides a scale; the hammer head is at the middle of the "ig1" unit, and the midpoint of the handle length is at the contact between "afa1" and "ig1". (Photo taken in September 2001.)

An upper ignimbrite deposit, labeled "ig2" in Figure 2, forms the uppermost part of the quarry wall. These ash-flow deposits correspond to the "Ig2E" ignimbrite package of Wilson and Hildreth (1997, p. 418). The base of the unit consists of a fine, white ash layer about 6 in. (15 cm) thick. Overlying this basal deposit, the rest of the ash-flow unit consists of light orange-pink pumice ash and lapilli with no well-defined layering. Lapilli are commonly 3 to 6 in. (7 to 15 cm) long, and blocks as much as 12 in. (30 cm) across can be seen. Wilson and Hildreth (1997, p. 421) report that this ash flow, which contains some pyroxene phenocrysts and Glass Mountain-derived xenoliths, is up to 425 ft (130 m) thick toward the southwestern margin of the Volcanic Tableland.

In summary, the Bishop ash deposits seen at this stop show the transition of eruptive products as the southern vent area for the Bishop Tuff migrated eastward. The earlier pyroclastic units were erupted from the south-central rim of the Long Valley caldera, away from the area of the Glass Mountain rhyolitic volcanic complex. The later deposits, on the other hand, were erupted from the eastern rim of the caldera, which lies within the source area for the Glass Mountain rhyolitic rocks.

RADIAL (ROSETTE) COLUMNAR JOINTING IN BISHOP TUFF.

Starting from the gate, **walk about 350 ft (110 m) up the road.** The purpose of the first part of this stop is to look at another slice of the Bishop Tuff stratigraphy that we saw at the pumice quarry north of Laws. The roadcut displays some of the same units that we saw in the quarry wall, but here the material is more indurated. The greater induration seen here is probably due to a higher temperature during emplacement of these deposits, compared to that of the pyroclastics deposited along the edge of the Volcanic Tableland.

The roadcut (Fig. 3) shows three packages of Bishop ash deposits: two pyroclastic flow units, with an air-fall ash deposit between them. The lower part of the roadcut exposes the same ash-flow deposit ("ig1" in Figs. 2 and 3) that we saw at the pumice quarry. Here, however, the material is sufficiently indurated to be described as a tuff, whereas at the quarry the deposit is more of a pumiceous ash deposit. This package of early ash-flow deposits makes up about 90 percent of the wall of the Owens River Gorge at this location. Very few xenoliths of Glass Mountain-derived rhyolitic rocks are found in the early ash-flow unit.

A broad, shallow swale was eroded into the surface of the early ash-flow deposit during the eruptive sequence, and some air-fall ash ("afa2" of Figs. 2 and 3) accumulated on the surface and was preserved in the swale. The air-fall deposit, which has a maximum thickness of 20 in. (50 cm) in the swale, has laminations that are on the order of $\frac{1}{4}$ to $\frac{1}{2}$ in. (about $\frac{1}{2}$ to 1 cm) thick. This air-fall unit was identified by Colin Wilson (oral communication, 2001) as part of the last package of air-fall ash deposits (the F9 unit of Wilson and Hildreth, 1997) produced by the great eruption. He reported that the air-fall ash contains xenoliths of Glass Mountain rhyolite and obsidian, which indicates that it was erupted from vents along the eastern rim of the Long Valley caldera.

Exposed in the upper part of the roadcut is a later ash-flow unit ("ig2" of Figs. 2 and 3) that overrode and buried the air-fall ash deposit. The top of the air-fall ash may have been eroded during emplacement of the overlying ash flows. A prominent parting occurs at the contact between the air-fall ash and the overlying ash-flow deposit. A high proportion of xenoliths in the later ash-flow deposits exposed in the roadcut are derived from Glass Mountain rhyolitic rocks, with the relative proportion increasing as one goes up the section (Colin Wilson, oral communication, 2001). This indicates that, as the later ash flows were being erupted, the vent areas were migrating eastward along the southern rim of the caldera, into the region occupied by the Glass Mountain volcanic complex.

Next, walk down the road, about 150 ft (50 m) past the locked gate. At this locality the Owens River Gorge is carved entirely in Bishop Tuff. The gorge here is about 450 ft (135 m) deep, which provides a minimum thickness for the tuff at this locality. The lower, more highly welded tuff is generally massive with irregularly developed jointing. The upper, essentially unwelded part of the tuff, however, has strikingly unusual columnar jointing that commonly forms radiating sets (Fig. 4). Column diameters typically range between 3 and 5 ft (1 and 1½ m), and columns have diverse orientations ranging from horizontal to vertical (Gilbert, 1938, p. 1836). If you want to photograph the rosette jointing, visit this stop in the afternoon.

The Bishop Tuff near the LADWP gate consists of very light gray to pale pink, agglutinated but only slightly welded, vitric pumice ash that weathers grayish orange pink. The tuff is porous, light in weight, and contains abundant pumice fragments, generally equidimensional, as well as plentiful phenocrysts of sanidine, quartz, and plagioclase. The latter phenocrysts consist almost entirely of unzoned oligoclase (An₁₃₋₂₅) (Wes Hildreth, written communication, 1976). Small xenoliths of basalt, hornfels, quartzite, and granitic rocks are included locally in the tuff (Putnam, 1960, p. 236) and serve to indicate the nature of the basement rock along the ring-fracture segment from which the ash flow was extruded (Hildreth and Mahood, 1986, p. 400-402).

In his geochemical study of the Bishop Tuff, Hildreth (1979, p. 49-61) found that Bishop Tuff minerals show progressive changes in more than 30 elements as a function of temperature, which he interpreted as indicating a systematic compositional change during the eruptive sequence. Silica content decreased from an initial 77 percent to about 75 percent toward the end of the sequence (Hildreth, p. 54). An important conclusion reached by Hildreth was that zoning of the magma was not due to transfer of phenocrysts by settling but rather that the zoning existed in the molten liquid prior to formation of the crystals. He (p. 67) inferred therefore that the zoned magma chamber developed by convection-driven diffusion in the liquid state. Hildreth's convection-diffusion model (Shaw and others, 1976) indicates that, in large-volume silicic magma chambers, major eruptions and subsequent reestablishment of chemical gradients could occur with a periodicity of several hundred thousand years. Note that the Bishop Tuff eruption occurred about 760,000 years ago.

In the welded part of the Bishop Tuff, which is not exposed along the road near the LADWP gate, the tuff is dense and locally glassy (although most of the glass has devitrified), and it contains flattened pumice fragments and deformed glass shards. The lower, more highly welded tuff can be seen by walking down the road past the gate and into the gorge, going about halfway to the bottom. There you can see for yourself pumice clasts

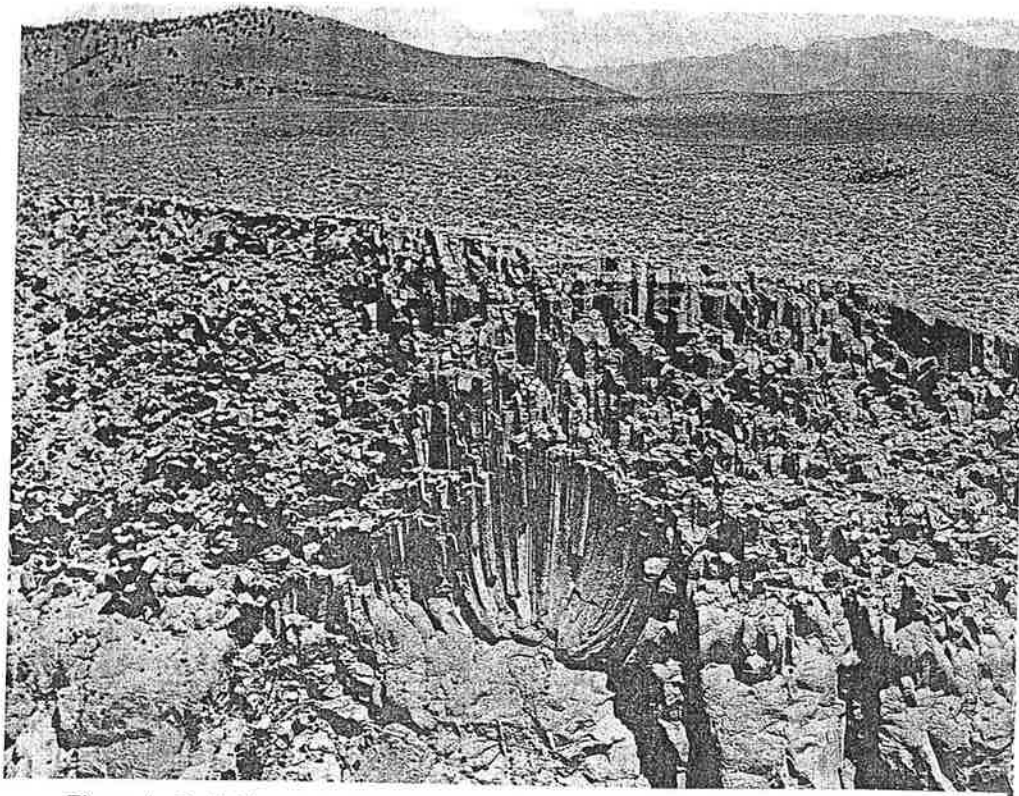


Figure 4. Radial (rosette) columnar jointing in Bishop Tuff at the Owens River Gorge, looking eastward from above the road to LADWP Powerhouse No. 1. The upper, more highly jointed part of the tuff is poorly welded to unwelded; the lower, less jointed part is more highly welded. Almost all of the tuff in the photograph is part of the early ash-flow unit ("ig1" in Figs. 2 and 3; "IglE" of Wilson and Hildreth, 1997) that was erupted from vents along the south-central part of the Long Valley caldera rim. (Photo taken in July 1976.)

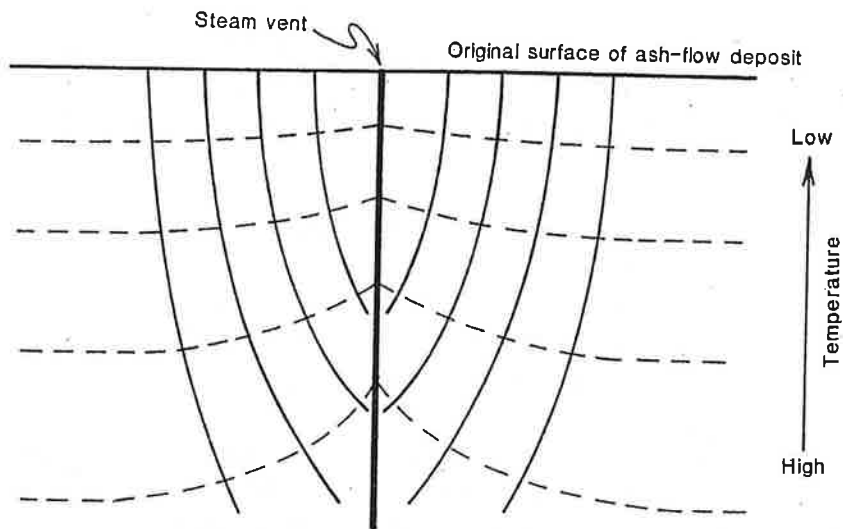


Figure 5. Cartoon sketch of the thermal regime around a fumarole (steam vent) in a cooling ash-flow sheet. Dashed lines are isotherms (contours of equal temperature), and solid lines are columnar joints, which coincide with the paths of heat flow. The thick vertical line is the steam or gas conduit. The heat of the steam causes elevated temperatures near the conduit, which deflects the isotherms upward. The columns have an approximately radial symmetry about the steam conduit. Compare this figure with the radial column array shown in Figure 4.

REFERENCES CITED:

- Bailey, R.A., Dalrymple, G.B., and Lanphere, M.A., 1976, Volcanism, structure, and geochronology of the Long Valley caldera, Mono County, California: *Journal of Geophysical Research*, v. 81, no. B2, p. 725-744.
- Bateman, P.C., 1965, Geology and tungsten mineralization of the Bishop district, California, *with a section on Gravity study of Owens Valley*, by L.C. Pakiser and M.F. Kane, *and a section on Seismic profile*, by L.C. Pakiser: U.S. Geological Survey Professional Paper 470, 208 p.
- Bateman, P.C., 1992, Plutonism in the central part of the Sierra Nevada batholith, California: U.S. Geological Survey Professional Paper 1483, 186 p.
- Bishop, K.M., 1999, Mega rock avalanche and rock slide deposits of the Owens Valley, eastern California, *in* Baldwin, J., Hughes, K., Sharp, G.M., Steiner, E., and West, M.D., *The Long Valley caldera, Mammoth Lakes, and Owens Valley region*, Mono County, California: South Coast Geological Society Field Trip Guidebook No. 27, 374 p.
- Bogaard, P. van den, and Schirnick, C., 1995, $^{40}\text{Ar}/^{39}\text{Ar}$ laser probe ages of Bishop Tuff quartz phenocrysts substantiate long-lived silicic magma chamber at Long Valley, United States: *Geology*, v. 23, p. 759-762.
- Chesterman, C.W., 1956, Pumice, pumicite, and volcanic cinders in California, *with a section on Technology of pumice, pumicite, and volcanic cinders*, by F.S. Schmidt: California Division of Mines Bulletin 174, 119 p.
- Curtis, G.H., 1968, The stratigraphy of the ejecta from the 1912 eruption of Mount Katmai and Novarupta, Alaska, *in* Coats, R.R., Hay, R.L., and Anderson, C.A., eds., *Studies in Volcanology*: Geological Society of America Memoir 116, p.153-210.
- Gilbert, C.M., 1938, Welded tuff in eastern California: *Geological Society of America Bulletin*, v. 49, p. 1829-1862.
- Hart, J., 1996, Storm over Mono: The Mono Lake Battle and the California Water Future: Berkeley, University of California Press, 211 p.
- Hildreth, W., 1979, The Bishop Tuff: Evidence for the origin of compositional zonation in silicic magma chambers, *in* Chapin, C.E., and Elston, W.E., eds, *Ash-Flow Tuffs*: Geological Society of America Special Paper 180, p. 43-75.
- Hildreth, W., and Mahood, G.A., 1986, Ring-fracture eruption of the Bishop Tuff: *Geological Society of America Bulletin*, v. 97, p. 396-403.

REFERENCES CITED: (Cont'd)

- Izett, G.A., Wilcox, R.E., Powers, H.A., and Desborough, G.A., 1970, The Bishop ash bed, a Pleistocene marker bed in the western United States: *Quaternary Research*, v. 1, p. 121-132.
- Kneiss, G.H., 1943, *Bonanza Railroads*, 2nd ed.: Stanford, CA, Stanford University Press, 148 p.
- Kurtak, J.M., 1997, *Mine in the Sky*: Anchorage, AK, Publication Consultants, 220 p.
- Lipshie, S.R., 2001, *Geologic guidebook to the Long Valley-Mono Craters region of eastern California*, 2nd ed.: Santa Ana, CA, South Coast Geological Society, 270 p.
- Lipshie, S., and Gray, R., 1998, Quaternary volcanism of the Long Valley caldera and Mono Craters region, California, in Caputo, M.V., and Grubb, B., eds., *Geology of the southeastern Sierra Nevada revisited: National Association of Geoscience Teachers, Far Western Section, spring field conference guidebook (April 17-19, 1998)*, p. 61-106.
- Metz, J.M., and Mahood, G.A., 1985, Precursors to the Bishop Tuff eruption: Glass Mountain, Long Valley, California: *Journal of Geophysical Research*, v. 90, no. B13, p. 11,121-11,126.
- Putnam, W.C., 1960, *Origin of Rock Creek and Owens River Gorges, Mono County, California*: University of California Publications in Geological Sciences, v. 34, no. 5, p. 221-280.
- Rinehart, C.D., and Ross, D.C., 1957, *Geology of the Casa Diablo Mountain quadrangle, California*: U.S. Geological Survey Geologic Quadrangle Map GQ-99, scale 1:62,500.
- Shaw, H.R., Smith, R.L., and Hildreth, W., 1976, Thermogravitational mechanisms for chemical variations in zoned magma chambers [abstract]: *Geological Society of America Abstracts with Programs*, v. 8, no. 6, p. 1102.
- Sheridan, M.F., 1970, Fumarolic mounds and ridges of the Bishop Tuff, California: *Geological Society of America Bulletin*, v. 81, p. 851-868.
- Sheridan, M.F., 1971, *Guidebook to the Quaternary geology of the east-central Sierra Nevada*: Friends of the Pleistocene, Rocky Mountains Section, XVI field conference, 60 p.
- Wilson, C.J.N., and Hildreth, W., 1997, The Bishop Tuff: new insights from eruptive stratigraphy: *Journal of Geology*, v. 105, p. 407-439.
- Wilson, C.J.N., and Hildreth, W., 1998, Hybrid fall deposits in the Bishop Tuff, California: a novel pyroclastic depositional mechanism: *Geology*, v. 26, p. 7-10.

Inyo Craters.

Three craters comprise the main part of the Inyo Craters themselves: the two lake-filled craters (Figs. 56 and 57) and another crater that surmounts Deer Mountain, the peak to the north (Fig. 55). The Inyo Craters chain actually includes more volcanic domes than craters: in addition to the three principal craters, it consists of at least six domes, including Deer Mountain. The rim of the Deer Mountain crater can be seen and easily recognized from the vicinity of the other two craters. The southern two craters with their lakes are quite impressive, and the southernmost is especially photogenic (Fig. 56). The southern lake is an opaque peasoup green or jade green, whereas the northern lake is a clear deep green color. The water of the northern lake is potable—I once saw a deer drinking it, and the creature seemed none the worse afterwards—but the southern lake's water doesn't look as though it would be very palatable.

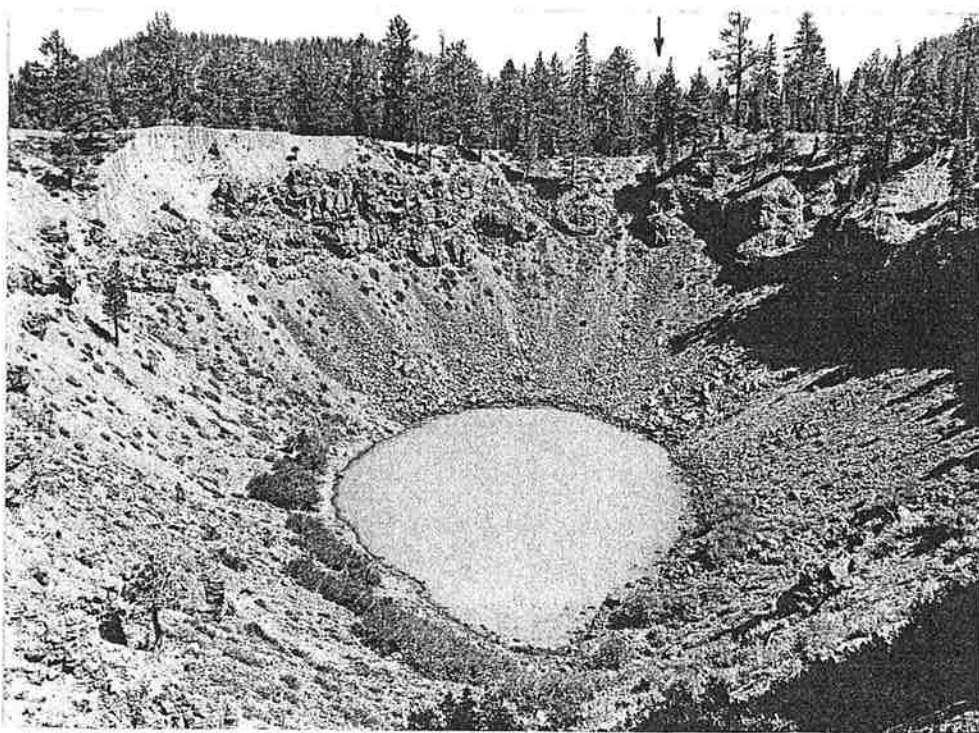


Figure 56. *Southernmost of Inyo Craters, looking south. Arrow (top) marks the location of a fault along which the east (left) block has been downdropped about 20 ft (6 m). An andesite flow, one of the mafic lavas that flowed into the north and south moats of the caldera, is exposed in the crater walls. Beyond the crater is a dome (upper left) of hornblende-biotite rhyolite, part of the moat rhyolite dated at 0.1 m.y. old. (Photo taken in July 1976.)*

The two craters with lakes are over 600 ft (180 m) in diameter and crudely funnel-shaped. The northern crater is about 130 ft (40 m) deep, and the southern one is more than 200 ft (60 m) deep. The craters originated as phreatic explosion pits, rather than being typical ash eruption craters. No tephra was produced during the formation of the craters. They were probably excavated when rising magma encountered a large volume of groundwater that had percolated downward into pore space in near-surface sediments and volcanic rocks (Rinehart and Huber, 1965). The magma superheated the water, and the resultant fluid pressure finally exceeded the confining pressure that was produced by the weight of the overlying rocks.

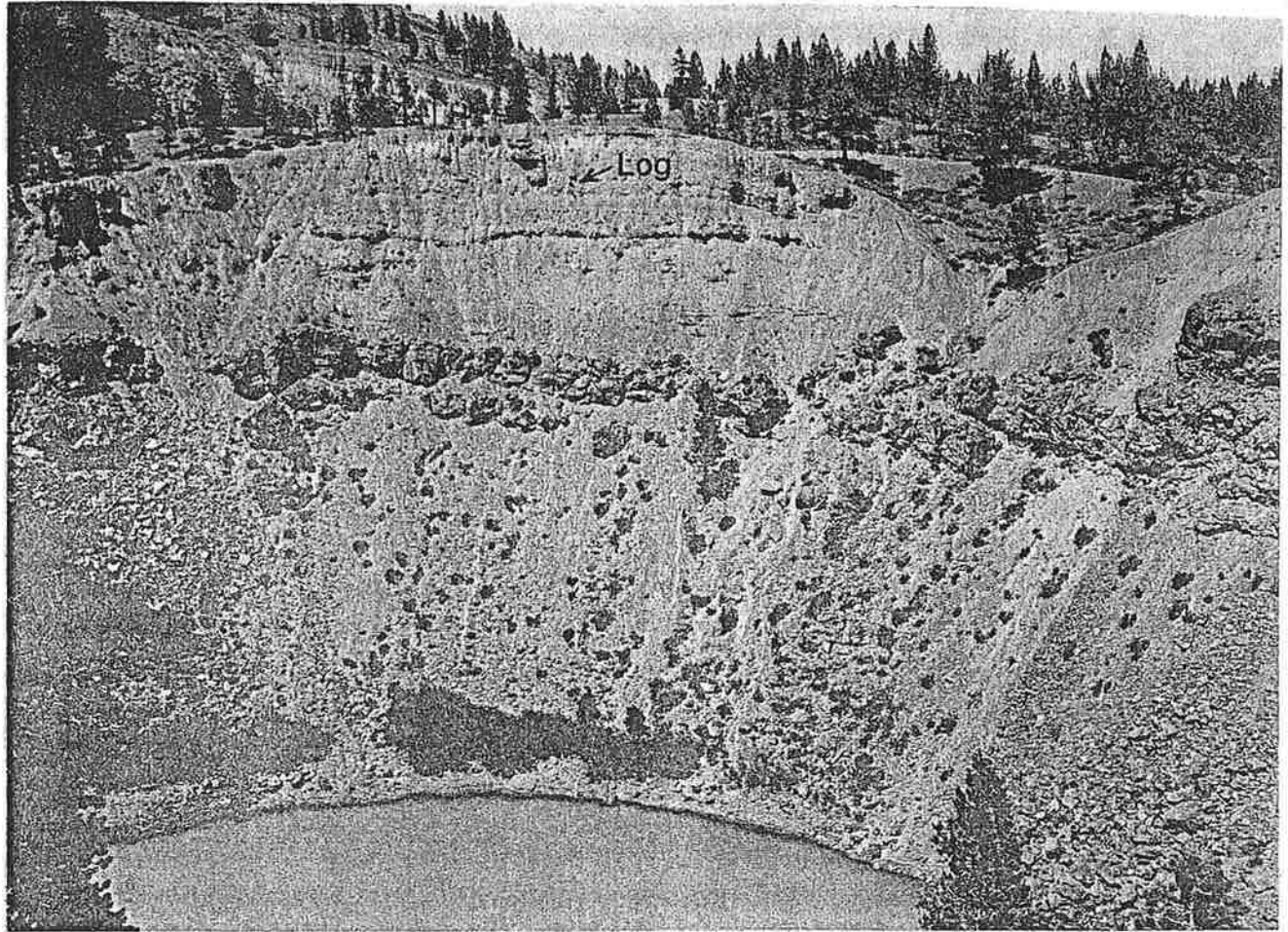


Figure 57. Northeast wall of southernmost Inyo crater. Overlying the andesite flow, the base of which is concealed by slopewash, is a thick section of tephra capped by layered phreatic explosion debris. The boundary between the tephra and the explosion debris is just below the prominent horizontal layer that casts a distinct shadow (about halfway between the crater rim and the top of the andesite flow). The location of the radiocarbon-dated log is indicated in the photo. Beyond the crater rim, part of the wall of the middle crater (upper left) can be seen at the base of Deer Mountain. (Photo taken in July 1976.)

Then the superheated water vaporized explosively, and the expanding steam hurled the overlying material upward and outward, blanketing the immediate area with a layer of debris. The layer is up to 50 ft (15 m) thick at the crater rim, but it thins precipitously outward, becoming unrecognizable at distances of several hundred feet (about 100 m) from the craters (Rinehart and Huber, 1965).

The craters and domes of the Inyo Craters chain extend northward from the northwest quadrant of the Long Valley caldera to the south end of the Mono Craters chain. Bailey and others (1976, p. 735) attributed the linear distribution of the Inyo domes and craters to alignment along a north-trending fracture that extends from the Long Valley caldera to the Mono Craters; the fracture runs subparallel to and east of the Sierra Nevada range front. Miller (1985) went one step further and suggested that the Inyo Craters eruptions occurred along a north-trending feeder dike that provided a conduit for the magma to reach the surface. To test the feeder dike hypothesis, an inclined hole was drilled in 1987 just southwest of the southern Inyo crater. The hole, which plunged 68° (*i.e.*, 22° from vertical) so as to go under the southern crater, intersected three breccia zones around 2000 ft (600 m) beneath the crater. The main breccia zone was interpreted to be a vertical feeder dike for the Inyo Craters eruptions. The rising rhyolite magma followed an older feeder dike for one of the late Pleistocene basaltic lavas that flowed into the north moat of the caldera (Eichelberger and others, 1988, p. 13,215-13,218).

A series of discontinuous, north-trending, down-to-the-east faults has been mapped from Mammoth Mountain northward to the Mono Craters (Huber and Rinehart, 1965; Kistler, 1966a); the longest segment of this system is the Hartley Springs fault (Fig. 18). A small fault that belongs to this system cuts the southeast quadrant of the rim of the southern Inyo crater (Fig. 56), relatively downdropping the east part of the rim by about 20 ft (6 m). The fault offsets phreatic explosion debris and thus postdates the craters.

A massive flow of dark gray andesite with a silica content of about 56 percent (Huber and Rinehart, 1967, pl. 1) is exposed in the wall of the southern crater and is probably covered by talus and slopewash in the northern lake-filled crater. The andesite flow has not yet been radiometrically dated, but it is believed to be late Pleistocene in age and to postdate the Rhyodacite of Mammoth Mountain (Huber and Rinehart, p. D16). It is presumably part of the mafic lava complex that was erupted into the west moat and flowed eastward into the north and south moats of the caldera after emplacement of the resurgent dome. The mafic moat lavas that have been dated by the K-Ar method have ages that range from about 230,000 to 60,000 years (Mankinen and others, 1986, p. 637-638).

Overlying the andesite is a zone of tephra layers about 30 ft (10 m) thick. Rinehart and Huber (1965) identified two distinctive tephra types in the zone: (1) a lower, fine-grained, reddish ash and lapilli deposit, which they correlate with the source vent for the andesite flow, and (2) an upper, light-colored ash and lapilli layer about 6 to 8 ft (2 to 2½ m) thick that probably had a different source. On top of the upper layer is a light gray to white pumice lapilli layer about 4 to 6 ft (1¼ to 2 m) thick that is widespread

throughout the region (Rinehart and Huber, 1965). Wood (1977b, p. 92) identified this pumice layer as his tephra 1 (see Stop 35), which he dated at 720 ± 60 years B.P., or around A.D. 1240.

Overlying the tephra is a heterogeneous aggregation of explosion debris from the craters. The explosion debris contains clasts of a variety of lithologies up to several feet (about a meter) across in a poorly sorted matrix of fine-grained material. Clasts include rounded cobbles of granitic and metamorphic rocks that Rinehart and Huber (1965) interpreted as being derived from glacial or stream gravel that may underlie the andesite. A radiocarbon date determined for an uncharred log (Fig. 57) from the middle third of the debris layer gave an age of 650 ± 200 years B.P. for the phreatic explosion that formed the craters (Rinehart and Huber, 1965). The uncharred condition of the log indicated that it had not been killed by a prior pumice ash eruption and that it was either still alive or lying on the pumice (tephra 1) layer at the time of the phreatic explosion.

Wood (1977b, p. 92) decided to redate a specific 20-year growth increment of the log sampled by Rinehart and Huber because of advances in radiocarbon dating techniques since the time of their dating. He found that the tree died 550 ± 60 years ago, which places an upper limit on the age of the explosive event and indicates that the craters were formed between A.D. 1340 and 1460. Curry (1971, p. 35) reported that local Paiute Indian legends supposedly tell of volcanic eruptions in the region. If so, they may refer to the phreatic explosions that formed the Inyo Craters. Or they could just as well refer to the extrusion of some of the Inyo domes about 50 to 100 years earlier.

It thus appears that major volcanic activity has occurred in the region within the last 500 to 600 years, and it seems reasonable, based on the record of the past several thousand years, to expect further volcanic eruptive activity within the next 500 years. An observation that Mark Twain (1872, p. 271) made long ago about the volcanic islands of Mono Lake can just as well be applied to the Inyo Craters today: although this crater has gone out of active business, there is still some fire left in its furnaces. And the same holds true for the Long Valley caldera, as is evidenced by the seismic activity that began in 1978 and continues today.

Future eruptions could have devastating effects on the water supply for the City of Los Angeles. The city at one time obtained as much as 80 percent of its water supply from the Mono Basin and Owens Valley (Hopson, 1991, p. 49, 53-54). Today it gets 65 percent of its water from that region, with the remainder coming from the Metropolitan Water District (20 percent) and local Los Angeles wells (15 percent) (Larry Jackson and Cliff Plumb, LADWP, oral communications, 2000).

Permian potholes at Reward Mine/ Late Pleistocene Potholes at Fossil Falls

Cal Stevens

Reward Mine: The potholes exposed south of the Reward Mine were first recognized by Kirk (*in* Knopf, 1918). These potholes are cut vertical to bedding in the presently almost vertically dipping, very hard, siliceous conglomerate of the Lower Permian Reward Member of the Lone Pine Formation. The potholes were formed after deposition and lithification of the Reward Conglomerate and prior to deposition of non-resistant strata that have since been removed from the potholes by erosion. The potholes are cut in progressively older strata northward showing that the river forming them flowed northward.

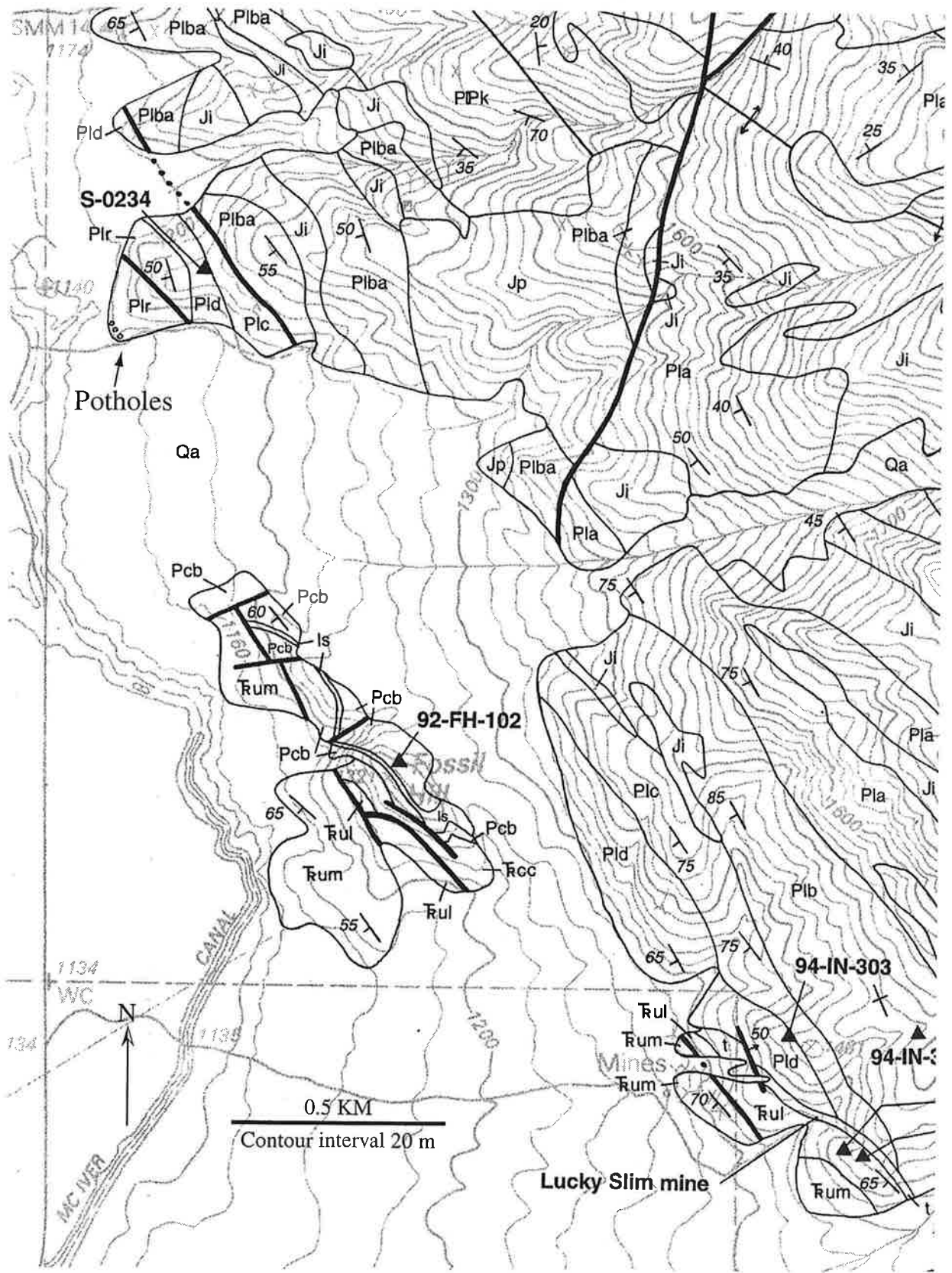
The rocks overlying the Reward Conglomerate are nowhere exposed, so the precise age of the potholes is uncertain. Regional relationships, however, suggest that their formation is post-Early Permian to Early Triassic.

Fossil Falls: Fossil Falls, carved in Pleistocene basalt, are a relic of glacial times when Owens Lake was overflowing and the Owens River continued flowing southward, the runoff ultimately reaching Manley Lake in Death Valley. Basalt flows in this area were erupted between 400,000 and 10,000 years ago and the falls were formed during the Tioga glacial stage which ended about 10,000 years ago (Sharp and Glazner, 1997). The falls have been essentially dry since then.

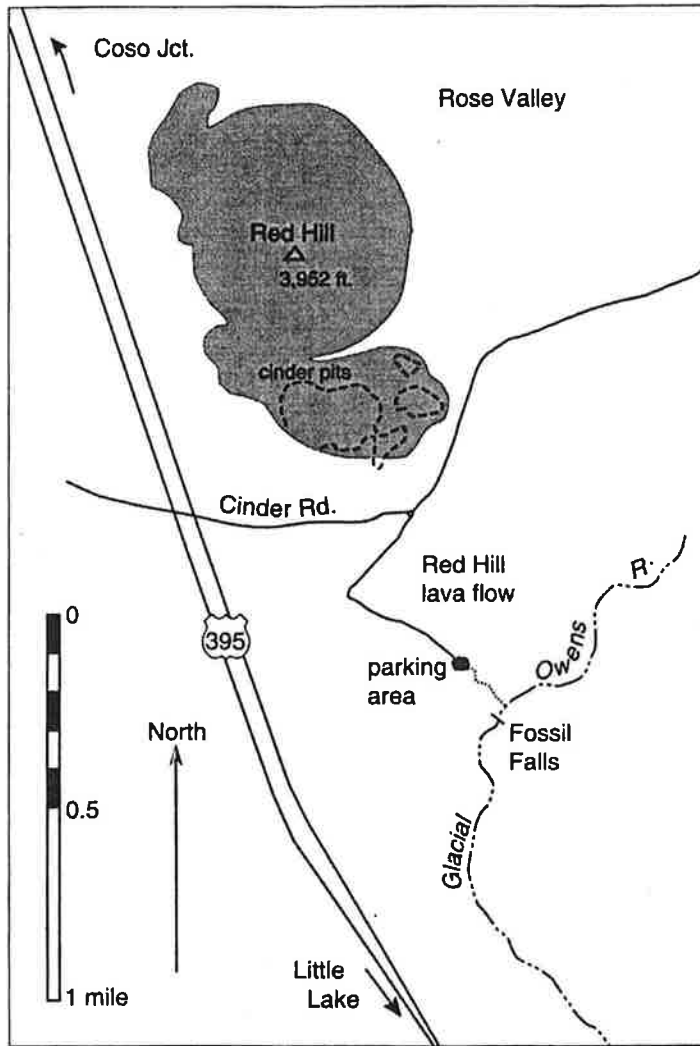
A connected series of potholes was eroded into the basaltic bedrock channel of a steep cascade that led downstream to the final drop of Fossil Falls. The Permian-Triassic potholes exposed near the Reward Mine are very similar to these potholes at Fossil Falls, and probably formed in a similar, high-gradient stream channel.

References:

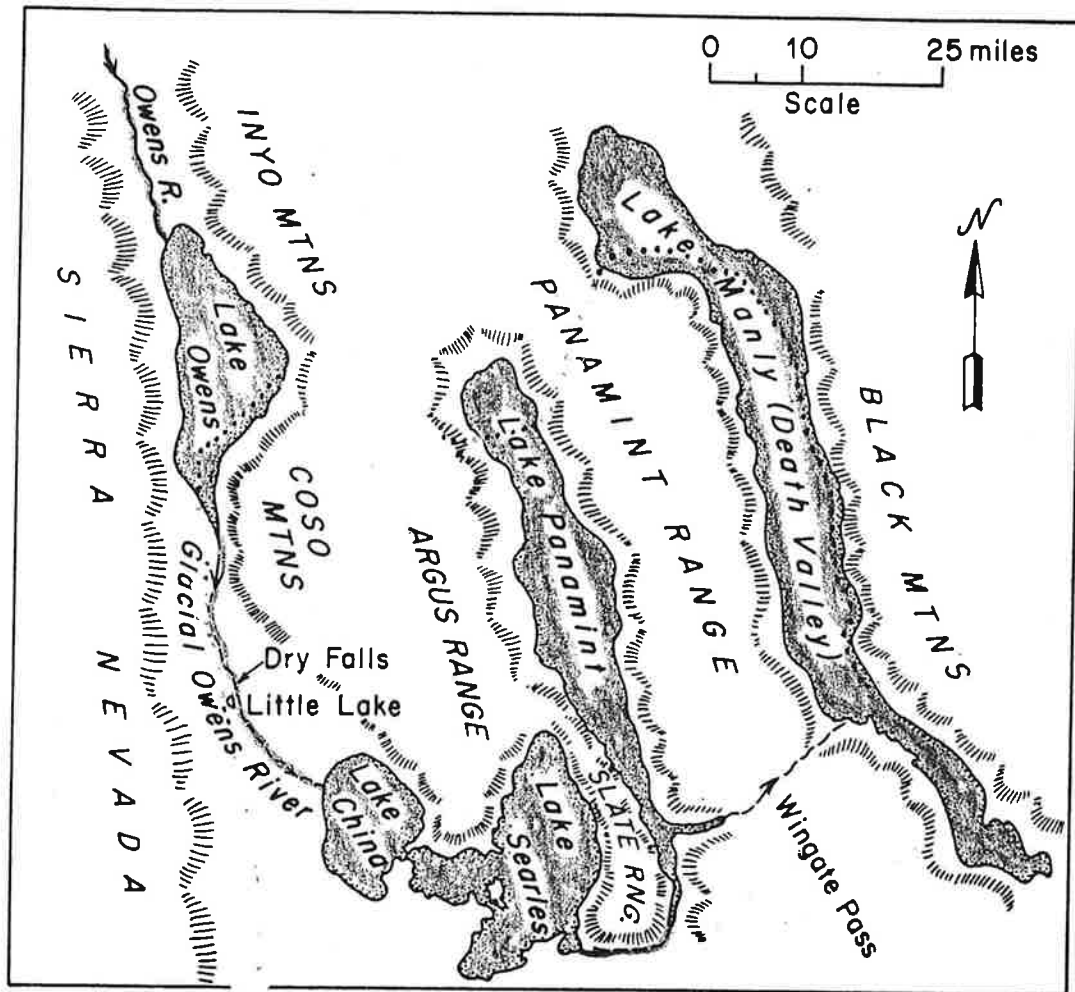
- Knopf, A., 1918, A geologic reconnaissance of the Inyo Range and the slope of the southern Sierra Nevada: U S Geological Survey Professional Paper 110, 130 p.
- Sharp, R.P., and Glazner, A.F., 1997, Geology underfoot in Death Valley and Owens Valley: Missoula, Montana, Mountain Press, 319 p.



Map of part of Union Wash 7.5' quadrangle in southwestern Inyo Mountains showing location of potholes at upper exposed surface of Permian Reward Conglomerate (unit Plr). Modified from Stone et al. (2000).



Map of Fossil Falls area (from Sharp and Glazner, 1997).



Pluvial lakes and connecting river system in eastern California during Plio-Pleistocene time.

COSO VOLCANIC AND GEOTHERMAL FIELD (Jorge Vazquez and George Dunne)

Introduction:

Just behind the prominent "whaleback-shaped" rhyolite dome on the horizon just east of Rose Valley lies a geothermal energy field. At the surface, the high heat flow in the area is expressed in the form of numerous fumaroles, mud volcanoes, and hot springs. It has been exploited for electrical power via a joint venture between Los Angeles Dept. of Water and Power, Southern California Edison, and the U.S. Navy, on whose land it lies.

Energy and development aspects of the Coso Geothermal field:

- Four power plants housing nine turbine-generator sets produce a maximum of 270 megawatts that is used by the China Lake Naval Air Weapons Station, with excess power sold into the state power grid.
- The four plants were constructed between 1987 and 1990.
- About 90 production wells tap very hot water (200° -325° C) at between 1 km and 2 km depth, which flashes to steam as it is piped up to the surface.
- Water recovered from the condensed steam is reinjected into the field through about 40 wells
- The operators believe the field will support electricity production for an additional 25 to as much as 50 years

Geology and Magmatic History:

Late Cenozoic volcanism initiated at approximately 6 Ma and erupted through basement composed of pre-Cenozoic granitoids and metamorphic rocks (Figure 1; Duffield et al., 1980). Since circa 4 Ma, approximately 35 km³ of basaltic to rhyolitic lavas and tuffs have erupted in the region of the Coso Range; about 30 km³ of this was emplaced in Pliocene time between circa 4 Ma and 2.5 Ma (Duffield et al., 1980). A second, distinctly bimodal, eruptive phase began about 2 Ma (Pleistocene) and may be thought of as continuing today. This second phase has to date produced approximately 2 km³ of high-silica rhyolite erupted to form small-volume domes, tuff rings, and fallout deposits, and approximately 3 km³ of basalt erupted to form cinder cones and lava flows. Similar to the Pliocene buildup, the volumetric flux of silicic eruption during the Pleistocene volcanic phase exhibits a increase over time (Duffield et al., 1980).

Bacon et al. (Bacon, 1981) assigned the 38 Quaternary high-silica rhyolite extrusions of the younger phase to seven groups, each of which consisted of chemically similar lavas that had similar apparent eruption ages. The oldest rhyolites are two domes with ages of 1 Ma and 0.5 Ma, which are distinct from all younger rhyolites in that they are relatively crystal rich and have different radiogenic isotope compositions (Bacon et al., 1984). The rest of the rhyolites are less than 250,000 years old and are generally aphyric.

Bacon (1982) suggested that a time-predictable relation between magma volume and the repose between Pleistocene eruptions indicates that extension controls the tapping of magma at Coso. Subsequent studies have confirmed that the eruptive products of the younger phase of volcanism lie within an extensional stepover connecting an echelon right-normal faults. GPS monitoring over the past 15 years reveals the region within this stepover is extending along a NW-SE direction at a rate of about 6.5 mm/yr. Extension within this stepover area has thinned the crust and allowed compensatory rise of asthenospheric mantle to relatively shallow levels. Resulting decompression melting apparently created the magma reservoir under this area. The subsurface region of magma storage is delimited by a concave-downward domain of crust at approximately 5-8 km depth that delays and reflects seismic waves, and is seismically inactive (Reasenberg et al., 1980; Manley and Bacon, 2000).

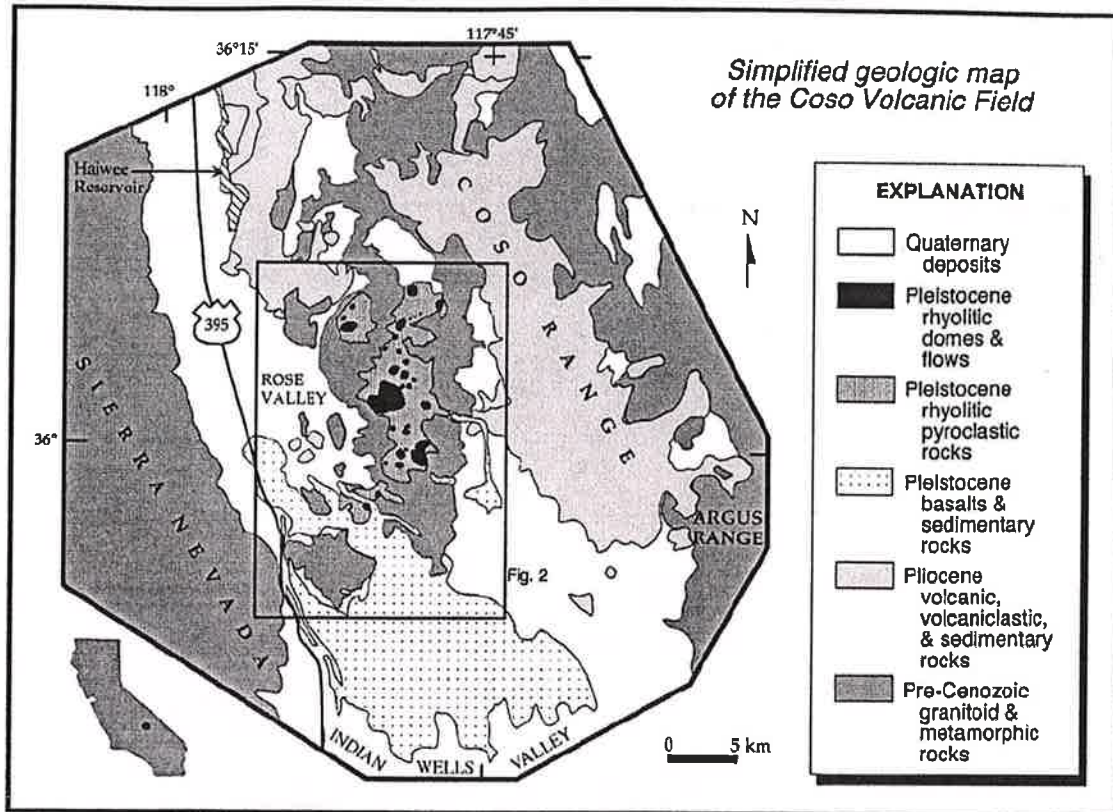
Bacon (1982) concluded that a voluminous subvolcanic reservoir was established by ca. 250 ka based on the age of hydrothermal deposits. Based on the observation that basaltic magma has not vented within the cluster of Pleistocene rhyolites in the last 600,000 years, the rhyolitic reservoir did not solidify between its major eruptive pulses (Manley and Bacon, 2000). A secular variation in mineral equilibria suggests that the depth of rhyolite storage has migrated from 10 km to 6 km in the last 300,000 years (Manley and Bacon, 2000). A secular increase in the volume of erupted magma suggests that the Coso volcanic system is a growing volcanic system, and may be in the prelude to a caldera-forming eruption (Bacon, 1985).

The basaltic and rhyolitic products of late Pleistocene volcanism are visible near Little Lake. While traveling on Highway 395, late Pleistocene basalt is exposed along the edges of the Owens River and crossed by the road at several locations. East of the road, Pleistocene rhyolite domes, tuff rings, and basaltic lavas and cinder cones are visible in the Coso Range. A prominent cinder cone (Red Hill) is exposed adjacent to Highway 395 near Little Lake. A basaltic lava that flowed southward from Red Hill yields a cosmogenic ^3He exposure age of ~60 ka (Cerling,

1990). Diversion of the ancestral Owens River scoured the margin of the Red Hill basalt near Little Lake and sculpted the smooth outcrops at Fossil Falls (Duffield and Smith, 1978). The scoured surface at Fossil Falls yields an exposure age of ca 15 ka, suggesting a late Pleistocene flood event (Cerling, 1990). Other basalts exposed along the Owens River at Little Lake (and south along Highway 395 near Indian Wells Valley yield K-Ar ages of 150 ka to 500 ka.

References:

- Bacon C.R., 1982, Time-predictable bimodal volcanism in the Coso Range, California. *Geology* 10: 65-69.
- Bacon C.R., MacDonald R., Smith R.L., Baedeker P.A., 1981, Pleistocene high-silica rhyolites of the Coso volcanic field, Inyo County, California. *Journal of Geophysical Research* 86:10,223-10,241.
- Bacon C.R., 1985, Implications of silicic vent patterns for the presence of large crustal magma chambers. *Journal of Geophysical Research* 90: 11,243-11,252.
- Bacon C.R., Kurasawa H., Delevaux M.H., Kistler R.W., Doe B.R., 1984, Lead and strontium isotopic evidence for crustal interaction and compositional zonation in the source regions of Pleistocene basaltic and rhyolitic magmas of the Coso volcanic field, California. *Contributions to Mineralogy and Petrology* 85: 366-375.
- Cerling, T.E., 1990, Dating Geomorphologic surfaces using cosmogenic ^3He : *Quaternary Research*, v. 33, p. 148-156.
- Combs, J, 1980, Heat flow in the Coso geothermal area, Inyo County, California. *Journal of Geophysical Research* 85: 2411-2424.
- Duffield, W.A., and Smith, G.I., 1978, Pleistocene history of volcanism and the Owens River near Little Lake, California: *Journal of Research of the U.S. Geological Survey*, v. 6, p. 395-408.
- Duffield W.A., Bacon C.R., Dalrymple G.G., 1980, Late Cenozoic volcanism, geochronology, and structure of the Coso Range, Inyo County, California. *Journal of Geophysical Research* 85: 2381-2404.
- Duffield W.A., Bacon C.R., 1981, Geologic Map of the Coso volcanic field and adjacent areas, Inyo County, California: U.S. Geological Survey Miscellaneous Investigations Series, Map I-200.
- Lanphere, M.A., Dalrymple, G.B., and Smith, R.L., 1975, K-Ar ages of late Pleistocene rhyolitic volcanism in the Coso Range, California: *Geology*, v. 3, p. 339-341.
- Manley C.R., Bacon C.R., 2000, Rhyolite thermobarometry and the shallowing of the magma reservoir, Coso volcanic field, California. *Journal of Petrology* 41: 149-174.
- Monastero, F.C., Katzenstein, A.M., Miller, J.S., Unruh, J.R., Adams, M.C., and Richards-Dinger, K, 2005, The Coso geothermal field: A nascent metamorphic core complex: *Geological Society of America Bulletin*, v. 117, p. 1534-1553.
- Reasenber P, Ellsworth W, Walter A (1980) Teleseismic evidence for a low-velocity body under the Coso geothermal area. *Journal of Geophysical Research* 85: 2471-2483.
- Sass, J., and Priest, S., 2002, Geothermal California: Geothermal Resources Council Bulletin, Sept-Oct, p. 183-187.



Simplified geologic map of Coso volcanic field. From Manley and Bacon (2000).

